Power Quality Studies in Distribution Systems Involving Spectral Decomposition

Dissertation

zur Erlangung des akademischen Grades

Doktoringenieur
(Dr.-Ing.)

von mgr. inż. Andrzej Bachry
geb. am 05.11.1971 in Lubań/ Polen

genehmigt durch die Fakultät Elektrotechnik und Informationstechnik
der Otto-von-Guericke-Universität Magdeburg

Gutachter: Prof.-Dr.-Ing. habil. Zbigniew Styczynski
Prof. Dr.-Ing. habil. Bernd Oswald
Prof. Dr.-Ing. habil. Tadeusz Łobos

Promotionskolloquium am 17. Juni 2004

Andrzej Bachry

Power Quality Studies in Distribution Systems Involving Spectral Decomposition

Otto-von-Guericke-Universität Magdeburg

Magdeburg 2004

Bachry, Andrzej:

Power Quality Studies in Distribution Systems Involving Spectral Decomposition

(Untersuchungen zur Spannungsqualität in Verteilungsnetzen unter Verwendung der Spektralanalyse)

Otto-von-Guericke-Universität Magdeburg, 2004

Magdeburg, Univ., Diss., 2004

mojemu Tacie

Danksagung

Die vorliegende Arbeit entstand während meiner Tätigkeit als wissenschaftlicher Mitarbeiter an der Fakultät Elektrotechnik und Informationstechnik, Lehrstuhl für Elektrische Netze und Alternative Elektroenergiequellen (LENA) der Otto-von-Guericke-Universität Magdeburg.

Mein besonderer Dank gilt Herrn Prof. Dr.-Ing. habil. Z. A. Styczynski für die Anregung zu dieser Arbeit und für seine freundliche Unterstützung während der letzten Jahre. Die wertvollen Diskussionen mit ihm gaben mir wichtige Impulse zur meiner fachlichen als auch zur persönlichen Weiterentwicklung.

Herrn Prof. Dr.-Ing. habil. B. Oswald danke ich für die Übernahme des Koreferates und die guten Hinweise, die zur Verbesserung der Qualität dieser Arbeit beigetragen haben.

Für die Übernahme eines weiteren Koreferates und das sowohl meiner Arbeit als auch meiner beruflichen Karriere entgegengebrachte große Interesse möchte ich mich bei Herrn Prof. Dr.-Ing. habil. T. Łobos herzlich bedanken.

Herrn Prof. Dr.-Ing. habil. H. Mecke danke ich für die Übernahme des Vorsitzes der Promotionskommission und Herrn Prof. Dr.-Ing. habil. J. Raisch für seine Mitarbeit in dieser Kommission.

Herrn Prof. Dr. rer. nat. habil. J. Nitsch danke ich für die Leitung der DFG-Forschergruppe, in deren Rahmen diese Arbeit entstanden ist.

Den Kolleginnen und Kollegen am Institut und am Lehrstuhl, vor allem Dr.-Ing. Antje Orths, Dr.-Ing. Mathias Purmann, Dipl.-Ing. Günter Heideck und Dipl.-Ing. Hans-Dieter Musikowski gilt mein besonderer Dank für die anregenden Diskussionen und vor allem für das angenehme Arbeitsklima, das ich während meiner Tätigkeit richtig genossen habe. Weiterhin gilt mein Dank Frau Sarah Thomforde, BA, für die sprachliche Korrektur des englischen Textes.

Den Hilfsassistenten und Diplomanden, insbesondere Herrn Dipl.-Ing. Tobias Wittmann, Herrn Dipl.-Ing. Marco Bierwirth, Herrn Dipl.-Ing. Cezary Dzienis und Herrn Matthias Schulze, die im Rahmen ihrer Arbeiten Beiträge zu dieser Arbeit geleistet haben, sei an dieser Stelle ebenfalls gedankt.

Mein Dank gilt auch der Abteilung Betriebstechnik, Sachgebiet Elektrotechnik des Dezernats Technik und Bauplanung der Universität Magdeburg, welche die Durchführung von Messungen im Universitätsnetz ermöglichte und unterstützte.

Der Deutschen Forschungsgemeinschaft danke ich für die finanzielle Unterstützung.

Einen sehr wichtigen Anteil an meiner Arbeit hat auch meine Frau Andzelika und meine Familie, die mich jederzeit zur Seite gestanden haben.

Erlangen, August 2004 Andrzej Bachry

Acknowledgements

This thesis was completed during my work as a research assistant at the Faculty of Electrical Engineering and Information Technology, Chair for Electric Power Networks and Renewable Energy Sources of the Otto-von-Guericke-University in Magdeburg, Germany.

Foremost I would like to express my deep gratitude to Prof. Dr.-Ing. habil. Z. A. Styczynski for his encouragement to do this work and his ongoing kind support during my stay in Magdeburg. The valuable discussions with him gave me many important impulses that contributed considerably to both my scientific and personal development.

I would like to thank Prof. Dr.-Ing. habil. B. Oswald for being the co-reporter and for his important advice which certainly improved the quality of this work.

I am also very grateful to Prof. Dr.-Ing. habil. T. Łobos for being the second co-reporter and for his interest in this work and his engagement in my professional career.

Moreover, I would like to thank Prof. Dr.-Ing. habil. H. Mecke for accepting the role of Chairman of the Dissertation Commission and Prof. Dr.-Ing. habil. J. Raisch for his work in the Commission.

At this stage, I would like to express my gratitude to Prof. Dr. rer. nat. habil. J. Nitsch, the Leader of the DFG-Research Group in which I was honored to work, for his favorable attitude.

Furthermore, my personal sincere thank goes out to all my colleagues at the Institute of Electric Power Systems and at the Chair LENA, especially to Dr.-Ing. Antje Orths, Dr.-Ing. Mathias Purmann, Dipl.-Ing. Günter Heideck and Dipl.-Ing. Hans-Dieter Musikowski for inspiring discussions and, above all, for the pleasing work environment which I really enjoyed. I thank also Ms. Sarah Thomforde, BA, for her efforts in the corrections and proof of the English text.

I am also much indebted to all my students, especially to Dipl.-Ing. Tobias Wittmann, Dipl.-Ing. Marco Bierwirth, Dipl.-Ing. Cezary Dzienis and Mr. Matthias Schulze, who through their various research projects all contributed to the accomplishment of this work.

Finally, I thank the Abteilung Betriebstechnik, Sachgebiet Elektrotechnik of the Dezernat Technik und Bauplanung of the University in Magdeburg for their support and for giving me the opportunity to carry out the measurements in the University power network.

I would like to thank to Deutsche Forschungsgemeinschaft for financial support.

A very important part of this work goes to my wife Andzelika and my family, who have given me ongoing encouragement, trust and support.

Erlangen, August 2004 Andrzej Bachry

1 INTRODUCTION

The development of technology over the years, especially the progress of power electronics applications, has brought about many technical conveniences and economical profits, but it has simultaneously created new challenges for power system operation studies. Driven by challenging environmental constraints, liberalization of the energy market and privatization of the power supply industry, power systems are more and more often operating at their maximal performance limits - and frequently beyond them - to maximize asset utilization. To avoid serious functional problems from occurring under these conditions, the system's secure and reliable operation needs to be maintained regarding various aspects of power system operation. One of the main topics of special concern is an aspect of wide power quality area which deals with, among others, voltage characteristics, one of which is control and prediction of harmonics and interharmonics [1].

Since the quality of electrical power, e.g. the voltage at the point of common coupling, has become an important feature of consumer goods on the market, the interest in finding, describing and above all, in forecasting system behavior grows continuously. On the one hand, an extensive use of power electronic loads, especially in distribution networks, introduces new inconveniences to proper system operation and demands an analytical method to forecast serious power quality problems before they occur. On the other hand, the development of standards can help to keep the disturbances within the limits which simultaneously influences the proper voltage waveform within the system. Obviously, in standards, the tendency in the setting up compatibility levels, e.g. for the voltage harmonics, shows a direct convergence to the increasing number of harmonic sources.

The facts that conventional power supply systems are designed to operate with sinusoidal waveforms and electric utilities strive to supply customers with reliable power of good "quality" that does not represent a damaging threat to their equipment conflicts with the steep development that the power electronic industry has undergone lately. This incoherent development results in the introduction of appliances that are more sensitive to the quality of power supplied and simultaneously, during their normal operation they introduce distortion to the steady-state current and voltages. These circumstances have set the basis for paying considerable attention to the quality of electrical power, intensely addressing the issue of voltage distortion, a major form of which is harmonic distortion [2].

1.1 AIM AND STRUCTURE OF THE WORK

The aim of this work is to develop a method that combines a qualitative overview study of the distribution power system with the goal of forecasting the most sensitive places to harmonic or interharmonic waveform distortion within it, and to provide a detailed analysis that gives quantitative answers to the distortion at the specific node. The qualitative analysis enables one to get a general outlook of the studied power system from the harmonic and interharmonic point of view. It can be of special interest in cases of widespread systems. In cases of detailed study of harmonic assessment over a power system, this general approach can be used as a first stage of a complete method for determining those nodes of the system to which special attention should be paid during the modeling process. It enables the next stage, the detailed measurement-based modeling with the help of constructed admittance matrices that acquire for the interaction effects between the load and the network.

Since distribution systems are operating nowadays with a high content of power electronic-based equipment that draw distorted currents and cause self-generated interference in the supply voltage, polluting it and propagating the distortion within the system, the need to understand the phenomena is stronger than ever because the damaging effects of harmonics can no longer be ignored [3]. The proper system arrangement avoiding capacitor failure or transformer and neutral conductor overheating demand analytical methods which require proper mathematical models to assure reliable system operation both in existing and in planned distribution systems [4].

The objective of the approaches that up to now have been generally applied to study such issues is the investigation of power quality problems after they have occurred – ‘reactive’ approaches. Therefore, there is a strong demand to introduce a ‘pro-active’ approach which will give the opportunity to predict serious power quality problems before they occur. Moreover, the detailed analysis of the distribution system in which many types of non-linear loads have a big influence on the quality of voltage is very difficult, and it cannot be applied to make a whole overview of the potential problems that can arise. Therefore, it is very important to know in advance how the power system, especially the distribution network, as in case of this work, will behave under distorted conditions: what susceptibility level at which point in the system can be expected.

The structure of a novel method presented in this work can be simplified as presented in Fig. 1.1.

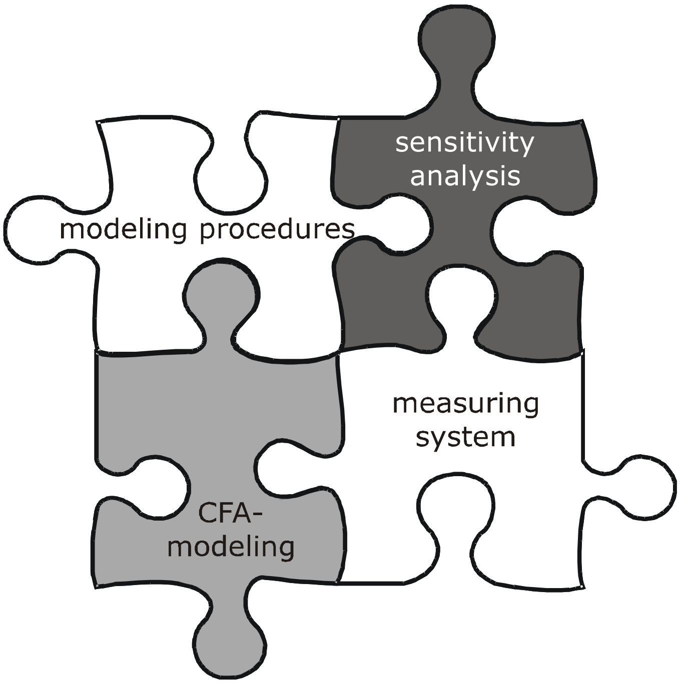

Fig. 1.1 General concept of the method proposed in this work

The method involves the co-operation of the four elements shown. Using the system data the modeling procedure is used in the qualitative sensitivity analysis to provide the information of which nodes in the studied system require special attention. Then, the measurement-based modeling process can be applied for quantitative information of the distortion at those nodes. In this case the information about the disturbing loads must be available. Therefore, the development of a proper measurement system is essential for the method. The system serves not only as a base for power quality surveys, in which the level of disturbances can be measured and therefore the real danger can be recognized, but it is used to acquire the information about distortion directly at clamps of a disturbing load.

Such construction of the proposed hybrid-method is very user friendly since the information is filtered by the sensitivity-step of the method that emphasizes only the places that are the most sensitive to disturbance, i.e. the places at which small changes in the disturbing current injection invoke considerable changes of the voltage distortion level.

Within the text, the work is structured in the following way.

The introductory part of Chapter 2 is devoted to clarify the term *power quality* within the framework of electromagnetic compatibility (EMC) and within the horizon of the political and economical aspects. The second section of the chapter covers the description of actual standards relating the EMC and the power quality (PQ) norm development in the standardization process. The third section is devoted to general classification of the EMC events and regards their implications on the electrical system equipment with respect to steady-state issues. The last, fourth, part of this chapter is devoted to the PQ area itself and concentrates on the classification of sources and effects connected with the low-frequency steady-state disturbances in power systems, like harmonics and interharmonics. This part builds a comprehensive basis for considerations presented in the next chapters of this work.

In Chapter 3 a description of the measurement system developed in the scope of this work to acquire and analyze waveform distortion indices in distribution networks is presented. The measuring instrumentation set-up together with data conditioning and exporting modules of the monitoring system are presented along with the theoretical background used as the basis for the evaluation algorithms that were implemented to the monitoring system.

The first section of Chapter 4 includes a concise review of the modeling and analysis of harmonics in power networks. The second section is devoted to measurement-based methods for the power quality evaluation in distribution networks. At first, in the third section the influence of the network structure on the propagation of harmonics is discussed together with comments on the measurement-based modeling process. Then, a new algorithm for the description of the interaction between the source of waveform distortion (non-linear loads) and the sink (distribution network) is introduced. This modeling approach is based on the description of the non-linear load in harmonic domain with the help of a specially constructed admittance matrix that allows for representing the load-network interaction near the working point of the load with a good exactness.

In the first section of Chapter 5 the mathematical background of the inherent structure theory of the networks is described and the extension of this analysis to the case of power system harmonics is presented. The second section contains the analysis of a power quality survey made in a real distribution system. Exemplary results are described and discussed regarding the network structure. Outgoing from this practical example the nodal admittance matrices of this system are then subjected to sensitivity analysis involving eigenvalue analysis. The measurement and calculation results are then compared and discussed.

2 POWER QUALITY - STATE OF ART

The phenomenon of disturbances caused by power system equipment resulting in a non-ideal waveform of the supply voltage is as old as the power network itself. First considerations made at the end of the 19th century identified transformers and rotating machinery as the main source of the waveform distortion [4]. The development of technology over the years, especially the growth of the use of switched power semiconductor devices has brought about many technical conveniences and economical profits, but on the other hand it has exerted a continual growing influence on the power system's operating conditions. This ever increasing process is stimulated mostly by the way the power system has changed under new challenges imposed by the prescriptions on the energy market introduced by many countries [5]. The resulted thereby growing share of renewable energy sources in power systems increases this process additionally, so that an increasing interest in maintaining of both proper voltage characteristic and continuity of supply can be observed.

Since nonlinear equipment has become a part of the world's directives for energy saving those changes have no alternative and in the coming years it can be expected that most of the loads in distribution systems will have a nonlinear character [6]. Considering the fact that at the distribution level the share of resistive load will decrease due to the above mentioned offensive of the power-electronic-controlled loads the problem of maintaining the proper quality of supply will become more severe than it is today [7]. This is why harmonics, interharmonics and other conducted forms of energy pollution are causing some alarm. Always present in electrical networks, they are now proliferating to epidemic proportions [8]. As a result, new challenges for power system operation studies have been created giving a decisive impulse to the growing interest in the wide power quality area, which is spread from fields relating to the problems of EMC, like emission or compatibility limits and voltage or current characteristics to the traditional power system areas of voltage continuity studies in terms of reliability and availability considerations [9].

To set the scene, in the first section of this chapter the subject of power quality and its placement within the EMC considering standardization work in this area is discussed. In following, a brief description of the main deviations from the ideal waveforms and their effect on power system operation is presented. The next section concentrates on the waveform distortion phenomena in terms of harmonics and interharmonics sources and describes their effects on power systems. The last section is devoted to the costs connected with poor power quality and discusses the dispersed generation influence on the quality of supply in terms of the voltage quality.

2.1 ELECTROMAGNETIC COMPATIBILITY (EMC) AND POWER QUALITY (PQ). DEFINITIONS FOR PQ

Electrical equipment has become increasingly complex in terms of the functions it fulfils and the way it interacts with other electrical equipment. As in the case of electric power systems this interaction takes place through the medium of the electricity network, which is the common source for all the system components. It arises because the power network, intended to transport the electrical energy at one base frequency (50 or 60 Hz) to the consumer, also provides a conduction path interlinking all equipment. As a result of this increasing complexity, some types of electrical equipment today are more sensitive to deviations of the supply voltage. An increasing important feature is the cumulatively disturbing effect of emissions from equipment connected to the network in large numbers and operating simultaneously. Therefore, the consideration of this cumulative effect represents an essential element of emission limiting standardization, in order to meet the protection requirements of the EMC Directive of the European Commission [10].

According to [11] the EMC is defined as: *the ability of a device, equipment or system to function satisfactorily in its electromagnetic environment without introducing intolerable electromagnetic disturbances to anything in that environment*. Therefore, EMC has two major requirements. The first is to ensure that emissions of electromagnetic disturbances are limited to a sufficient degree, and the second is to ensure that equipment has a sufficient level of immunity to maintain adequate performance in the presence of the electromagnetic disturbances to which it is subjected. These requirements concern all electromagnetic disturbances, however a distinction is made between high frequency disturbances, affecting especially equipment having telecommunication or information processing functions, and low frequency disturbances, affecting equipment utilizing energy drawn from electrical power networks in general. Within EMC a distinction is made between radiated disturbances and conducted disturbances. Radiated disturbances are emitted (or transmitted) by one device and received by another device without the need of any conduction. Conducted disturbances need a conductor to transfer from one device to another. These conducted disturbances are within the scope of PQ, radiated disturbances, although also very important, are outside of the normal realm of power system engineering or power quality [12].

Concluding, there is a great deal of ground that is common to both EMC an PQ fields. The phenomena in connection with PQ are also electromagnetic disturbances, the emission of which needs to be limited and immunity from which is necessary for the proper functioning of the equipment [13].

Power quality as such a defined subject was introduced in early 1980`s and the term *power quality* has become one of the most prolific buzzwords in the power industry since the late 1980`s. However, till now there is still a lot of disagreement in the usage of this term, and in how to define it and what it really incorporates. The main objection against the use of this term is that one cannot talk about quality of a physical quantity like power. There are various term used instead of *power quality* [5]. As the first of these the term *voltage quality* can be mentioned. It is used especially in the European publications and is interpreted as a quality of the product delivered by the utility to the customers. A complementary definition to the previous term would be *current quality* concerned with deviations of the current waveform from the ideal one. Thus, where voltage quality has to do with what the utility delivers to the consumer, current quality is concerned with what the consumer takes from the utility. Both are of course strongly related and if either voltage or current deviates from the ideal it is hard for the other to be ideal. The next term: *quality of supply* can be a useful definition as long as one does not want to include customer's responsibilities, because the word *supply* clearly excludes active involvement of the customer. The supplementary term to the latter can be *quality of consumption*, but it is not in common use and therefore of no interest [5]. In standards the term *power quality* has gained some official status, as well. Within the Institute of Electric and Electronic Engineers (IEEE), in the USA, one of the Standards Coordination Committees (SCC), namely the SCC 22 has the name: *Power Quality* [14]. Although, within the documents (standards) of the International Electrotechnical Commission (IEC), the international standards setting organization, the term *power quality* did not appear officially until 2002, when in the draft of the IEC standard [15] the term *power quality* was used for the first time. It should be underlined that the acceptation of the term *power quality* is growing constantly. Judging by the content of the main contributions to this topic in recent years, *power quality* is generally used to express the quality of the voltage [9] and there is increasing acceptability of the latter interpretation, therefore, in this work the term *power quality* will be used in this context, as well.

As far as the *power quality* definitions are concerned, in [3] the authors describe *power quality* as an ultimately consumer-driven issue, giving the end-user the precedence and defining a power quality problem as: *any power problem manifested in voltage, current, or frequency deviations that results in failure or misoperation of customer equipment.* Moreover, the utilities may define power quality as reliability and show statistics that its system is, for example, 99.98 % reliable. Manufacturers of load equipment may define power quality as those characteristic of the power system that enable their equipment to work properly. The characteristics, however, can be very different depending on the criteria.

That is why the international standardization agencies have started to define and categorize power quality related phenomena on power systems. The definition given in the IEEE dictionary [16], which originates in the IEEE Emerald Book [17], describes power quality as *the concept of powering and grounding sensitive equipment in a matter that is suitable to the operation of that equipment*. In 2000 the IEC started its initiative on power quality which resulted in the development of the draft [15] and proposed the following definition of power quality: *Power quality is the set of parameters defining the properties of the power supply as delivered to the user in normal operating conditions in terms of continuity of supply and characteristic of voltage (symmetry, frequency, magnitude and waveform).* This definition created a lot of confusion because of the sudden limitation of power quality to the *normal operating conditions*. As a result, in the draft [15] the definition was changed to: *the characteristics of the electricity at a given point on an electrical system, evaluated against a set of reference technical parameters* (with a note saying that: *these parameters might, in some cases, relate to the compatibility between electricity supplied on a network and the loads connected to that network*). Moreover, in the German version of this draft (published in July 2003) the term *power quality* has been specified as "*Spannungsqualität"* which means, directly translated, *voltage quality*. Concluding, the definition of *power quality* is still a subject of discussion so that the development of the end-definition is a case of the future.

Summarizing the discussion above, it can be stated that however various publications use the term *power quality* with slightly different meanings and other sources use similar but slightly different terminology like *quality of power supply* or *voltage quality*, all these terms have one thing in common: they all deal with the interaction between the utility and the customer, i.e. between the power system and the load, respectively. The emphasis that is placed on this interaction is heightened nowadays, especially considering the fact that the era of information technology and information society brings new challenges to the reliability and quality of electrical supply. This is directly connected to the safety and functionality of the even bigger part of the critical structures in every country. In recent years this case has constantly received growing consideration. Programs like the Proposal for Development and Application of Security, Quality, Reliability, and Availability (SQRA) and Modeling for Optimizing Power System Configurations for the Digital Economy have already been launched in the USA [18]. They set patterns for defining security for strategic management and key elements for managing modern power systems serving an increasingly digital customer base introducing security programs to the critical structures like power systems on the political surface.

Additionally, security will be incorporated into power quality and reliability assessments, into automation and monitoring systems, utilizing measuring, assessing, and benchmarking of the security of electric power systems [18]. Regarding all these aspects a growing demand to develop less-cumbersome methods of the power quality and reliability evaluation can be expected to deal with the critical structures, like electric power systems to assure their secure and reliable operation.

2.2 CLASSIFICATION OF POWER SYSTEM ELECTROMAGNETIC PHENOMENA

The term *power quality* is put to use for a wide variety of electromagnetic phenomena on the power system. Therefore, in this section the classification of EMC events is presented, which is made in relation to the EMC - phenomena [19], [20], [21], [22] to describe a basis for considerations presented in this work.

Generally, as already stated in section 2.1, within EMC a distinction is made between radiated and conducted disturbances. While the conducted disturbances are within the scope of power quality, the radiated disturbances (although very important) are outside the normal realm of power system operation or power quality. The terminology presented in this work reflects the efforts being made on the international level to standardize definitions of power quality terms and categorize the phenomena. The IEC through its liaisons coordinates power quality standardization process together with IEEE SCC 22 and the Congress Internationale des Grand Réseaux Électriques à Haute Tension (CIGRE).

Within the IEC the electromagnetic phenomena are classified into three categories: low-frequency phenomena (<9 kHz), high-frequency phenomena (>9 kHz) and electrostatic discharge (ESD) phenomena [23]. Further, each phenomenon is divided into radiated and conducted disturbances depending on the medium within which they occur, thus building the six principal groups (shown in Fig. 2.1 as grayed ellipses). It is arguable that all of these phenomena can be considered as power quality issues. Therefore, within the power industry it is generally accepted that only the two conducted categories (shown in Fig. 2.1 within a gray rectangle) constitute power quality. The realm of power quality considerations presented in this work concentrates on the steady-state and quasi steady-state phenomena, which according to this classification are placed within the conducted low-frequency phenomena and are indicated in Fig. 2.1 by ellipses with white text. Transients are exempted from this group and belong to other groups according to this classification.

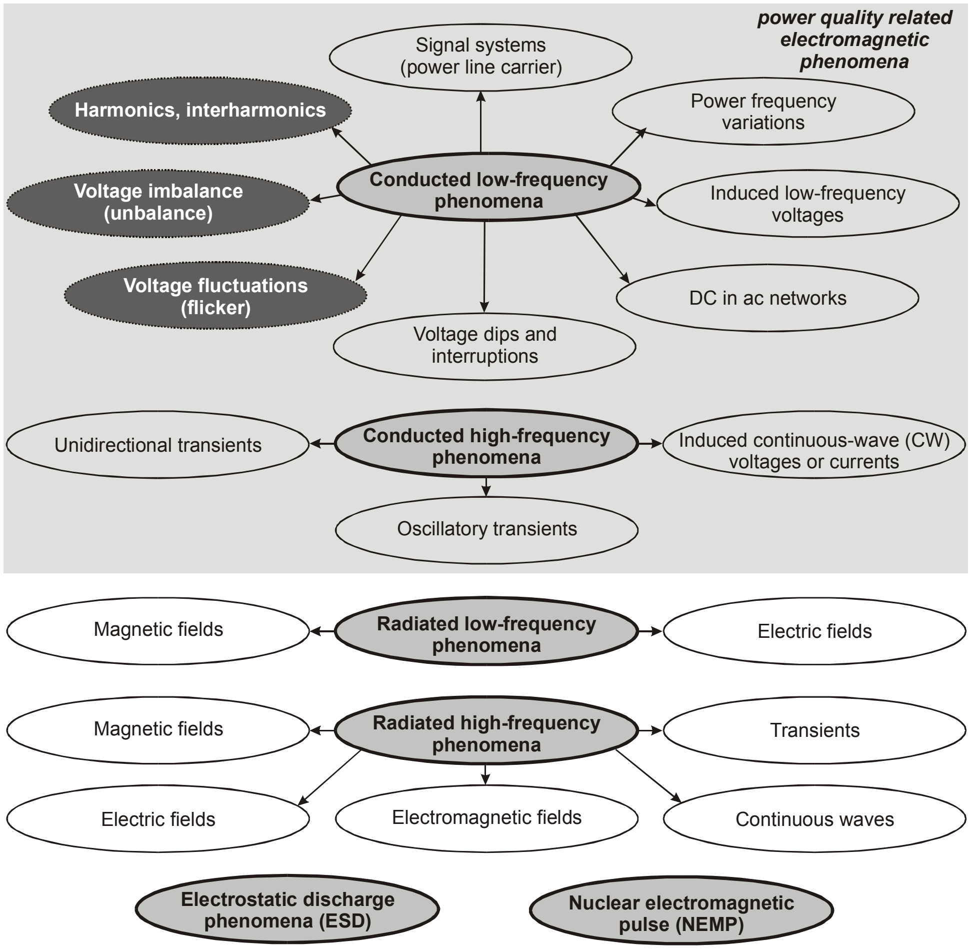

Fig. 2.1 Principal phenomena causing electromagnetic disturbances as classified by the IEC [23] and fields of interest of this work

From the power quality point of view the categorization of the events which are related to the power system area can also be made considering duration of the event as a main factor [24]. Table 2.1 presents the categorization of electromagnetic phenomena as it is used within the power quality community showing some useful comments to the terminology that can differ, especially between the U.S. power quality community and that used in IEC publications. This categorization of events on power systems considers typical physical characteristic of the event regarding spectral contents and amplitude. As far as the described quantity is concerned, all events presented in Table 2.1 describe voltage-based phenomena, so that the contents of Table 2.1 can be regarded as a voltage quality categorization. In this work the steady-state phenomena, which are covered by the group of waveform distortion, are subjected to further considerations. Therefore, within the next sections the steady-state phenomena, especially harmonics and interharmonics, are subjected to detailed considerations, i.e. the problematic of power systems under operating conditions is described and the radiated disturbances are not included in the analysis.

Table 2.1 Categorization of Power System Electromagnetic Phenomena

Duration	*category*	*typical voltage module*	*characterization*
	Transients		
	Impulsive		**IMPULSIVE** transient is unidirectional in polarity and mainly caused by **LIGHTNING**
<50 ns	*Nanosecond* (5 ns rise)		
50 ns - 1 ms	*Microsecond* (1 µs rise)		
>1 ms	*Millisecond* (0.1 ms rise)		
	Oscillatory		**OSCILLATORY** transient is bi-directional in polarity,can be caused by ferroresonance or trafo energization, capacitor bank energization, or a local system response to impusive transient
5 µs	*High frequency* (0.5 - 5 MHz)	0 - 4 pu	
20 µs	*Medium frequency* (5 - 500 kHz)	0 - 8 pu	
0.3 - 50 ms	*Low frequency* (<5 kHz)	0 - 4 pu	
	Short-duration variations (*IEC terminology: Voltage Dips and Interruptions*)		
0.5 - 30 cycles	Instantaneous		**INSTANTANEOUS** phenomena occur at fault conditions, by energization of large loads - like motor starting, by equipment failure or control malfunction
	Interruption	<0.1 pu	
	Sag (IEC: Dip)	0.1 - 0.9 pu	
	Swell	1.1 - 1.8 pu	
30 cycles - 3 s	Momentary		**MOMENTARY and TEMPORARY** phenomena occur by delayed reclosing of the protective device
	Interruption	<0.1 pu	
	Sag (IEC: Dip)	0.1 - 0.9 pu	
	Swell (*called also: momentary overvoltage*)	1.1 - 1.4 pu	**SAG** occurs between the time a fault initiates and the protective device operates
3 s - 1 min	Temporary		
	Interruption	<0.1 pu	**SWELL** occurs by switching off a large load or in unfaulted phases by e.g a single-phase-to-groun fault
	Sag (IEC: Dip)	0.1 - 0.9 pu	
	Swell	1.1 - 1.2 pu	
< 10 s	**Power frequency variations**		occur by faults on bulk power trans-mission systems, or at large source generation going off-line
>1 min	**Long-duration variations**		
	Interruption, sustained	0 pu	
	Undervoltages (*sometimes used: brownout*)	0.8 - 0.9 pu	**UNDERVOLTAGES and OVER-VOLTAGES** are caused by load variations on the system and system switching operations
	Overvoltages	1.1 - 1.2 pu	
Steady state	**Voltage unbalance** (*sometimes used: imbalance*)		**UNBALANCE** results from. e.g blown fuses or load conditions
	Waveform distortion		
	DC offset	0 - 0.1 %	**DC offfset** can be caused by geo-magnetic disturbance or power converters assymetry
	Harmonics (typ. 0 - 50^{th} harm.)	0 - 20 %	**Harmonics and interharmonics** are described in details in further sections
	Interharmonics (0 - 9 kHz)	0 - 2 %	
	Notching		**Notching** is a result of commutation processes in power electronic
	Noise (broadband, 9 - 200 kHz)	0 - 1 %	**Noise** is a result of superimposing of unwanted elctrical signals upon power systems voltage or current
	Voltage fluctuations (<25 Hz) *called also: FLICKER*	0.1 - 7 %	**FLICKER**: Systematic variation of the voltage envelope or a series of random voltage drops

Summarizing, power quality, like quality in other goods and services is difficult to quantify. There are standards for voltage and other technical criteria that may be measured, but the ultimate measure of power quality is determined by performance and productivity of end-user equipment. The framework of standards in the power quality area is the subject of the next section.

2.3 FRAMEWORK OF THE WORLD-WIDE STANDARDS FOR PQ

Since many of the electromagnetic disturbances are generated as a result of the particular way in which some utilization equipment makes use of the supplied energy, limitation of emissions from users' equipment is as vital for PQ as it is for EMC. In fact, it has always been a condition of the contract for electricity supply that the user has to avoid disturbing the network and other users. Thus, meeting the EMC requirements and resulted application of EMC emission standards is very important for power quality. Equally, given the technical as well as the economic reality that power quality can be never ideal, it is important that the EMC immunity standards be implemented, so that the equipment utilizing the electricity supply can continue to operate satisfactorily in the real conditions of the electromagnetic environment, of which the power networks are a significant part [13].

Therefore, the implementation of the EMC Directive [10] is very important for power quality. In the standards reference is often made to *compatibility level* (Fig. 2.2). This EMC term is defined as *the specified electromagnetic disturbance level used as a reference level in a specified environment for co-ordination in the setting of emission and immunity limits* with a note: *by convention, the compatibility level is chosen so that there is only a small probability that it will be exceeded by the actual disturbance level* [11], [25].

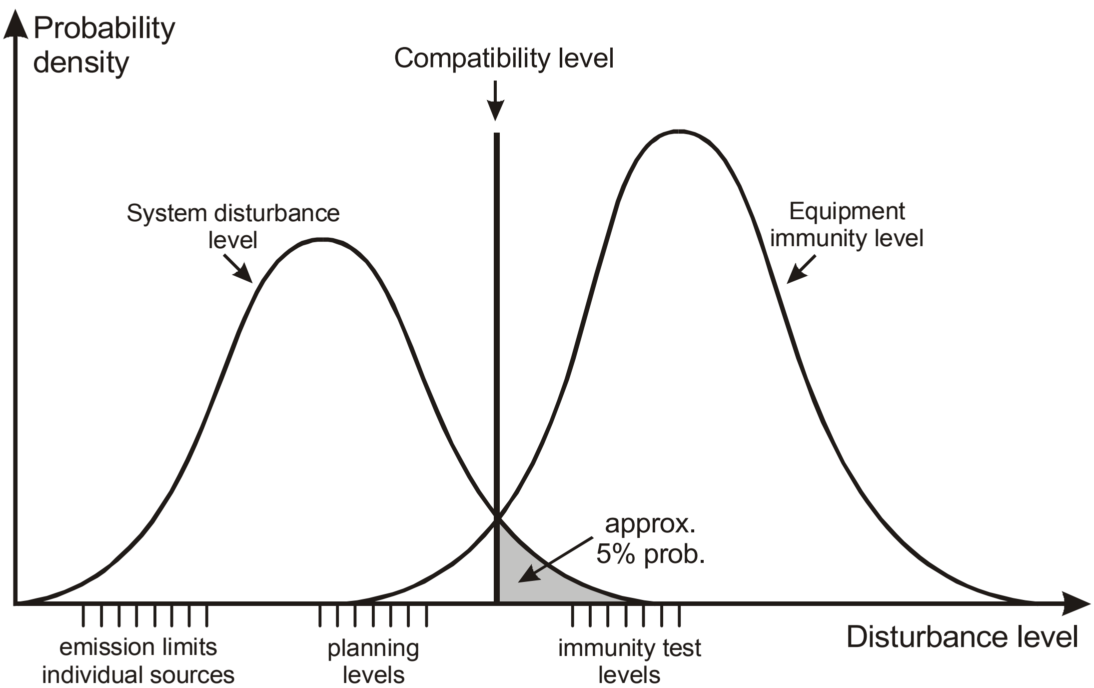

Fig. 2.2 General concept of the electromagnetic compatibility in electrical power networks [26]

Compatibility limits are set by experience in order to give guidance for setting appropriate emission limits and immunity requirements, and are also aimed at the reduction of complaints about mal-operation (both of loads and of system components). By definition, compatibility levels do not represent rigid limits, but are expected to be exceeded with a low probability and only to a small percentage of place.

The significance of this level and its relationship to emission and immunity limits are also a subject of the Annex A to the standard [27] and can be explained by Fig. 2.2. The system disturbance level which arose through the emission of the disturbances underlies to time and place spread because of the fact that the sources of disturbances are statistically overlaid. On the other hand there is also a statistical distribution of the equipment immunity level. Even devices from equal production series can have different immunity levels, moreover, their immunity level can drop in the presence of more than one disturbing phenomena. So the surface below the crossing point of both distribution curves corresponds to the minimum probability of equipment failure. Therefore, compatibility level is generally placed at or near this crossing point driven by the general thought to minimize the costs for the necessary measures to be done at both the system and equipment side. The tendency here is to set the compatibility level at such a level of disturbance which can be expected in the environment, allowing for a small probability (~ 5 %) of its being exceeded (Fig. 2.2).

In relation to *power quality* the compatibility level is intended to represent a measure for the cumulative disturbance level in a given environment, and is expected to be exceeded very rarely. This is why in this work the measured values are compared with compatibility levels. From a power quality perspective, any tendency for the actual cumulative disturbance level to exceed the compatibility level would be that electricity users' equipment would be jeopardized to get degraded in its intended operation by disturbances coming from the electricity networks. Also the networks themselves would be hindered in their function of delivering the electrical energy in form of a voltage with the intended characteristics to the customers. Moreover, the compatibility level is interpreted only as a benchmark for the immunity level, i.e., it is usually specified by the equipment manufacturers without further safety margin. As a replacement for the missing margin each energy supply company specifies its internal planning levels (Fig. 2.2), which serve for network planning and to limit the larger consumers disturbance emissions appropriately. The emission of the mass devices, i.e. individual sources, is limited according to correspondent standards [26].

The development of the standards is an issue which many structures within world-wide electronic and electrotechnical organizations are currently working on. Within this work only the civil standards will be taken into account, military are excluded. The analysis of the standardization process for the latter can be found in [28].

2.3.1 International EMC standards and norms committees

Within the IEC the work related to EMC has been carried out by the International Special Committee on Radio Interference (CISPR), which was set up in 1934 as a joint committee of international organization including the IEC, and later became a special committee under the sponsorship of IEC. The Technical Committee 77 (TC 77) was organized in 1974 as a technical committee of the IEC to deal broadly with electromagnetic compatibility standards. TC 77 and CISPR are technical committees with horizontal functions having responsibility for developing emission limits and measurement requirements to achieve EMC. In general, CISPR is responsible for emissions above 9 kHz, and TC 77 for emissions below 9 kHz. TC 77 has also the responsibility for developing the basic standards for immunity of products. Members of CISPR are the National Committees of the IEC and many international organizations. Important institutions responsible for the standardization work within EMC area and their responsibility fields are shown in Fig. 2.3.

All EMC publications and standards developed by IEC including CISPR and other standardization bodies can broadly be placed in four categories which are shortly presented and described in Table 2.2.

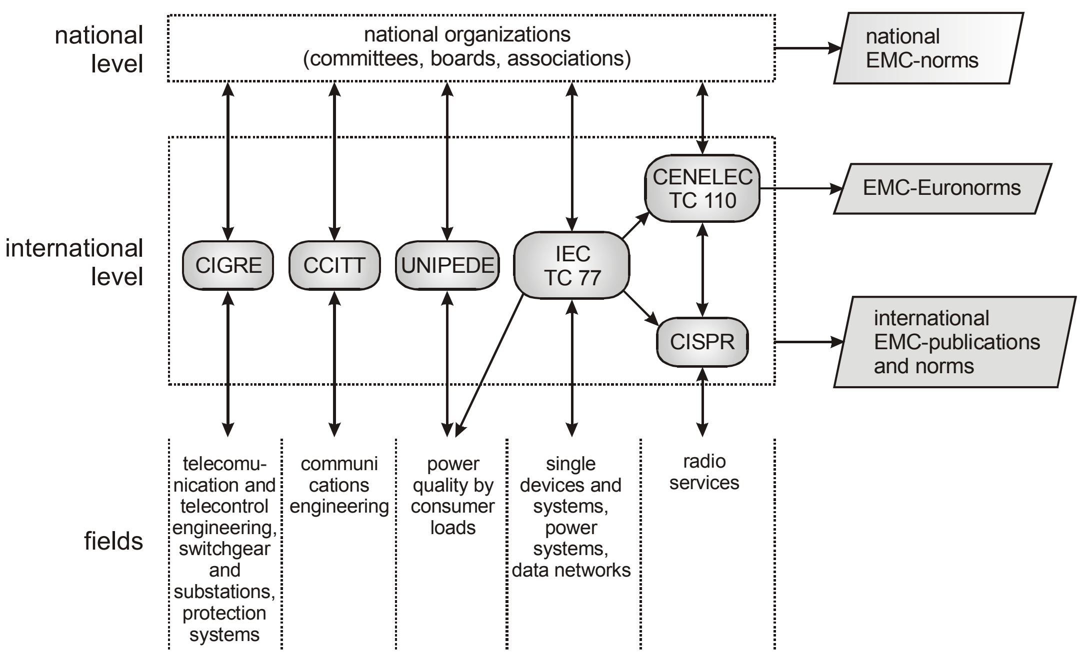

Fig. 2.3 Important institutions responsible for the development of standards in EMC [21]

Table 2.2 Classification of EMC publications and standards within IEC [26]

Type	Contents	Considerations
Basic EMC Publications	may be standards or technical reports; are general and hence not dedicated to specific product families or products; concern: terminology, description of EMC phenomena, specification of compatibility levels, general requirements for the emissions limitation, recommendations for test levels, measuring and testing methods, classification of the environment;	should be identified on the front page by the indication: "BASIC EMC PUBLICATION"; references to it should be included in Generic- and Product-standards;
Generic EMC Standards	specify set of essential requirements, test procedures and generalized performance criteria applicable to product and systems operating in EMC environment, in particular: specify a limited number of essential emission and immunity tests, max. emission levels as well as min. immunity test levels; concern requirements and tests related to emission and immunity;	should be identified on the front page by the indication: "GENERIC EMC STANDARD"; do not include detailed measurement and test methods, but refer for that purpose to the Basic EMC Publications;
Product Family EMC Standards and **Product EMC Standards**	define specific requirements and tests procedures dedicated to particular products and product families; may take either the form of a separate publication or the form of one dedicated clause in a comprehensive Product Family / Product Standard;	should not deviate from the Basic EMC Publications or only in exceptional cases and a justification should be given;

2.3.2 Standards and norms related to steady-state PQ phenomena

Since the early 20th century the electricity suppliers have been in the position to standardize their product - electricity. An ever increasing application of this kind of energy within everyday life has lead to the situation where the customer is used to the safe use of electricity in all fields of private and business life, at any time and with a quality level which allows him or her to operate any kind of electrical equipment with an appropriate reliability [13]. Having recognized the importance of creating a standardization which ensures compatibility between supply networks and customers' electrical equipment connected thereto, within the IEC a framework of EMC standards considering the low frequency conducted disturbances in public distribution power networks is under development. A standard-unification process between international standards organizations is also on the way. The framework of standards for compatibility levels, emission limits, immunity levels and measurement methods for the PQ steady-state related measures, as classified in Table 2.1, is summarized in Table 2.3.

Table 2.3 Framework of IEC standards describing PQ related phenomena

compatibility levels	emission limits	immunity levels	measurement methods
	harmonics and interharmonics		
IEC 61000-2-2 - LV networks and IEC 61000-2-12 for MV networks; IEC 61000-2-4 - for industrial installations at IPC (in plant point of coupling) establishing three classes according to required immunity of equipment;	IEC 61000-3-2 - harmonic current emissions applicable to electrical and electronic equipment having an input current up to and including 16 A per phase, public low-voltage ac distribution systems; IEC 61000-3-12 - draft standard, electrical and electronic equipment with a rated input current exceeding 16 A, up to 75 A per phase, public low-voltage ac distribution systems;	IEC 61000-4-13 proposes different immunity levels in accordance with different performance criteria;	generally, measurement instrumentation is proposed in draft IEC 61000-4-30, detailed prescriptions are defined in IEC 61000-4-7 for testing individual items of equipment related to emission limits given in product standards as well as for the measurement of harmonic currents and voltages in supply systems;
	voltage fluctuations / flicker		
IEC 61000-2-2 for LV networks and IEC 61000-2-12 for MV networks; compatibility levels for flicker also discussed in EN 50160, with P, with P_{lt} lower or equal to 1 during 95% of the time;	for emission, the limits for equipment having an input current up to and including 16 A per phase connected to the LV supply network are given in IEC 61000-3-3; IEC 61000-3-11 for equipment with a rated input current exceeding 16 A, up to 75 A per phase;	IEC 61000-4-14 together with the performance criteria and the immunity measurement method;	IEC 6100-4-14, IEC 61000-4-15 and IEC 60868; analogously in newly issued draft - IEC 61000-4-30;
	unbalance		
IEC 61000-2-2 and IEC 61000-2-12;	--	IEC 61000-4-27 defines the immunity levels of equipment from unbalance;	specified in IEC 61000-4-27 with symmetrical component method; analogously in newly issued draft - IEC 61000-4-30;

As far as the historical development of the compatibility levels within the IEC standards framework is concerned, the newly published standard [27] allows the Total Harmonic Distortion factor (THD) of the voltage to be 11 % for a short period of time, and sets the long-term limit to 8 %, analogously to the previous version of this norm [25], however there were no short-term exceptions. In the first versions of standards, THD was set to only 5 %. This development shows that the trend is to allow for more distortion in the distribution networks in the future. The standards that deal with emission limits in low voltage networks are established only for equipment having an input current up to and including 16 A per phase; for highly rated equipment the limits are still up for discussion. The technical report IEC 61000-3-4 covers the discussion on the limits to such equipment and the draft standard IEC 61000-3-12 is planned to set the limits in public low-voltage systems.

For general power quality assessment the newly issued draft-standard [15] covers all conducted low-frequency phenomena and prescribes respective measurement instrumentation to achieve repetitive and comparable measurement results that allow for the holistic measurement of power quality indices independent of the instrument used and the environmental conditions. It covers all typical steady-state power quality phenomena like harmonics, interharmonics, voltage unbalance as well as the unpredictable ones like surges, sags, spikes, brown-outs and outages. The study of those phenomena is out of realm of this work.

Within the IEEE the standard [29] established limits on harmonic currents and voltages at the point of common coupling (PCC) or at the point of metering. This standard allows for 5 % THD at the distribution system voltage level, a new edition of that will cover also interharmonic limits it is on the way [30].

There also exists a European product standard [31] that describes electrical energy in low voltage and middle voltage supply networks as a whole product, including its drawbacks. This standard defines the main characteristic of the electromagnetic environment as the voltage characteristic at the customer's supply terminals in public distribution systems under normal operating conditions. It takes up the matter of the compatibility levels for the voltages describing the electromagnetic environment as it is now, not as it should be, and not even as it will be in the future [5]. The underlying thought is that the situation will not worsen and that it is up to the utilities to ensure this. The compatibility levels presented in it are only slightly different from those in [27]. The major difference is within the harmonics of order 15th and 21st where according to [31] the limits are set for both orders to 0.5 %, in [27] they are 0.4 % and 0.3 %, respectively.

The limited values are based in every standard on 95 % of the measurement period. As far as the allowance for the remaining 5 % of the time is considered, there is a lot of discussion at the moment, especially regarding the long-term phenomena limits. For example, regarding voltage magnitude requirements, according to the standard 'only' during 95 % of the week the voltage should not exceed the magnitude limits. In the other eight and half hours in this week the voltage magnitude can vary randomly and that will be in compliance with the standards. A bit anxiety is also connected with the fact that for some disturbance phenomena like harmonics severity levels are rising, and therefore a long-term perspective is required [13].

Knowing the standardization aspects of the steady-state power quality phenomena following a detailed characterization of the sources of harmonics and interharmonics and their effect on the power system operation is presented.

2.4 SOURCES OF HARMONICS AND INTERHARMONICS AND THEIR IMPLICATIONS TO THE DISTRIBUTION SYSTEMS

As previously mentioned the first considerations made at the end of the 19th century identified transformers and rotating machinery as the main source of the waveform distortion since they use magnetic materials that are operated very close to - and often in - the non-linear region for economic purposes. However, the development of technology over decades, especially the underlined growth of the use of switched power semiconductor devices has resulted in rapid proliferation of the harmonics and interharmonics within power systems, so that the harmonics introduced by rotating machinery are considered negligible compared to those introduced by power electronic devices. Transformers can in some circumstances inject certain portions of harmonic or interharmonics to the system, but the critical phenomena can be connected with the case of resonance (i.e. ferroresonance) [2].

Harmonics and interharmonics of a waveform can be defined in terms of its spectral components in the quasi-steady state over a range of frequencies. Table 2.4 provides an effective mathematical definition assuming that f_1 is the fundamental frequency of a power system and h is harmonic order:

Table 2.4 Mathematical definitions of waveform in terms of its spectral components

Harmonic	$f = h \cdot f_1$, where h is an integer > 0
Interharmonic	$f \neq h \cdot f_1$, where h is an integer > 0
Sub-harmonic[1]	$f > 0$ Hz and $f < f_1$
dc	$f = 0$ Hz ($f = h \cdot f_1$, where $h = 0$)

For general purposes the *harmonic sources* can be divided into three categories [8]:

1) A large number of distributed non-linear components of small rating (i.e. mass-products), consists mainly of: single phase diode bridge rectifiers, power supply of low voltage appliances (Switch Mode Power Suppliers: SMPS in TV sets, PCs and other IT equipment), and gas discharged lamps.

[1] The term sub-harmonic does not have any official definition and is treated as a special case of interharmonics for frequency components less than the power system frequency f_1. The term has appeared in several references and is in general use in the engineering community so it is mentioned here for completeness. The use of sub-synchronous frequency component is preferred, as it is more descriptive of the phenomena.

2) Large and continuously randomly varying non-linear loads, refers mainly to electric metal-melting arc furnaces with power rating in tens of MW connected directly to the transmission network. The furnace arc impedance is randomly variable and extremely asymmetrical, where the carbon electrodes in contact with steel have dissimilar impedances between the positive and negative flows of current. The same character has resistance welding, where the copper electrodes and the steel being welded have dissimilar impedances between the positive and negative flows of current, and

3) Large static power converters and transmission system level power electronic devices. Static Power Converters are used more extensively for controlling loads. There are many forms of SPC: rectifiers, inverters, cycloconverters, single-phase, three-phase, twelve-pulse, six-pulse, but all have the same character, they are all non-linear, so that they require current from the power system that is non-sinusoidal.

The analysis of power system with large loads 2) and 3) is well described in [4], [8] and the connection of such is mainly subjected to network operator requirements, so that the level of distortion can be obtained analytically. Unlike 2) and 3), the big amount of loads of small rating 1) makes it difficult to analyze its effects directly; therefore it is up to the network structure to ensure the proper operation of those devices in the electromagnetic environment. This demands that the new methods acquire system structure characteristic regarding the effects of potential harmonics- and interharmonic- injecting loads. Currently, a strong trend in decreasing the amount of linear, resistive loads can be observed. Like with the air conditioners which are replaced by the power electronic controlled ones the danger of resonance is increasing. This is why the description of the electromagnetic environment of the power system under normal operating conditions has become an issue recently, and why harmonics, one of several forms of energy pollution, are of special interest.

As far as the *impact of harmonics* on power system equipment is concerned it can be generally stated that harmonics are causing equipment (both in networks and in user’s installations) to be subjected to voltages and currents at frequencies for which it was not designed. The effects of such exposure usually are not instantly visible but can have serious consequences in the medium and long term. Practically speaking, the most important implications of harmonics to the power systems can be summarized as follows:

- derating of network equipment, such as cables and overhead lines, due to additional harmonic currents;

- derating and overheating of transformers, particularly due to saturating effect in the iron core;
- premature aging of network equipment and consumer appliances, due to their unwanted exposure to the excessive harmonic currents or voltages;
- neutral conductor overload, due to cumulative action of currents at harmonic orders of odd multiples of three;
- additional Joule losses in conductors and losses due to eddy currents in transformers;
- stress to the power factor correction capacitors at customer's installations, mostly due to the amplification of the normal operating current by a resonance.

In particular the detrimental effect of certain harmonics can be regarded as follows:

The second harmonic has a tremendous impact on peak voltage asymmetry. One half-cycle has a higher peak voltage than the next half cycle and this effect can be accentuated in the presence of other harmonics [7]. There are many loads sensitive to peak voltage asymmetries. For single-phase and three phase rectifiers with large dc filter capacitors, these devices start injecting dc in response to the 2nd harmonic. The dc is biasing transformers and causes saturation. It causes the voltage zero-crossings to be unequal and disturbs the 6-pulse rectifiers as well [32]. Sources of the 2nd harmonic are e.g.: three-phase half-controlled rectifiers or blasted arc furnaces. However, there are not many field cases reported on annoyances caused by the 2nd harmonic. It is looked upon as a very aggressive harmonic; however its presence in supply voltage is not high, slightly more than 0.5 %. Other even harmonics are very rare, therefore not reported here.

The third harmonic (or triplens, i.e. ninth, fifteen, twenty first, ...) is mainly zero-sequence: It raises the potential of the neutral. It has a much stronger effect on communication lines than the 5th and the 7th, because it loads the neutral conductor causing additional losses in the neutral current path, even when the load is balanced but nonlinear. The third, when zero-sequenced, it is one of the most dangerous ones. When is positive or negative sequenced, it is not as harmful.

The fifth was and still is a predominant component in the harmonic mix observed in the voltage [33]. The world wide measurements campaigns have confirmed its significant appearance at every power system voltage level, documenting its steady increasing level even at the high voltage level (about 2 % on many transmission networks) [13]. Harmonic surveys documented in [13] show a steady increase of the 5th harmonic level over the last three decades. This increase can be estimated as a constant growth of 1 % point over each 10-year period.

The harmonics of order seven, eleven, thirteen are also present in supply voltages. However their levels are lower than the fifth and are oscillating from about 2 % to around 1 %. Their stronger presence is mainly caused by resonance phenomena within a power system. The same goes for harmonics of higher orders.

Interharmonics can be thought of as the inter-modulation of the fundamental and harmonic components of the system with any other frequency components [34]. The basic standard IEC 61000-2-1 defines interharmonics as follows: *Between the harmonics of the power frequency voltage and current, further frequencies can be observed which are not an integer of the fundamental. They can appear as discrete frequencies or as a wide-band spectrum.* Interharmonics are produced by a relatively small subset of power system loads and as such can be viewed as less important. Nevertheless, due to the continual development in the construction of such electronic loads and their increasing penetration in distribution systems interharmonics have also become a growing topic in power quality study [30]. Chief among *interharmonic sources* is a general class of power electronic devices - the static frequency converters. Cycloconverters, a special case of the latter, were introduced in early 1970's and are well-established units in a variety of applications such as rolling mill drives or railroad traction. Another source of interharmonic currents is an arcing load. This includes such loads like arc furnaces or arc welders. The analysis dealing with the measurement of interharmonic currents and their impact on the distribution system is complex [35]. Induction motors with wound rotor using subsynchronous converter cascades or other doubly fed configurations can also be the source of interharmonics. Another group of modern loads that is becoming more popular these days, like ovens, furnaces, die heaters and spot-welders is a source of interharmonics, as well. As a result of such power electronic increases within the power system, interharmonics are becoming an important class of power system phenomena.

The *impact of the interharmonics* of frequencies higher than fundamental system frequency is generally the heating effect caused in the same fashion as with harmonic currents. Additionally, an overload of series tuned filters, communications interference or ripple control and power line carrier interference, and current transformer saturation can be mentioned as further impact to the power system. In frequencies near the fundamental one the lamp flicker is probably the most familiar impact of interharmonics to power system operation. But the interharmonics that excite torsional oscillations in turbo-generator shafts can be a significant one, representing the greatest potential financial impact [30].

2.5 OTHER ASPECTS

The quality of electrical power has become a very important feature of consumer goods on the market. European Directive [36] calls for electricity to be considered a product like any other and its producer, the electrical utility, to be liable for the quality of its electricity - the power quality. With the electric industry undergoing change, increased attention is being focused on power quality in terms of its continuity and voltage quality and also in terms of costs connected with maintaining power quality.

There is strong discussion about the costs that result from poor power quality. These additional costs are mainly generated due to the two main reasons: voltage uncontinuity, i.e. supply interruptions > 3 min, and voltage quality, i.e. harmonics and other voltage quality events [37]. Excluding costs for the voltage uncontinuity (outages), which can be estimated at about 150 billion $ in the USA [18], the costs of poor power quality are estimated at the level of about 20 to 30 billion € within the European Union and at 40 billion $ in the USA, each year [37]. Much of the costs are due to the heating effect caused by harmonics. In Germany, it is estimated that about 0.8 % of the electricity bill is due to additional Joule losses caused by harmonics [38]. This subject will not be directly broadened in this work, although there exists a strong connection to the method presented in the next chapters concerning the economical aspects of the method. Summarizing, the tendency is clear that in the future, some utility companies may impose a penalty for users producing harmonics, or may charge for better power quality.

Switched power semiconductor devices are used extensively in the renewables grid connecting equipment, which greatly influence the distribution system's normal operating conditions and cause self-generated interference. Together with the development of distributed energy sources, like wind power plants, the generated power is not as 'clean' as it used to be. Interaction between the connected load and the facility electrical systems with an ever growing part of distributed weather dependent and electronically controlled energy producers and the impact of loads with adverse electrical characteristics will account for more and more power quality problems [3].

Some of the power quality aspects of the distribution network with a large share of renewables, namely the voltage band and voltage controllability, were subjects of a German national research project EDISon[2]. Within the project models of renewable energy sources have been developed and used for simulation in distribution networks [39], [40]. Several cases were carried out to study the behavior

[2] The project EDISon (Electricity Distribution Integrating Systems of New Generation, Storage and Coupling Technologies and Using Advanced Information and Communication Systems for the Dispatch) was founded by the Federal Ministry for Economy and Technology in Germany.

of renewables in the network and simultaneously to analyze the impact of distributed generation on power system operation [41]. It was discovered that the appropriate usage of communication systems to control the renewables like fuel cell units, combined heat and power units, middle-voltage coupling units and battery storage can provide advantages not only to voltage quality but also increase the security and efficiency, especially of large distribution grids [42]. Some other aspects of the presence of renewables as voltage ride-through and voltage control were analyzed as well. A new power system planing tool including the above mentioned models for networks with presence of dispersed generation was developed and studied in [43].

However, the increasing presence of dispersed generation in power networks presents challenges which in turn increase pressure on the existing power network equipment to conform to the EMC and PQ standards to assure reliable and secure operation at even more sophisticated supply structures. Nevertheless, to draw conclusions on power quality in a distribution system, extensive measurements are indispensable to erect a basis for extended analytical case studies within power systems.

3 POWER QUALITY MONITORING SYSTEM FOR DISTRIBUTION NETWORKS

This chapter describes a power quality monitoring system which was developed to acquire and analyze waveform distortion indices in distribution networks. The measuring instrumentation set-up together with data conditioning and exporting modules of the monitoring system are presented in the first part of the chapter. The next section includes a description of the evaluation modules, where major measures relating to the PQ monitoring are introduced with respect to the norms and standards that were presented in the previous chapter. The last section covers the theoretical background used as the basis of the power evaluation algorithm that was implemented as an external module of the monitoring system.

3.1 GENERAL CONCEPT OF THE MONITORING SYSTEM

Waveform distortion and voltage unbalance have become very important factors that essentially decrease the efficiency of both power supply systems and the consumers connected to them. Direct measurement in the network nodes is required in order to get valid information on these power quality indices. Many surveys have shown that most customer power quality problems originate within the customer facility [3], [8], [13]. It is clear that monitoring is essential for both power suppliers and users to ensure optimal power system performance and effective energy management. Moreover, it provides information about power flow and demand and helps to identify the cause of power system disturbances.

A measurement system was developed to gain knowledge about long-term power quality behavior within a studied distribution power system. The system was used to acquire the load data within the distribution system and, above all, to gather the practical information which was then used to compare it with the analytical considerations presented in Chapter 5. Beside the possibility to make long-term power quality surveys within the power system, additional modules were also developed and integrated in the structure of the monitoring system (Fig. 3.1). An additional module allows for short-term emission measurements directly at the clamps of disturbing loads. Moreover, export of raw-data in predefined formats is possible using the *exporting module* (Fig. 3.1), so that a later analysis using external software can be made. A *power resolution module* can be used to perform power calculations at the cross-section of disturbing loads utilizing data exported in ASCII-format. Within the integrated graphical user interface (GUI) on-site presentation of the measurement results and their analysis can be performed as well.

Such a structure as the developed monitoring system enables one to study both the behavior of the system in a long-term perspective, i.e. observing and comparing trends of the PQ indices over a long period of time, and to also measure and analyze power quality problems that arise at the cross-section of disturbing loads or at the connection point of renewables. A synthesis of these types of information is possible within the monitoring system using an unified information exchange interface between the system components, dented as arrows in Fig. 3.1. Such a synthesis is essential for analysis and evaluation of the power quality related problems.

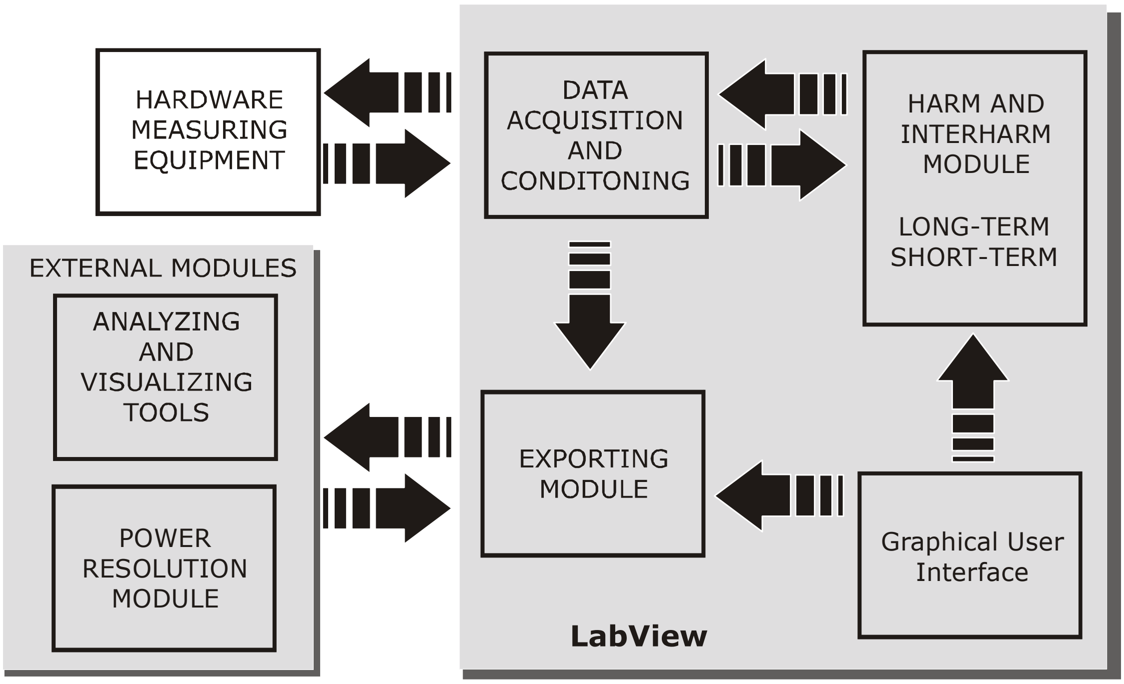

Fig. 3.1 Power quality monitoring system - general scheme

The integration of the above mentioned goals in one power-quality-monitoring-system is realized based on the program-system LabView®, which consists of a good user interface, a graphical programming structure and a wide driver library. Therefore, it is predestinated for integrating many composite tasks that makes the usage of multiple hardware instruments necessary and need a flexibility within wide data gathering procedures. However, some task involving matrix calculation procedures or power calculations have been realized outside the LabView environment, being integrated directly in Matlab®, or evaluated in MS Excel®. Besides extending the system flexibility this solution enables one to use the optimal software platform, which is dedicated for definite tasks, like Matlab for matrix operations. The menu tree of the system is presented in Fig. 3.2.

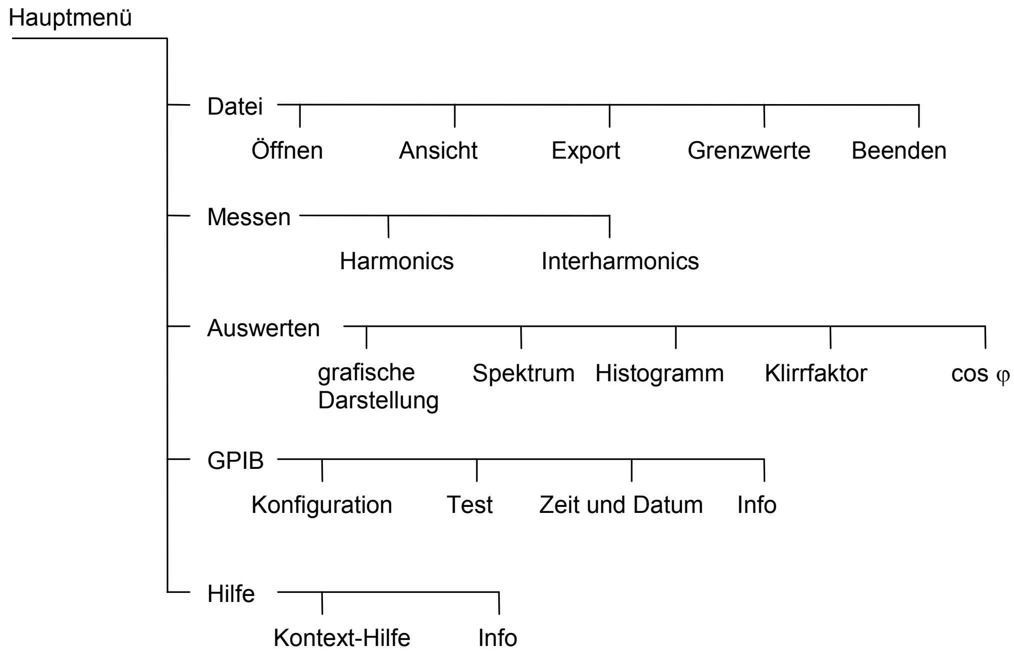

Fig. 3.2 The menu-tree of the measurement system [44]

During an on-site analysis measurement results are evaluated and visualized internally (Auswerten, Fig. 3.2) within the LabView environment. The analyzed measurement data can be both displayed on the screen of the measurement system (Fig. 3.3) or exported as graphical data so that they can be used by establishing a measurement protocol.

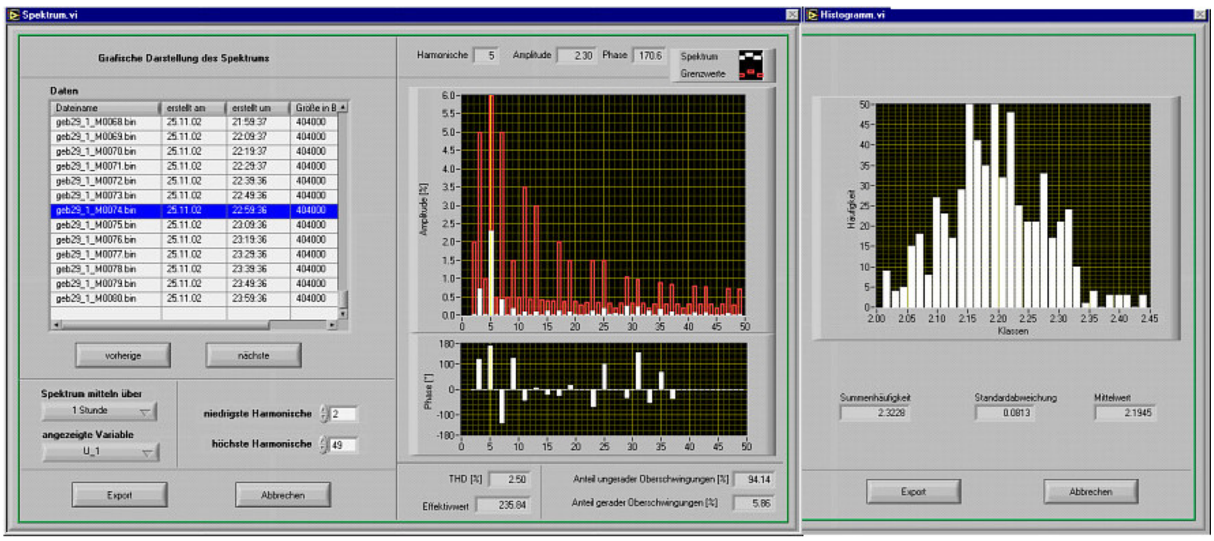

Fig. 3.3 Exemplary result window and a statistical analysis window

The next sections of this chapter are devoted to the detailed description of the modules of the developed monitoring system from Fig. 3.1.

3.2 DATA ACQUISITION, CONDITIONING AND EXPORTING MODULES. MEASUREMENT INSTRUMENTATION

To acquire the information about power quality at a network node or at clamps of a disturbing load a lot of information has to be captured and processed. It is therefore necessary to properly manage the data, so that low-time-consuming and standard-related evaluation can be optimally made for both cases. For that, within the LabView environment, a software-supported data acquisition module (Fig. 3.1) has been developed utilizing two different hardware solutions. They were adopted to function on the common software platform, so that a flexible, automatic and software-controlled collection of the measuring data is possible. The *data acquisition and conditioning module* (Fig. 3.1) covers a software interface that communicates with both hardware instruments used for long-term power quality monitoring and short-term measurements at the cross-section between disturbing load and power supply, respectively. The interface makes the conditioning of the acquired data in order to achieve a standardized output data format that is then utilized by other modules of the system from Fig. 3.1.

General requirements regarding the instrumentation intended for the measurement of harmonic currents and voltages in supply systems as well as for testing individual items of equipment related to emission limits are given in standard [45] which expires at the end of October 2005 and are treated the same way in its newest version [46]. The general structure of the instrument is based on the use of the Discrete Fourier Transform (DFT) through its implementation algorithm Fast Fourier Transform (FFT) technique[1]. The instrument is comprised of an input circuitry with an anti-aliasing filter, an A/D converter including sample-and-hold unit, a DFT-processor providing the Fourier coefficients and is complemented by the external parts devoted to current assessment and/or voltage assessment. For determining the coefficients synchronous sampling and an employment of a rectangular window are described in the standard [46]. Other waveform processing techniques are not included there, they shall, however, state the same range of uncertainty as for the described DFT method.

[1] Generally, the Fourier analysis is used to convert time domain waveforms into their frequency components and vice-versa [47]. The Fourier series represents the special case of the Fourier Transform (FT) applied to a periodical signal [48], [49]. In practice, data are often available in the form of sampled time function, represented by a time series of amplitudes, separated by fixed time intervals of limited duration. When dealing with such data a modification of the FT, namely the DFT is applied. The implementation of DFT, by means of the FFT algorithm [50] forms the basis of spectral and harmonic measurement systems and is therefore integrated in the hardware of a modern data acquisition system.

As far as the other techniques for obtaining the complete frequency spectrum of periodic and non-periodic voltage and current waveform are concerned, the usage of wavelets [51], neural networks [52], fuzzy logic [53] or other advanced signal processing methods are also of interest [54], [55]. Since the development of a norm-based measuring system was the goal of this work, the other methods have not been implemented, so that the monitoring system employs FFT with the rectangular window during data pre-processing, as it is described in the standard [46]. However, an extension of the system to include all or some of above mentioned method can be an interesting scientific and engineering task for future investigations.

For *long term measurements* in power quality surveys the LEM Wide Band Power Analyzer System NORMA D6200 [56] equipped with high-accuracy current probes and voltage grips was used for the data acquisition. The developed data acquisition and conditioning module is used in this case to control the data flow and to set-up the internal instrument settings at the beginning of the survey in order to acquire conformity with the standard. The communication between software and hardware is made via IEEE-488.2 interface (GPIB). Moreover, a user friendly interface has been created to help with the set-up of the measurement. The usage of this instrument allows one to capture the voltage direct at the low voltage side of the transformers, i.e. at 230/400 V. The currents can be captured using current probes that measure current ranging from 5 to 1000 A. In cases of large cross-sections like bus-bars, Rogowski-coils are used, but with less accuracy.

The total measurement error of such a system configuration is composed from the error introduced by the voltage and current probes used, the error of the data acquisition system and the error in the signal processing units. Table 3.1 summarizes the technical data of the system and considers the measurement accuracy.

Due to the fact that in the new standard [46] the length of the analysis window was changed to 200 ms, new technical requirements to the data acquisition system were imposed. Since the instrument LEM NORMA turned out to be inflexible and therefore unable to handle this change, a new hardware solution had to be introduced to the measurement system - a data acquisition card NI-6120 [57] was implemented. The technical features of the card make the implementation of the new guidelines possible. Together with changes made within the program the possibility to perform *short-term measurements* at clamps of disturbing loads was also introduced. The updated program includes the newly defined measuring window and new data evaluating procedures and utilizes analogous user-interface, having comparable measurement uncertainty.

Table 3.1 Technical specifications and measurement accuracy

Voltage channel		*Current* channel with jaws	
max. input voltage	1500 V (rms)	input range	5 A .. 1000 A
input impedance	10 MΩ	transformation ratio	1000 A / 1 V
A/D resolution	16 bit	A/D resolution	16 bit
frequency range	0 Hz .. 1 MHz	frequency range	10 Hz .. 30 kHz
sampling rate	35 kS/s .. 70 kS/s	sampling rate	35 kS/s .. 70 kS/s
accuracy 50 Hz .. 1 kHz	± (0.05 % of the measured value (mv) + 0.01 % of the measured range (mr))	accuracy 50 Hz, 5 kHz	± 0.2 %, ± 0.4%
type of connection	4 mm secure slide-on receptacle	max. cross-section of the conductor	54 mm
accuracy of the DFT module		± 0.02 %	
additional error of FTT (adverse conditions, i.e. loss of synchronization)		± (0.6 % of mv + 0.1 % of mr)	
accuracy of IEEE-488.2 interface (GPIB)		± 0.15 % of mv	
typical accuracy at frequencies below 2 kHz (VOLTAGE)	~ ±0.2 % of mv	typical accuracy at frequencies below 2 kHz (CURRENT)	~ ±1 % of mv by Rogowski coil: ~ ±2 % of mv

The data *exporting module* prepares the raw data and/or the processed data into a suitable form that can be accepted by one of the standard software programs (e.g. Matlab or MS Excel or Origin®). The advantage of such a monitoring system construction lies in its flexibility in data exchange. This enables the sub-tasks, like the calculation of power or visualization of chosen measurement results, to be completed utilizing standard software. Therefore, such a module broadens the possibilities of the measurement data utilization and that, in turn, enables one to take full advantage of such a constructed monitoring system.

3.3 HARM AND INTERHARM MODULES. BASIC MEASURES FOR HARMONICS AND INTERHARMONICS ASSESSMENT

The data processing within the harm and interharm modules of the monitoring system from Fig. 3.1 is made according to norm guidelines utilizing the basic measures calculated using measurement data prepared in the appropriate way. The implemented algorithm utilizes theoretical background that defines the indices for harmonic and interharmonic distortion with respect to the new measurement guidelines introduced in [46]. Below, a comprehensive description of the main measures, as proposed in the international standards is presented with respect to the harmonic and interharmonics distortion as implemented into the developed harm and interharm modules of the monitoring system.

There are several measures, which define the most common indication of the presence of harmonics. The first is *Total Harmonic Distortion* (THD) which can be calculated for either voltage or current, and for the voltage can be defined as in (3-1):

$$THD = \sqrt{\sum_{n=2}^{H} \left(\frac{U_n}{U_1} \right)^2} , \tag{3-1}$$

where: U_n is the root mean square (rms) value of the harmonic component of order n of the voltage, U_1 is the rms value of the fundamental component of the voltage [27]. In some publications the THD for the voltage is often noted as $THDu$, or in American nomenclature $THDv$. The definition (3-1) is in accordance with IEEE standard [29] and with the definition used in the European product standard for the voltage characterization [31], as well. However, the value of H - being the maximal order of harmonic that is taken into account during the calculation of this quantity - is defined in each standard differently. In [29] and [31] H it is set to be equal to 40, in the [27] H is defined to be, generally 50, but can also be 25 in cases of low risk of resonance at higher orders. It is also possible to calculate THD for the current ($THDi$), but in this case it is worthwhile to point out that $THDi$ would refer to the present value of the fundamental frequency current, which may sometimes be misleading that small current, which has high $THDi$, is dangerous. To avoid this in [29] the calculation of $THDi$ referring to the fundamental of the peak-demand current rather than the fundamental of the present sample has been proposed. In this way calculated quantity (3-2) is called *Total Demand Distortion* or simply TDD:

$$TDD = \frac{\sqrt{\sum_{n=2}^{H} I_n^2}}{I_L} , \tag{3-2}$$

where: I_n is the magnitude of individual harmonic components (rms) and I_L is the maximum demand load current at fundamental frequency (rms). The limits of TDD are based on the I_{sc}/I_L ratio, where I_{sc} is the short-circuit current at the point of common coupling (PCC) between the customer (load) and the utility (power supply).

THD is the measure of the effective value of the harmonic components of a waveform, in other words, the potential heating value of whole harmonics in relation to the fundamental frequency. It is, therefore, a very useful quantity for many applications. It provides a practical estimation of how much extra heat will be realized when a distorted voltage is applied across the resistive load, and it gives an indication of the additional losses caused by the current flowing through the conductor. However, since the voltage stress within a capacitor is related to the peak value not to the heating value of the voltage waveform, the THD can not be a good intimation in such cases. Hence, two other quantities utilizing weighting principle were proposed to evaluate the additional thermal impact of harmonic voltages on capacitors working without burden and on inductive elements like windings, induction motors, etc. [45].

As previously underlined, the newly issued international standard [46] introduces a set of several measures that are calculated with a new resolution, which enables the interharmonics to be treated separately from harmonics. The basic idea is that the measurements should be made within a 200 ms time window, which means that in the scope of this standard the time window has a width of 10 (for a 50 Hz system) or 12 (for a 60 Hz system) fundamental periods. The sampled data are then subjected to the DFT or, in general, to its smarter version FFT, which results in a 5 Hz resolution of FFT-bins at the output of the FFT processor. These bins are then subjected to a grouping and smoothing procedure. The task of the first procedure is to properly give back the spectral energy of the measured signal, dividing it into harmonic and interharmonic components. The second procedure is employed during long-term measurement to acquire long-term compliance with limits and is realized by statistical handling of the data according to the relevant standard, e.g. such as IEC 61000-3-2.

The grouping procedures that are recommended in standard [46] are comprehensively shown in Fig. 3.4 and Fig. 3.5 regarding the building process of the groups and subgroups of harmonics and interharmonics, respectively.

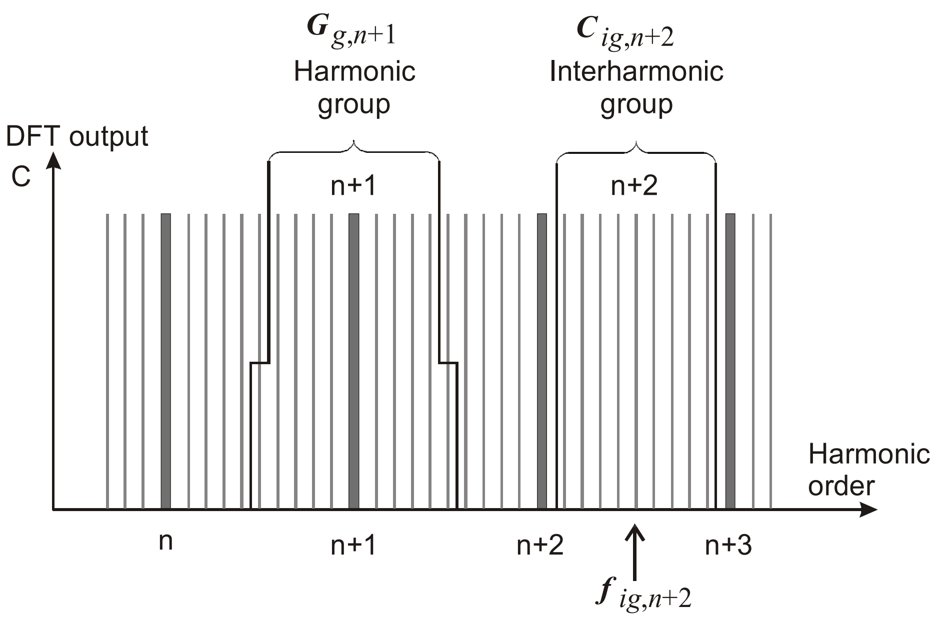

Fig. 3.4 Grouping of DFT-bins into the harmonics and interharmonics groups [46]

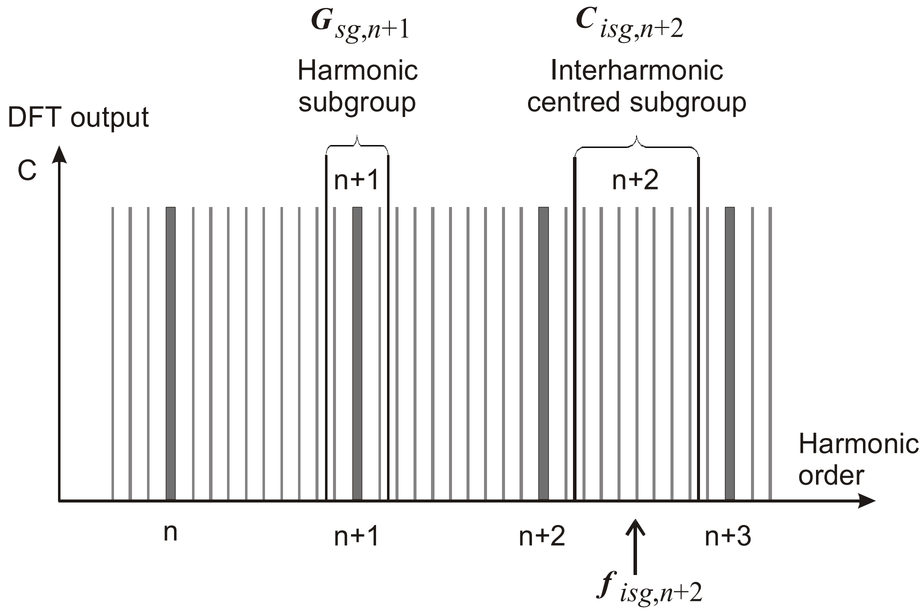

Fig. 3.5 Grouping of DFT-bins into the harmonics and interharmonics subgroups [46]

In Fig. 3.4 $G_{g,n}$ represents the effective value of a harmonic group (3-3):

$$G_{g,n} = \sqrt{\frac{C_{k-5}^2}{2} + \sum_{i=-4}^{4} C_{k+i}^2 + \frac{C_{k+5}^2}{2}}\ , \tag{3-3}$$

where C_k is a rms value of a spectral component corresponding to an output bin, k and i being running-integer numbers. By analogy, the rms value of an interharmonic group (3-4) at the frequency $f_{ig,n}$ (Fig. 3.4) can be defined:

$$C_{ig,n} = \sqrt{\sum_{i=1}^{9} C_{k+i}^2}\ . \tag{3-4}$$

However, the two measures above should not be used together because harmonic groups $G_{g,n}$ include all of the energy of the measured signal, and its presentation together with interharmonic groups $C_{ig,n}$ will lead to misunderstandings resulting from the overestimation of the energy included in the measured signal. On the contrary, Fig. 3.5 shows that sub-grouping procedure should be made simultaneously for harmonics and interharmonics to fully represent the frequency spectrum of the signal. The rms value of a harmonic subgroup (3-5) is defined:

$$G_{sg,n} = \sqrt{\sum_{i=-1}^{1} C_{k+i}^2}\ , \tag{3-5}$$

and, correspondingly, the rms value of an interharmonic subgroup (3-6) at the frequency $f_{isg,n}$ (Fig. 3.5):

$$C_{isg,n} = \sqrt{\sum_{i=2}^{8} C_{k+i}^2} \,. \tag{3-6}$$

In compliance with the above mentioned grouping methods the following measures have been integrated into the harm and interharm modules of the monitoring system according to the definition proposed in [46]. The first measure is *Total Harmonic Distortion* (THD) (3-7):

$$THD = \sqrt{\sum_{n=2}^{H} \left(\frac{G_n}{G_1} \right)^2} \,, \tag{3-7}$$

where G_n is the effective value of a harmonic component being identical with the rms value of a spectral component C_k .This measure is identical with that presented in (3-1), but here it is defined as a single bin coming from the FFT processor precisely at the frequency which is an integer multiplication of the fundamental frequency. The next measure is called *Group Total Harmonic Distortion* ($THDG$) (3-8):

$$THDG = \sqrt{\sum_{n=2}^{H} \left(\frac{G_{g,n}}{G_{g,1}} \right)^2} \,, \tag{3-8}$$

and, consequently, the *Subgroup Total Harmonic Distortion* ($THDS$) (3-9):

$$THDS = \sqrt{\sum_{n=2}^{H} \left(\frac{G_{sg,n}}{G_{sg,1}} \right)^2} \,, \tag{3-9}$$

Next, the *Partial Weighted Harmonic Distortion* factor ($PWHD$) (3-10) is introduced:

$$PWHD = \sqrt{\sum_{n=Hmin}^{Hmax} \left(\frac{G_n}{G_1} \right)^2} \,. \tag{3-10}$$

However, in the standard [27] additional measures in the presence of interharmonics are proposed which partially overlap [35] definitions described in [46]. The *Total Distortion Content* (TDC) (3-11) has been defined as:

$$TDC = \sqrt{Q^2 - Q_1^2} \,, \tag{3-11}$$

where Q is the total rms value for either current or voltage and Q_1 is the rms value of the corresponding fundamental component[2]. As a relation of TDC to the respective fundamental component the *Total Distortion Relation* (TDR) (3-12) has been introduced as well:

[2] Original notation from the standard has been maintained.

$$TDR = \frac{TDC}{Q_1} = \frac{\sqrt{Q^2 - Q_1^2}}{Q_1}. \tag{3-12}$$

For practical purposes several indices are also defined which are specific to the type of equipment being affected by harmonics. The *K - factor* is used to describe the impact of harmonics on losses in power system equipment and is often used in de-rating of equipment, e.g. to dimension the transformers which are intended to work in connection with harmonic-producing equipment [29]. The *Telephone Influence Factor* (*TIF*) is a measure describing the telephone noise that originates from harmonic current and voltages in power systems. The *psophometric current* weighting system is used in the EU[3] to provide a reasonable indication of the interference from each harmonic, taking into account the response of the telephone equipment and the sensitivity of the human ear [58]. The practical considerations dealing with the usage of these indices are discussed in the works [59], [60] and [61], where the EMC studies of a real voltage booster system for railway power systems have been made.

3.4 POWER RESOLUTION MODULE. DEFINITIONS OF POWER COMPONENTS UNDER NON-SINUSOIDAL CONDITIONS

The harmonic pollution in distribution systems affects the power properties of such circuits. The power definitions under non-sinusoidal conditions are widely discussed [62], [63], [64] and quite a lot literature which has been published dealing with power definitions [65], [66]. Some of the works were focused on how to figure out the power in some cases based on simulations and measurements using selected approaches and definitions [67].

During construction of the monitoring system, the main methods of power resolution were chosen and implemented in the external evaluation module of the system (Fig. 3.1) to investigate the usefulness of each method in the scope of its practical implementation. This chapter presents the theoretical background of the methods implemented into the *power resolution module* of the monitoring system.

The first method is that of Budeanu [68] which was developed in the early 20th century and is still the best known and the most popular method in industry. The next one is that of Czarnecki [69], which builds upon the work introduced by Fryze [70] and the last one is that of the IEEE Working Group [71] which was developed mainly with contributions done in the works of Filipski [72] and Emmanuel [73]. All of these approaches are eligible to implement their algorithms into the power quality measurement and evaluation system and in the following section the theoretical background of these three approaches will be presented.

[3] For similar purposes in the USA *C-Message index* is used.

3.4.1 Basic power definitions and Budeanu reactive power definitions

For the algorithm used in the power resolution module, it is useful to represent the harmonic voltage (3-13) and current (3-14) measured at a cross-section as complex, rms-scaled, time dependent quantities which are formed by summing the constituent n-th order time-dependent complex, root-mean-square scaled quantities over the harmonic range:

$$\underline{U}_n(t) = U_n \cdot e^{j(n\omega_1 t + \alpha_n)} = \underline{U}_n \cdot e^{jn\omega_1 t}\,, \tag{3-13}$$

$$\underline{I}_n(t) = I_n \cdot e^{j(n\omega_1 t + \beta_n)} = \underline{I}_n \cdot e^{jn\omega_1 t}\,. \tag{3-14}$$

The complex $\underline{U}_n$ and $\underline{I}_n$ represent the n-th order harmonic phasor values of voltage and current, with α_n and β_n being the phase angles of the voltage and current harmonics, respectively.

In practice (3-15) and (3-16) represent the general form of the measurable time dependent quantities for voltage and current[4], respectively [67]:

$$u(t) = \sqrt{2}\,\boldsymbol{Re}\left\{\sum_n \underline{U}_n(t)\right\}, \tag{3-15}$$

$$i(t) = \sqrt{2}\,\boldsymbol{Re}\left\{\sum_n \underline{I}_n(t)\right\}. \tag{3-16}$$

The total time-dependent *real power* (at all harmonic orders) at a measuring cross-section (3-17) can be defined:

$$p(t) = \sum_n \sqrt{2}\,\boldsymbol{Re}\{\,\underline{U}_n(t)\,\} \cdot \sqrt{2}\,\boldsymbol{Re}\{\,\underline{I}_n(t)\,\}. \tag{3-17}$$

When substituting in (3-17) for $\underline{U}_n(t)$ and $\underline{I}_n(t)$ from (3-13) and (3-14) and after a manipulation the expression (3-18) is obtained:

$$p(t) = \sum_n \left[U_n \cdot I_n \cdot \boldsymbol{sin}(2n\omega_1 t) \cdot \boldsymbol{sin}\,\varphi_n + U_n \cdot I_n \cdot (1 + \boldsymbol{cos}(2n\omega_1 t)) \cdot \boldsymbol{cos}\,\varphi_n\right]. \tag{3-18}$$

Integrating of (3-18) over the fundamental period yields (3-19):

$$P = \sum_n U_n \cdot I_n \cdot \boldsymbol{cos}\,\varphi_n\,, \tag{3-19}$$

[4] The scalars (and physically measurable) time-dependent voltage $u(t)$ and current $i(t)$ are denoted in some European countries as an imaginary part of the complex quantities, so that in equations (3-15) and (3-16) instead of operator Re the Im is used. This is a subject of a convention and in this work the notation proposed in (3-15) and (3-16) is used.

which is an average power or *active power* over all the considered harmonic orders, with $\varphi_n = \alpha_n - \beta_n$. According to Budeanu the instantaneous imaginary power (3-20) is defined as the power which is in quadrature to the real power (3-17), i.e.:

$$q(t) = \sum_n \sqrt{2}\,\boldsymbol{Re}\{\,\underline{U}_n(t)\,\} \cdot \sqrt{2}\,\boldsymbol{Im}\left\{\underline{I}_n(t)^*\right\}, \tag{3-20}$$

where the asterisk denotes a vector of the conjugate values. Then, analogously treated, this leads to (3-21):

$$q(t) = \sum_n \left[U_n \cdot I_n \cdot \boldsymbol{sin(}2n\omega_1\, t\boldsymbol{)} \cdot \boldsymbol{cos}\,\varphi_n + U_n \cdot I_n \cdot \boldsymbol{(}1 + \boldsymbol{cos(}2n\omega_1\, t\boldsymbol{))} \cdot \boldsymbol{sin}\,\varphi_n\right] \tag{3-21}$$

and the average of this expression (3-22) is termed by Budeanu as the *reactive power*:

$$Q = \sum_n U_n \cdot I_n \cdot \boldsymbol{sin}\,\varphi_n\,, \tag{3-22}$$

Since the cosine-function in (3-19) forces P to be the arithmetic sum of the real powers in all harmonic orders, the sine-function in (3-22) may result in a zero value for Q, while the constituent harmonic orders have non-zero values, which leads to misleading interpretations of the measured reactive power. Originally defined by Budeanu distortion power D can be obtained from (3-23):

$$S^2 = P^2 + Q^2 + D^2\,, \tag{3-23}$$

and it can be ambiguous as well.

3.4.2 Czarnecki power theory

To avoid misleading interpretation of non-active powers under distorted and/or unbalanced conditions Czarnecki has proposed another concept of power resolution in circuits with non-sinusoidal waveforms [74]. This theory is based on the decomposition of currents into orthogonal components with the main goal being interpretation of power phenomena. The work can be seen as a complementary one to the theory developed by Akagi and Nabae [65]. Czarnecki defines non-active powers as the product of the rms value of voltage by the rms value of current components. This concept is based on the following assumptions: since the currents and power flow in three-phase circuits do not depend on the reference voltage, any voltage can be added to the supply voltage without any affect on the power phenomena. However, such a voltage may change the apparent power. Thus, it affects the value of the power factor in circuits with unbalanced loads [69]. Only the currents, active and reactive powers do not change with the change of the voltage reference. Therefore, an increase in the apparent power with the load unbalance should be explained in terms of the current rms value.

Decomposition is based on the partitioning of the set of N harmonic orders into two subsets N_A (3-24) and N_B (3-25), namely:

$$\text{if } P_n \geq 0 \text{ then } n \in N_A, \tag{3-24}$$

$$\text{if } P_n < 0 \text{ then } n \in N_B, \tag{3-25}$$

where P_n is the active power transmitted from the source to the load at the n-order harmonic frequency amounts to (3-26):

$$P_n = \boldsymbol{Re}\{\underline{S}_n\} = \boldsymbol{Re}\{\underline{U}_n^{\,T} \cdot \underline{I}_n^{\,*}\}. \tag{3-26}$$

The asterisk in (3-26) denotes a vector of the conjugate values and the vectors of voltage and currents are calculated as complex root mean square (crms) values for each harmonics. In three-phase circuits corresponding quantities can be obtained for line-to-ground voltages (3-27) and line currents (3-28) defining vectors:

$$\underline{\boldsymbol{U}}_{\boldsymbol{n}} = [\underline{U}_{Rn}, \underline{U}_{Sn}, \underline{U}_{Tn}]^T \text{ and} \tag{3-27}$$

$$\underline{\boldsymbol{I}}_{\boldsymbol{n}} = [\underline{I}_{Rn}, \underline{I}_{Sn}, \underline{I}_{Tn}]^T. \tag{3-28}$$

The observed line-to-ground voltages are arranged in the vector $\boldsymbol{u}$ (3-29) and line currents are described by the vector $\boldsymbol{i}$ (3-30), which can be expressed:

$$\boldsymbol{u} = [u_R, u_S, u_T]^T = \sum_{n \in N} u_n = \sum_{n \in N} [u_{Rn}, u_{Sn}, u_{Tn}]^T = \sqrt{2} \cdot \boldsymbol{Re} \sum_{n \in N} [\underline{U}_{Rn}, \underline{U}_{Sn}, \underline{U}_{Tn}]^T \cdot e^{jn\omega_1 t}, \tag{3-29}$$

$$\boldsymbol{i} = [i_R, i_S, i_T]^T = \sum_{n \in N} i_n = \sum_{n \in N} [i_{Rn}, i_{Sn}, i_{Tn}]^T = \sqrt{2} \cdot \boldsymbol{Re} \sum_{n \in N} [\underline{I}_{Rn}, \underline{I}_{Sn}, \underline{I}_{Tn}]^T \cdot e^{jn\omega_1 t}, \tag{3-30}$$

respectively [69].

An explanation for this decomposition lies in the direction of the energy flow. When the load is passive, linear and time-invariant, then each of the harmonic active power P_n can not be negative. However, if any of these conditions is not fulfilled, the harmonic currents may be generated in the load, so that the energy at that frequency may be transmitted back to the source ($P_n < 0$). As a result, this decomposition enables one to decompose the current (3-31), the voltage (3-32) and the active power (3-33) observed at the cross-section into the following components:

$$\boldsymbol{i} = \sum_{n \in N} \boldsymbol{i}_n = \sum_{n \in N_A} \boldsymbol{i}_n + \sum_{n \in N_B} \boldsymbol{i}_n = \boldsymbol{i}_A + \boldsymbol{i}_B. \tag{3-31}$$

$$\boldsymbol{u} = \sum_{n \in N} \boldsymbol{u}_n = \sum_{n \in N_A} \boldsymbol{u}_n + \sum_{n \in N_B} \boldsymbol{u}_n = \boldsymbol{u}_A - \boldsymbol{u}_B \,. \tag{3-32}$$

$$P = \sum_{n \in N} P_n = \sum_{n \in N_A} P_n + \sum_{n \in N_B} P_n = P_A - P_B \,. \tag{3-33}$$

The currents $\boldsymbol{i}_A$ and $\boldsymbol{i}_B$ are mutually orthogonal [69] and their rms values defined in (3-34) and (3-35) as the *Euclidean vector norm*[5]:

$$\|\boldsymbol{i}_A\| = \sqrt{\langle \boldsymbol{i}_A, \boldsymbol{i}_A \rangle} = \sqrt{\sum_{n \in N_A} \left(I_{Rn}{}^2 + I_{Sn}{}^2 + I_{Tn}{}^2 \right)} = \sqrt{\sum_{n \in N_A} \|\boldsymbol{i}_n\|^2} \,, \tag{3-34}$$

$$\|\boldsymbol{i}_B\| = \sqrt{\langle \boldsymbol{i}_B, \boldsymbol{i}_B \rangle} = \sqrt{\sum_{n \in N_B} \left(I_{Rn}{}^2 + I_{Sn}{}^2 + I_{Tn}{}^2 \right)} = \sqrt{\sum_{n \in N_B} \|\boldsymbol{i}_n\|^2} \,, \tag{3-35}$$

fulfil the relationship (3-36):

$$\|\boldsymbol{i}\|^2 = \|\boldsymbol{i}_A\|^2 + \|\boldsymbol{i}_B\|^2 \,. \tag{3-36}$$

Likewise, the relationship for the voltage (3-37):

$$\|\boldsymbol{u}\|^2 = \|\boldsymbol{u}_A\|^2 + \|\boldsymbol{u}_B\|^2 \,. \tag{3-37}$$

yields to the statement describing the *apparent power* S (3-38), which was defined in a similar form by Buchholz [75] and then extended by Czarnecki:

$$S^2 = \|\boldsymbol{u}\|^2 \cdot \|\boldsymbol{i}\|^2 = S_A{}^2 + S_B{}^2 + S_F{}^2 \,, \tag{3-38}$$

where the three components can be described in equations (3-39), (3-40) and (3-41), respectively:

$$S_A = \|\boldsymbol{u}_A\| \cdot \|\boldsymbol{i}_A\| \,, \tag{3-39}$$

$$S_B = \|\boldsymbol{u}_B\| \cdot \|\boldsymbol{i}_B\| \,, \tag{3-40}$$

$$S_F = \sqrt{\|\boldsymbol{u}_A\|^2 \cdot \|\boldsymbol{i}_B\|^2 + \|\boldsymbol{u}_B\|^2 \cdot \|\boldsymbol{i}_A\|^2} \,. \tag{3-41}$$

The last quantity (3-41) also occurs in single-phase circuits under distorted conditions and is called by Czarnecki *forced apparent power*. By comparing equations (3-33) and (3-38) it can be observed that the presence of bi-directional transmission of active power reduces the transmitted useful power P, while increasing the apparent power S due to an increase in the voltage and current rms values.

[5] See in Appendix 8.1 for further explanations.

At unidirectional transmission with all $P_n \geq 0$, the set N_B is empty. This means that $S_B = S_F = 0$, and $S = S_A$. Therefore, the partition into two sub-sets of harmonics allows for the construction of two sub-circuits, in which that part to which the active power is delivered can be considered a passive circuit. An equivalent circuit can be found for each of them with the same apparent power S_n and current i_n at voltage u_n as observed in the original circuit. Considering a symmetrical load that is equivalent (index e) with respect to the complex apparent power $\underline{\boldsymbol{S}}_n$, at the terminal RST (or L1L2L3) to original load then, its phase admittance (3-42) can be found and it should be equal to:

$$\underline{\boldsymbol{Y}}_{en} = G_{en} + jB_{en} = \underline{\boldsymbol{S}}_n^{\;*} / \|\boldsymbol{u}_n\|^2 , \tag{3-42}$$

for $n \in N_A$, otherwise $\underline{\boldsymbol{Y}}_{en} = 0$. Such a load draws the current (3-43):

$$\boldsymbol{i}_b = \sqrt{2} \cdot \boldsymbol{Re}\left\{ \sum_{n \in N_A} \underline{\boldsymbol{Y}}_{en} \cdot \underline{\boldsymbol{U}}_n e^{jn\omega_1 t} \right\} , \tag{3-43}$$

which is the part of the current $\boldsymbol{i}_A$. With respect to the active power P_A the load is equivalent to a symmetrical resistive load of conductance (3-44):

$$G_d = P_A / \|\boldsymbol{u}_A\|^2 . \tag{3-44}$$

The current (3-45) of this load, equal to:

$$\boldsymbol{i}_d = G_d \cdot \boldsymbol{u}_A = \sqrt{2} \cdot \boldsymbol{Re}\left\{ \sum_{n \in N_A} G_d \cdot \underline{\boldsymbol{U}}_n e^{jn\omega_1 t} \right\} \tag{3-45}$$

is the part of $\boldsymbol{i}_A$ as well, and can be considered the active component of the current $\boldsymbol{i}_b$ and of the current $\boldsymbol{i}_A$ and is therefore named *active current*. This term was first proposed by Fryze [70], but it was defined only for single-phase circuits; Czarnecki has extended this concept to the three-phase circuits. The remaining component of the current $\boldsymbol{i}_b$ (3-46):

$$\boldsymbol{i}_b - \boldsymbol{i}_d = \sqrt{2} \cdot \boldsymbol{Re}\left\{ \sum_{n \in N_A} (G_{en} - G_d + jB_{en}) \cdot \underline{\boldsymbol{U}}_n e^{jn\omega_1 t} \right\} \tag{3-46}$$

is decomposed into the *scattered current* (3-47):

$$\boldsymbol{i}_s = \sqrt{2} \cdot \boldsymbol{Re}\left\{ \sum_{n \in N_A} (G_{en} - G_d) \cdot \underline{\boldsymbol{U}}_n e^{jn\omega_1 t} \right\} \tag{3-47}$$

and the *reactive current* (3-48):

$$\boldsymbol{i}_r = \sqrt{2} \cdot \boldsymbol{Re}\left\{ \sum_{n \in N_A} jB_{en} \cdot \underline{\boldsymbol{U}}_n e^{jn\omega_1 t} \right\}. \tag{3-48}$$

Therefore, the current $\boldsymbol{i}_b$ (3-49) is composed of the three orthogonal components:

$$\boldsymbol{i}_b = \boldsymbol{i}_d + \boldsymbol{i}_s + \boldsymbol{i}_r \tag{3-49}$$

and draws the current of an equivalent symmetrical load which has the same active power, P_A, and the same complex apparent power, $\underline{S}_n$, as the original unbalanced load with current $\boldsymbol{i}_A$.

However, due to this unbalance the current $\boldsymbol{i}_A$ may differ from $\boldsymbol{i}_b$ by a component $\boldsymbol{i}_u$:

$$\boldsymbol{i}_u = \boldsymbol{i}_A - \boldsymbol{i}_b\,, \tag{3-50}$$

which is termed *unbalanced current*. In conclusion, current $\boldsymbol{i}_A$ (3-51) is decomposed into four components, which are mutually orthogonal:

$$\boldsymbol{i}_A = \boldsymbol{i}_d + \boldsymbol{i}_s + \boldsymbol{i}_r + \boldsymbol{i}_u\,, \tag{3-51}$$

and are orthogonal also to the $\boldsymbol{i}_B$, the fifth component of the load current $\boldsymbol{i}$, so that, extending (3-36) to (3-52):

$$\|\boldsymbol{i}\|^2 = \|\boldsymbol{i}_d\|^2 + \|\boldsymbol{i}_s\|^2 + \|\boldsymbol{i}_r\|^2 + \|\boldsymbol{i}_u\|^2 + \|\boldsymbol{i}_B\|^2\,. \tag{3-52}$$

As a result, this decomposition enables one to write the apparent power from (3-38) in a more detailed form (3-53):

$$S^2 = P_A{}^2 + D_s{}^2 + Q_r{}^2 + Q_u{}^2 + S_B{}^2 + S_F{}^2\,, \tag{3-53}$$

where the constituent powers, written in (3-54), (3-55) and (3-56):

$$D_s = \|\boldsymbol{u}_A\| \cdot \|\boldsymbol{i}_s\|\,, \tag{3-54}$$

$$Q_r = \|\boldsymbol{u}_A\| \cdot \|\boldsymbol{i}_r\|\,, \tag{3-55}$$

$$Q_u = \|\boldsymbol{u}_A\| \cdot \|\boldsymbol{i}_u\|\,, \tag{3-56}$$

cause the apparent power increase due to source loading with scattered, reactive and unbalanced currents. It is important to note that in (3-53) active power does not appear. Therefore, the equation for active power (3-33) should always accompany the apparent power equation (3-53).

With unidirectional flow of the active power the apparent power equation (3-53) can be simplified into the form (3-57):

$$S^2 = P^2 + D_s{}^2 + Q_r{}^2 + Q_u{}^2 . \tag{3-57}$$

To summarize, the theory of the orthogonal decomposition of current (3-52) provides an explanation for the reasons for which the source current $\boldsymbol{i}$ is usually higher than necessary for the active power transmission. Each of the currents in this equation occurs due to different physical phenomena.

3.4.3 IEEE Working Group definitions for power

The concept presented in [71] is based on the main assumption that the goal of energy transmission is to deliver as much of the power as possible through a 50 Hz positive sequence component to the consumer. Therefore, it makes sense to separate the fundamental and the harmonic components from each other. Using the rms values of the voltage (3-58) and current (3-59):

$$U = \sqrt{\sum_n U_n{}^2} , \tag{3-58}$$

$$I = \sqrt{\sum_n I_n{}^2} , \tag{3-59}$$

the harmonic rms-components can be separated into their fundamental and harmonic components, (3-60) and (3-61), for voltage and current, respectively:

$$U^2 = U_1^2 + U_H^2 , \tag{3-60}$$

$$I^2 = I_1^2 + I_H^2 , \tag{3-61}$$

with (3-62) and (3-63):

$$U_H^2 = \sum_{n \neq 1} U_n^2 , \tag{3-62}$$

$$I_H^2 = \sum_{n \neq 1} I_n^2 , \tag{3-63}$$

respectively. From (3-60) and (3-61) the apparent power is defined in (3-64):

$$S^2 = (U \cdot I)^2 . \tag{3-64}$$

This can then be divided into two main components (3-65):

$$S^2 = S_1^2 + S_N^2\,, \tag{3-65}$$

where S_1 is the *fundamental apparent power*, which is in turn resolved in (3-66) into the *fundamental active power* P_1 and *fundamental reactive power* Q_1 according to the well-known equation used under pure 50 or 60 Hz sinusoidal conditions:

$$S_1^2 = (U_1 \cdot I_1)^2 = P_1^{\,2} + Q_1^{\,2}\,. \tag{3-66}$$

The second component in (3-65) is named *non-fundamental apparent power* S_N, and consists of three components (3-67):

$$S_N^2 = (U_1 \cdot I_H)^2 + (U_H \cdot I_1)^2 + (U_H \cdot I_H)^2\,. \tag{3-67}$$

Because of the fact that the first component is the product of fundamental rms voltage and harmonic current, it is named *current distortion power*, and usually it is a dominant term in (3-67). along the same lines, the second term is named *voltage distortion power*, and it is a reflection of the voltage distortion at the bus. The third term, called *harmonic apparent power* S_H is further divided in (3-68) *into total harmonic active power* P_H, and *total harmonic non-active power* N_H[6]:

$$S_H^2 = (U_H \cdot I_H)^2 = P_H^{\,2} + N_H^{\,2}\,. \tag{3-68}$$

It is worthwhile to recognize that while a direction of flow may be assigned to P_1 and Q_1, no direction of flow may be assigned to the three components in (3-67).

Dividing (3-67) by (3-66) yields *normalized non-fundamental distortion power* (3-69):

$$\left(\frac{S_N}{S_1}\right)^2 = \left(\frac{I_H}{I_1}\right)^2 + \left(\frac{U_H}{U_1}\right)^2 + \left(\frac{U_H \cdot I_H}{U_1 \cdot I_1}\right)^2, \tag{3-69}$$

which can be drawn in (3-70) using the quantity defined in (3-1):

$$\left(S_N/S_1\right)^2 = \left(THDi\right)^2 + \left(THDu\right)^2 + \left(THDi \cdot THDu\right)^2\,. \tag{3-70}$$

When $THDi$ > 20% and $THDu$ < 5% then (3-70), with only a small error, simplifies to (3-71):

$$S_N/S_1 \cong THDi\,. \tag{3-71}$$

[6] Original notation from the document [71] has been maintained.

The normalized non-fundamental distortion power provides a relatively good indication of the level of harmonic pollution. The total power factor or *true power factor* is defined by equation (3-72):

$$PF = \frac{P_1 + P_H}{S}, \tag{3-72}$$

however, the *displacement power factor* (3-73):

$$dPF = \frac{P_1}{S_1} \tag{3-73}$$

carries information about uncorrupted fundamental power flow.

For three phase circuits the IEEE Working Group introduced the term *system apparent power* S_e, also called *equivalent apparent power* (3-74):

$$S_e = 3 \cdot U_e \cdot I_e, \tag{3-74}$$

where

$$U_e = \sqrt{\frac{U_R^2 + U_S^2 + U_T^2}{3}} \quad \text{and} \tag{3-75}$$

$$I_e = \sqrt{\frac{I_R^2 + I_S^2 + I_T^2}{3}}. \tag{3-76}$$

Voltages in (3-75) are line-to-neutral rms voltages calculated according to (3-58). For three-conductor systems the equivalent voltage U_e may also be calculated using (3-75) with line-to-neutral voltages measured with help of an artificial neutral point, or from line-to-line rms values (3-77):

$$U_e = \sqrt{\frac{U_{RS}^2 + U_{ST}^2 + U_{TR}^2}{9}}. \tag{3-77}$$

As for the single-phase case, analogously named values for powers in three-phase circuits can be obtained. However, in the case of an unbalanced system, another component of apparent power is defined in [71]. The degree of unbalance in the fundamental apparent power S_{e1} (3-78) can be divided into two terms:

$$S_{e1}^2 = S_{1+}^2 + S_{u1}^2, \tag{3-78}$$

where the first component is the *positive-sequence fundamental apparent power* calculated with rms values of the positive-sequence fundamental voltage and current, and the second one is named *unbalanced fundamental apparent power*.

The three approaches are implemented in the algorithm of the external module of the power quality monitoring system from Fig. 3.1. The module consists of several MS Excel spreadsheets in which calculations are made automatically by the macros that are prepared to deal with the standardized data input that come from the exporting module. In work [76] and [77] power calculations utilizing the module are described in detail. The calculations made at the cross section between the resistance welder and the power supply show that the concept of active power calculation is quite similar for all three theories. However, calculation of Budeanu's reactive power tends to fail especially when huge waveform distortion is present in the system [77]. So, the usage of the terms defined by Budeanu, e.g. distortion power, can be misleading and should be forsaken for cases with strong waveform distortion in the power system.

4 MEASUREMENT-BASED EVALUATION OF POWER QUALITY IN DISTRIBUTION SYSTEMS UNDER BALANCED AND UNBALANCED CONDITIONS

A concise review of the modeling and analysis of harmonics in power networks is presented in the first section of this chapter. The state of art in modeling of the power system elements for frequencies higher than fundamental one is presented. The next part of this chapter is devoted to measurement-based methods for the power quality evaluation in distribution networks. In section 4.2 the influence of the network structure on the propagation of harmonics is discussed together with comments on the measurement-based modeling process. The last section of this chapter introduces a new algorithm for the description of the interaction between the source of waveform distortion (non-linear loads) and the sink (distribution network). This modeling approach is based on the description of the non-linear load in harmonic domain with the help of a specially constructed admittance matrix that allows for representing the load-network interaction near the working point of the load with good precision.

4.1 TECHNIQUES FOR HARMONIC AND INTERHARMONIC ANALYSIS

Harmonic studies are an important component of power system analysis and design [78]. They are used to quantify the distortion in voltage and current waveforms at various points in a power system. Interest in the analysis of harmonics and their effect dates back to the early 1900’s but since the late 1970’s the subject has gained increasing attention due to the wide-spread use of static power converters [79], [80]. In general there are three main tendencies in the modeling philosophy: studies in time domain, frequency domain, and harmonic domain that can be viewed as a restriction of frequency domain modeling to integer frequencies but with all non-linear interactions modeled.

Time domain simulation consists of differential equations representing the dynamic behavior of the interconnected power system components. Mostly, calculations in time domain are used for simulations of transients and non-stationary disturbances in different time ranges [81]. In studies of load non-linearity there also exists time domain models that accommodate both steady-state and dynamic behavior. However, they include parameter derivation procedure and describe only small loads, like a fluorescent lamp or a desktop computer [82]. The resulting system of equations, generally non-linear, is solved using numerical integration. The derivation of harmonic information from time domain programs involves solving for the steady-state and then applying the FFT. This requires considerable computation for relatively small systems [83].

Frequency domain simulation in its simplest form provides a direct solution for the effect of specified individual harmonic injections throughout a linear system, without considering the harmonic interaction between the network and the non-linear components. The most commonly used model involves the use of single phase analysis, a single harmonic source and a direct solution [84]. The supply of three-phase fundamental voltage at points of common coupling is well balanced within strict limits, and under these conditions load flow studies are normally carried out on the assumption of perfect symmetry of network components. The same assumption is often made for the harmonic frequencies, even though there is no guarantee from the utilities of harmonic symmetry. The simulations based on models that did not account for the supply-voltage dependency of non-linear loads are very often burden with errors [85]. Therefore, such studies are eligible only for qualitative analysis.

To achieve better accuracy harmonic domain analysis, also called iterative harmonic analysis, is often performed. The increased power ratio of modern power electronic devices in relation to system short circuit power means that the principle of superposition that is used in frequency domain simulations does not apply. The harmonic injection from each source will, in general, be a function of that from other sources and the actual system state. Accurate results can only be obtained iteratively solving non-linear equations that describe the steady state as a whole. In many cases, it can be assumed that there are no other frequencies present apart from the fundamental frequency and its harmonics. This type of analysis, in harmonic domain, can be viewed as a restriction of frequency domain modeling to integer frequencies but with all non-linear interactions modeled. Standard methods are employed to obtain a set of accurate non-linear equations which describe the system steady-state mainly at the fundamental frequency [8]. After partitioning the system into linear regions and non-linear devices, these devices are described by isolated equations, depending on given boundary conditions to the linear system [9]. Then, the system solution is predominantly a solution for the boundary conditions for each non-linear device.

Summarizing, time domain simulation involving non-linear load behavior requires its mathematical description, e.g. in form of differential equations, which for most types of non-linear load are either difficult to establish or unknown. The drawback is also the lack of power flow constraints, i.e. constant power specification at load buses at the fundamental frequency. The analysis in frequency domain can be built on the standard information including impedances of system elements and the characteristic (spectrum) of the current (or in some cases voltage) injected by non-linear loads bringing fast solutions and an overview, qualitative analysis of the system. But the drawbacks here are considerable errors resulting from the non-linear nature of the harmonic phenomenon itself, and the difficulties in the giving back of the interaction between harmonic source and the network. The harmonic domain is a novel approach and due to the giving back of the load-network interaction it is predestined for quantitative studies. However, the simulation process is often burden with a time-consuming measurement and parameterization process.

In this work a combined approach is proposed that link the overview analysis in frequency domain with detailed modeling that is applied to the most important points in the system from the forecasted harmonic or interharmonic distortion point of view. In the following section the techniques being used for power system harmonic analysis are reviewed. The next sections are devoted to the measurement-based technique for evaluation of power quality in power systems.

4.1.1 Harmonic simulations

The concept of harmonic analysis in a power system can be composed as in Fig. 4.1.

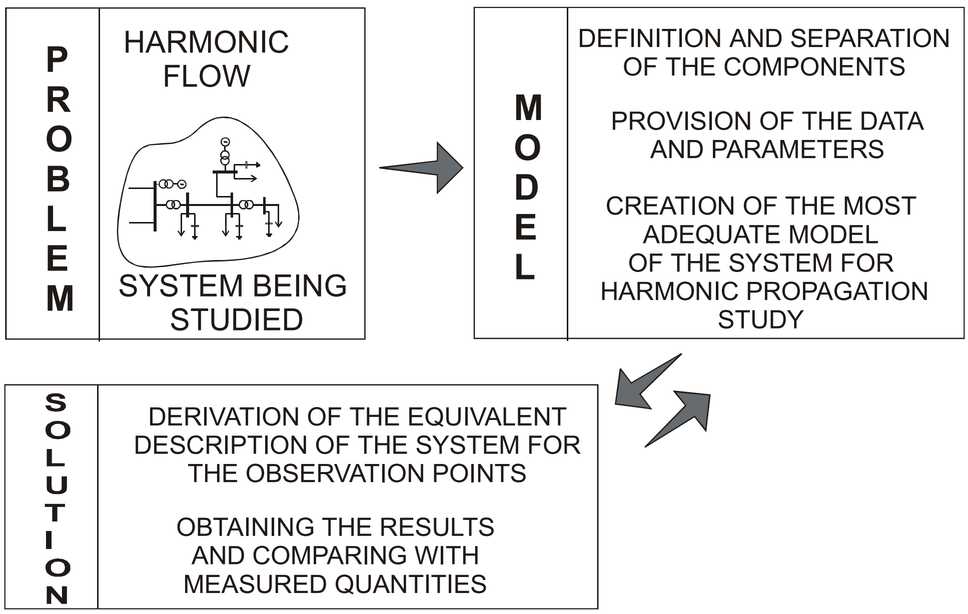

Fig. 4.1 Concept for harmonic distortion studies

In general, the problem of harmonic analysis can be cast mathematically as the solution of a network equation and a set of device equations at fundamental and harmonic frequencies. The network equation can be formulated in the form of a nodal admittance matrix or in a power flow equation form [78]. The device equation can be as simple as known current sources or as complex as control-variable dependent circuits. Which technique to use for a particular problem is determined by the available data (Fig. 4.1) keeping in mind the importance of using a method correspondent with input data accuracy. To conclude, a certain amount of information can be more readily retrieved in one domain than in the other. Mathematically both are equivalent.

In frequency domain there are two types of harmonic simulations: The first of these, the frequency scan, is the simplest and most commonly used technique for harmonic analysis. A scan calculates the frequency response characteristic at a particular bus or node. Usually, this is accomplished by injecting 1 A into the bus over a range of frequencies and then observing the resultant voltage. The resultant voltage is directly related to the system impedance in ohms. Frequency scan analysis is the best method for identifying resonance conditions. It has also been used in filter design. The second type, harmonic distortion simulations, use harmonic source characteristics of nonlinear loads (current spectrum) to determine current and voltage distortion levels at various points in the system. Harmonic source characteristics (current source) are obtained from field measurements, other simulation programs, or a library of typical waveforms. Distortion simulations are useful for evaluating component duty and determining harmonic limit compliance, i.e. [27] or [29].

Good harmonic prediction requires clear understanding of three closely related topics that can be summarized as in Fig. 4.2.

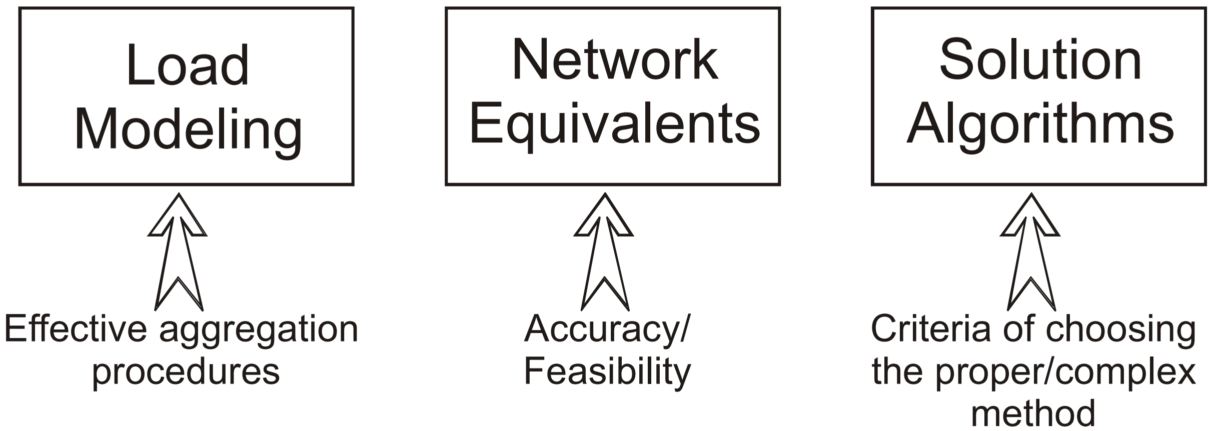

Fig. 4.2 General concept of power system components modeling methodology

The first topic is the non-linear load modeling with proper exactness and the choice of the right aggregate procedures for the linear load models. These tasks are in practice made difficult by insufficient information on the composition of the system loads and their dampening effect on the harmonic frequencies [86]. The second topic is the proper network equivalent, where one of the most important problems associated with developing a system model lies in how much of the system should be modeled exactly. Unfortunately, there are no hard-and-fast rules in this area. It is often more of a feel that is developed over time. A good starting point for harmonic studies is to model one or two buses back from the bus of interest (connection of non-linear load). The best method for determining the appropriate system model is to start with a small, simple circuit that accurately represents the phenomena, and then add more of the system details to determine their impact on the solution result [87]. And finally, third topic - the derivation of suitable solution techniques for the analysis to achieve a proper balance between complexity and accuracy for the study in question. Here the method-palette is stretched from time-domain methods through simple frequency domain solutions to composed solutions in harmonic domain. Harmonic simulation programs can be useful as tool at the introductory stage for the study on harmonic problems [87]. The following table presents the standardized procedure for using a harmonic simulation program to perform harmonic studies.

Table 4.1 Standardized procedure for harmonic simulations [87]

1. Identify the study objectives	The objectives will dictate the frequency range of interest, the modeling requirements, the variables to be investigated, and the types of output that are needed from the simulation.
2. Develop the system model	The extent of the system model depends on the capacitors and/or lines to be switched and the frequency range of interest. Obviously, it would be desirable if the model could include the entire system and you could just switch the device(s) of interest.
3. Draw a connection diagram and assign bus names.	The bus labels will be used in the harmonic data file for identification.
4. Develop component models	Each component model (transmission line, transformer, breaker, etc.) will depend on the frequency range of interest and the specific harmonic event being evaluated.
5. Run a fundamental steady-state solution case	This case will verify system connectivity and provides a sanity check on many of the system components. This is a very important step that must not be skipped.
6. Estimate the expected results	This can be done from previous studies, from the literature, or from hand calculations. It is important to know what to expect from the simulation so that major problems can be identified quickly.
7. Use a sensitivity analysis for unknown or important quantities	Important variables from the simulation should be evaluated to determine their impact on results. These could include capacitor bank size, transformer size, line length, source strength, etc.
8. Develop solutions	Possible solutions (i.e. filters) are evaluated and design specifications are developed.

4.1.2 General concepts for power system elements modeling

The process for completing a harmonic simulation consists of first collecting and developing the necessary data to represent the circuit to be modeled. Often this system representation is completed by "describing" the interconnection and component values. From the network structure point of view this procedure includes three important steps: modeling of the subsequent network connection point, modeling of the network elements and modeling of the load structure with harmonic sources. These three elements will now be described in detail.

A. Network impedance

Network impedance is a characteristic of the system that delivers electricity and plays an important role in relation to the disturbing effect of some devices connected to the network. In very general terms, a low impedance tends to reduce the disturbing effect [13]. In practice, the value of the network impedance varies considerably from point to point in the system. The disturbing action of loads is a function of the current they draw from or inject into the network. The disturbing effect on other users is a function of the voltage delivered to them, i.e. the conversion of the emitted disturbing current to the delivered disturbing voltage is a function of the impedances of the circuits through which the current flows – the network impedances.

Generally, for modeling purposes, the assessment of the impedance value can be done by calculating of the impedance point by point on the basis of the impedance characteristics of the network. A typical starting point in the simulations of the distribution systems is modeling of a subsequent utility system. The utility system can be represented by its impedance $\underline{Z}_{s,f}$ (4-1) that can be calculated at frequency f:

$$\underline{Z}_{s,f} = j \cdot \frac{k \cdot U_n^{\,2}}{S_k''} \cdot \frac{f}{f_1}, \qquad (4\text{-}1)$$

where U_n stands for nominal voltage at the fundamental frequency f_1, S_k'' is the short-circuit power at the point where the modeling process begins, e.g. at the PCC. The voltage factor c accounts for the not amenable effects by a short-circuit and can be found in the respective short-circuit calculation norms or in [88]. In many cases it is sufficient to represent the system as an inductance. When the information about X/R ratio in the system is available, the inclusion of the resistance can be made as well. The modeling of the superordinated system in the typical frequency range for harmonic and interharmonic studies allows for the application of (4-1).

B. Standard models of equipment elements

The data needed for modeling distribution system elements can be summarized as in Table 4.2.

Table 4.2 Summary of typical data for a distribution system harmonic study [83]

Device	Data needed
overhead lines, cables	phase and neutral conductor size, layout, length, or short circuit impedances; capacitance (when available)
transformers	turns ratio, connection diagram, short circuit impedance
capacitor banks	voltage rating, VAr rating, configuration (wye, grounded wye, or delta)
tuned filters	tuned frequency, voltage rating, VAr rating, configuration in detail

The middle voltage cables of the length l, are represented by their pi circuit, with both longitudinal (4-2) and transversal elements (4-3) expressed as frequency functions, where root by the resistance accounts for the skin-effect:

$$\underline{Z}_{k,f} = \left(R_1' \cdot \sqrt{\frac{f}{f_1}} + jX_1' \cdot \frac{f}{f_1} \right) \cdot l \,, \tag{4-2}$$

$$\underline{Y}_{ck,f} = j \cdot 100\pi \cdot \frac{f}{f_1} \cdot C_b' \cdot l \,. \tag{4-3}$$

The distribution step-down transformers are modeled as a series resistance R_t with the leakage inductance X_t calculated from available rated impedance voltage u_{kr} and rated ohmic voltage drop u_{Rr} [88]. The capacitances of the transformer are not considered because experience has shown that capacitances only start to have some effect at 10 kHz, well above the common harmonic frequencies present in power systems, i.e. 2.5 kHz [83]. The frequency dependence is included as in (4-4) so that the transformer model is based on the assumption that its X/R ratio is constant over the studied frequency range.

$$\underline{Z}_{t,f} = \left(R_t + jX_t \right) \cdot \frac{f}{f_1} \,. \tag{4-4}$$

In the detailed study more sophisticated transformer models are applied to account for the phase difference. The modeling methods of two, three and four-winding transformers can be found in [2].

The power factor correction capacitors in the distribution systems should be precisely placed and modeled as susceptances with linear frequency dependence. However, balanced positive sequence models are not sufficient when there are single-phase capacitor banks on the system. The same method is to be applied for the tuned filters.

C. Modeling the linear load structure and non-linear load representation

The term linear load describes a class of loads that if supplied by a sinusoidal source at fundamental frequency, produce only fundamental sinusoidal current. Some of residential loads, induction motors and synchronous motors are examples of linear load [86]. The modeling of these types of loads is presented in [2] in detail. The most popular method to acquire the loads admittances is their direct calculation from their power consumption. These values can be taken both from measurements and from the grid carrier's data. However, such load representation is often not sufficient in cases when composite structure of load is present. Since the representation of aggregate linear load structure has an influence on the frequency and the dampening effect of the resonance, [86] proposed effective methods for the acquisition of the aggregate linear load models. In the scope of this work, however, the modeling of the load and their influence on the analytical method proposed will be studied separately in cases presented in Chapter 5. Therefore, the detailed presentation will be omitted here.

The next area in the modeling of power system loads is the case of non-linear load representation. Generally, a current source representation is used or in cases when the source admittance is known, a Norton equivalent circuit is often used [78]. From a variety of sources the following three sets, according to classification presented in Chapter 2 of this work, can be separated from the modeling difficulty point of view:

(1) Large numbers of distributed non-linear components of small rating. These appliances present special simulation problem, since the statistical information of their content in the load mix must be provided. In the majority of cases, only minimal information on such characteristics is presented. The conclusion here is that only through extensive measurements can the necessary portion of information be won.

(2) Large and continuously randomly varying non-linear loads, like electric metal-melting arc furnaces or resistance welding. The difficulty lies in the variability of the current harmonic injections to be used in each particular study, which should be based on extensive experimental information obtained from measurements in similar existing installations.

(3) Large static power converters and transmission system level power electronic devices. Static power converters are used more extensively for controlling loads and are discussed in detail in [8], [32]. The modeling of such devices is subjected to a special research domain and will not be discussed in this work.

In general, by developing the power system model for harmonic and interharmonic study a simplification will always occur. Very often the goal of the study is to determine the model complexity. Some factors affecting system simplification include model development and simulation time which is not a significant factor nowadays. The power system equipment modeling methods are well established, but the area of proper load modeling is still not satisfactorily arranged. Traditional modeling methodology that is based on a direct solution in frequency domain is not sufficient to represent major groups of non-linear loads in distribution system studies. The modeling does not include the interaction effect between the distribution system and the electronically controlled loads. Standard calculation programs concentrate on impedance calculations over the chosen frequency range and do not include the 'interactive' phenomena, that the change of the supply harmonic voltage can have a big influence on the distortion currents drawing from the electronically controlled loads. It is, therefore, very important to improve the non-linear load modeling to include this important behavior.

It is appropriate to note that a large number of harmonic related problems encountered in practice need to be analyzed by a combination of the various methods to reach an improvement in the simulation exactness. This implies the usage of complex methods that combine the methods in a solution algorithm that is typical for the problem to be solved. The method developed in [89] obtains a harmonic load flow from iterations between i.e. the Norton equivalent circuits of non-linear elements and the linear network solutions at harmonic frequencies. Often, however, the methodology of the hybrid methods includes the modeling of the control circuits of the non-linear loads, like power electronic elements. Measurements in such cases may also be an essential component in the analysis.

In the following sections a measurement-based modeling of the distribution system elements is presented. A current spectrum of a big non-linear load is used to perform case studies to study the influence of the network configuration on the harmonic analysis.

4.2 MEASUREMENT-BASED MODELING OF THE DISTRIBUTION SYSTEM ELEMENTS

The studies based only on deterministic solutions are burdened with errors and allow only limited choice of the proper mitigation method. The level of distortion present in distribution systems is highly dependent on the load present both down and upstream of the distribution transformer. Even the system impedance can vary changing simultaneously harmonic content in the system [78]. Therefore, every single case on harmonic studies that should be realized with higher accuracy demands on-site measurements whose results can tune the model used and, in turn, improve its exactness.

In this section a three-step measurement-based modeling approach is proposed to study the influence of equipment modeling concepts on the harmonic propagation study of the system. It contains a proper model design, measurements obtaining the statistical profile of the existing distortion in the studied university system and the combined analysis to calculate distortion within it based on synchronized measurements in the system with a non-linear load - a resistive welding machine. The study of non-linear load influence on the system operation becomes especially important when loads with pulsed power like welding machines or electrical discharge machines are a part of the analyzed distribution system [77]. High current pulses - by welders pulses rise about 0.5 A/µs with peak value about 800 A (Fig. 4.3) on the low voltage level - demanded by these devices result in stronger voltage distortion and increase the possibility of improper system operation.

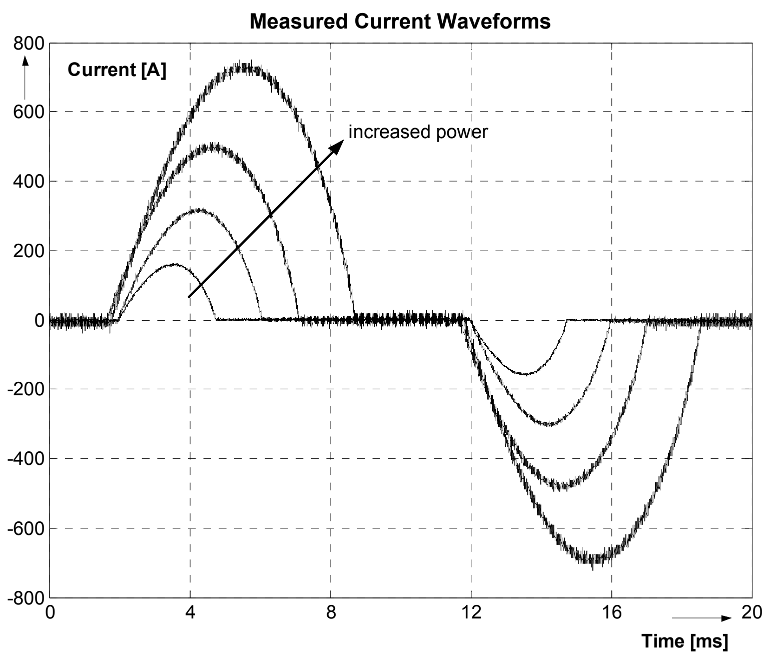

Fig. 4.3 Waveforms of the current demanded by the welder by distinct welding power

The elements of the distribution system are represented as frequency dependent impedances. The three-phase model used in these calculations (Fig. 4.4) utilizes equations proposed in [83], and described in the previous section.

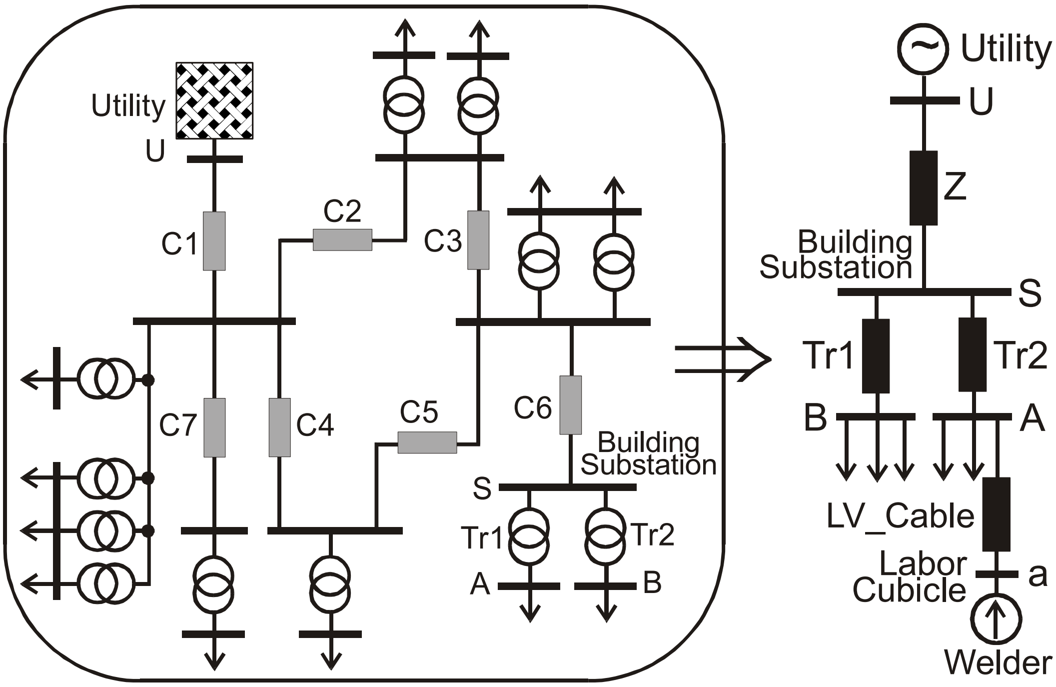

Fig. 4.4 The system and its simplification modeled for the welder case study

The utility system is represented by its impedance (4-1) and the middle-voltage cables are modeled according to (4-2, 4-3): The impedance of the low voltage cables, especially of the cable which supplies the welder, is modeled according to (4-2). The cable capacitance is in this case omitted. For the study of the low frequency conducted disturbances (i.e. within a frequency range 50 Hz – 2.5 kHz) this assumption can be made without a big influence on the modeling exactness [83].The transformer model is based on the assumption that its X/R ratio is constant over the studied frequency range, like in (4-4) with the vector group being modeled.

Such a formulated model is used to carry out the harmonic propagation study in the examined case using a harmonic simulation program [87]. The non-linear load representation consists of the harmonic spectrum of the welder current according to the data obtained from direct measurements. Introducing no other non-linear devices to the modeled system the information of the distortion injected by the single machine to the system can be obtained. Measurements and simulations of the welder current spectrum and the resulting voltage distortion on both ends of the supply cable are the subject of closest considerations in this section with regard to the question if and how the system elements modeling has an influence on the modeling exactness.

4.2.1 Distortion level profile determination at the welder connection bus

Using the measurement system described in the previous chapter long-term measurements of the quasi-stationary harmonics at the building substation (Fig. 4.4) were made to evaluate the harmonic "noise" in the supply voltage. The welder was not present during these measurements. Over the set of measurements a daily profile was created utilizing statistical distribution functions. From the measurement sets a grouping procedure was carried out to build 32 classes [45] and then according to the standard [45] a quantile of the rank 0.95 was calculated for every data set established during these quasi-stationary harmonic measurements.

Fig. 4.5 presents an exemplary daily profile of the *THD* factor for voltage and its main component the 5th harmonic (3rd being small) over a working day in one of the phases at the bus A. The profile was then used in case studies presented in following sections. It should be noted that this type of profile, with a characteristic higher level of 5th harmonic that has maximum in the night and minimum in the morning hours, has been measured also at other substations within this distribution system. A near look over the measurement survey will be given in Chapter 5.

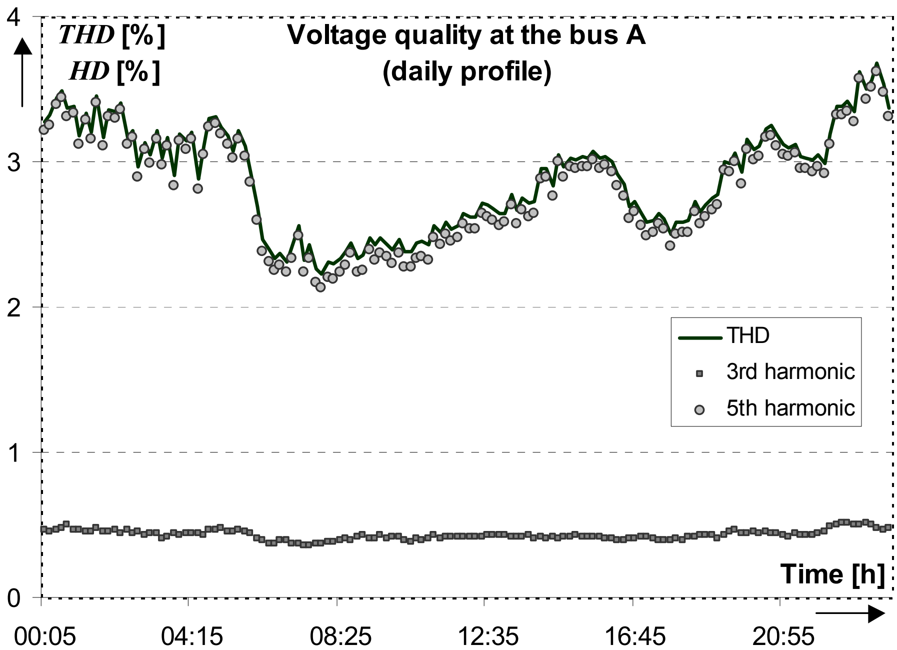

Fig. 4.5 Daily voltage quality profile at the bus A (no welder present)

4.2.2 Synchronized measurements - arrangement

To investigate the influence of non-linear loads on the voltage quality drop in a distribution system an industrial resistance welder – a pulsed power device - was installed in the laboratory room in one of the university buildings. This single-phase device with the maximal power of 350 kVA was supplied from the building substation via a separate low voltage cable with the length of about 100 m, so that the installation of the metering system was possible both at the device' clamps and the substation without any other load hanging on that cable [90]. The substation is a part of the university distribution system, a diagram representing the middle voltage network and its simplification used for the model is presented in Fig. 4.4.

The synchronous measurements were arranged as in Fig. 4.6. Four–channel oscilloscopes LeCroy AL584 and LeCroy 9314A were installed on both ends of the cable which supplied the welder: One at the device's clamps and the other at substation A (Fig. 4.6). The input channels were provided with signals coming from voltage differential probes Tektronix P5200 and Agilent N2772A and from current probes Tektronix A621 and Tektronix A6302. Synchronous triggering was realized through the trigger function on the current flank. The voltage signals were collected according to Fig. 4.6. This additionally enables one to measure the influence of the welder on the voltage at other, far buses in the system, e.g. bus B. The binary data recorded on both oscilloscopes over 100 ms were converted into ASCII files which then were used to calculate the quantities at each measuring point using Matlab's program involving FFT.

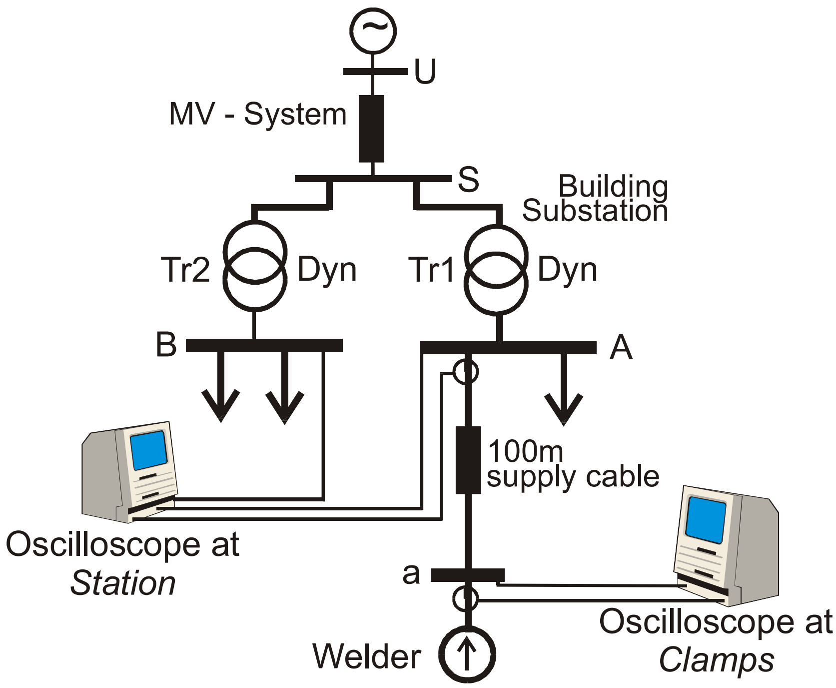

Fig. 4.6 Measurement setup in the studied distribution system

4.2.3 Voltage quality study – comparison simulations and measurements

The disturbances introduced by the welding device vary in accordance to changes in the welding power and influence the voltage quality at the substation bus. Fig. 4.7 presents the 3rd and 5th harmonic level measured at the device's clamps (point a in Fig. 4.6) and at the station (point A in Fig. 4.6) as a function of the device's welding power. It is interesting to see that the maximum distortion introduced by this machine into the supply voltage (Fig. 4.7) lies near the point of 40-50 % of the machine's maximal welding power and consists mainly of the 3rd harmonic.

The 3rd harmonic dampening along the cable is nearly constant over the whole power range, but the 5th dampening varies. This is because of the interaction between the 5th harmonic component present in the supply voltage (Fig. 4.5) and the component introduced by the welder. Due to the phase differences between them, i.e. the harmonic cancellation effect, the dampening has irregular values. This effect is then the main error source in the model described in following.

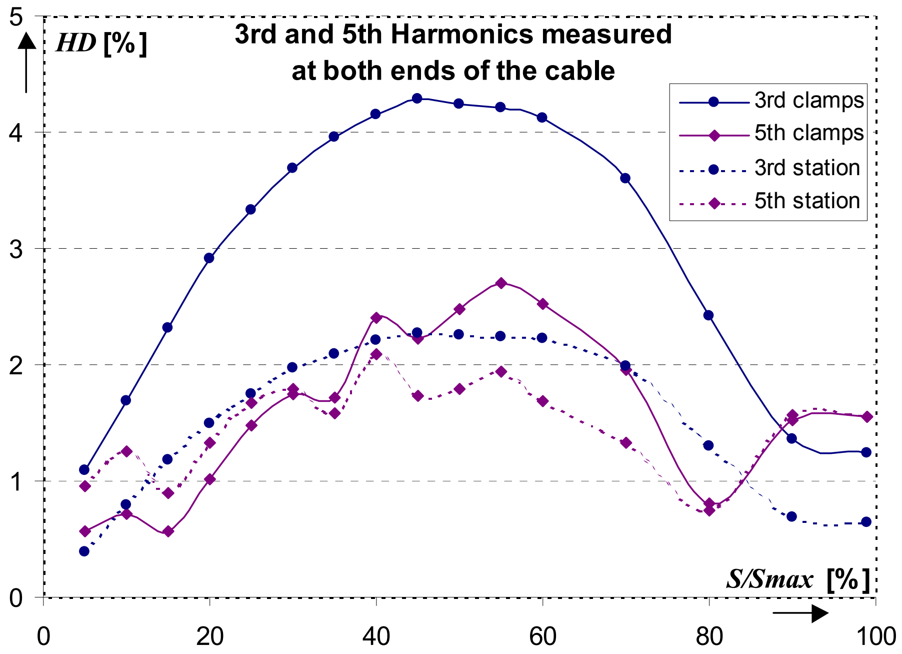

Fig. 4.7 Harmonic content of the voltage measured at the clamps (a) and station (A)

The simulations described here were made under the assumption that there is no harmonic noise present in this system. In other words, the supply voltage was assumed to be clear to receive its reaction only on that device. Furthermore, the differences between simulation and the real case can be obtained to clarify the influence of the background distortion.

Keeping in mind that in the voltage supplying the welder the biggest harmonic was the 5th (Fig. 4.5) the fact of the slight difference between measured and simulated curve can be explained (Fig. 4.8). The welder introduces more 5th component in the range of 50-70 % of maximal welding power. The difference between simulation and measurements is in this range bigger than for other power values. Again, the cancellation effect, not considered in the model, is responsible for these erroneous results.

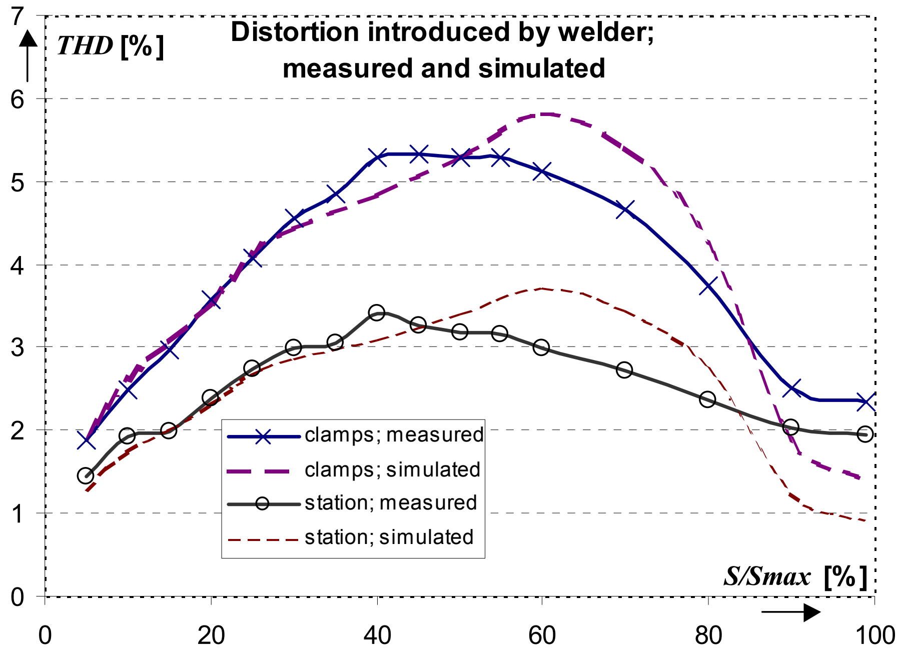

Fig. 4.8 Comparison between measurements and simulation results: Voltage distortion at both ends of the supply cable (points A, a in Fig. 4.6)

For the pathway: system-station-cable-load (U-S-A-a in Fig. 4.6) several cases were simulated to obtain the sensitivity of the solution to the model parameter changes. Also, the influence of the ratio power of device to short-circuit power at the substation A was examined. In the real system the short-circuit power to device power ratio is close to 100. Therefore, the distortion present at the station is not critical (Fig. 4.8). The harmonic voltage transported upstream (calculated at bus B, Fig. 4.6) is within a range 0.12 - 0.25 % *THD* (with the main 5th component – the propagation of the triple harmonic orders through *Dyn* transformers was blocked). During measurements the effect of the welder on the voltage distortion at substation B was not observable due to background "noise" – in this case around 2.5 % *THD* with the 5th harmonic as the main component (Fig. 4.5).

Fig. 4.9 presents the case study considerations, when the length of the cable, its frequency dependency and the short-circuit power at the substation were changed.

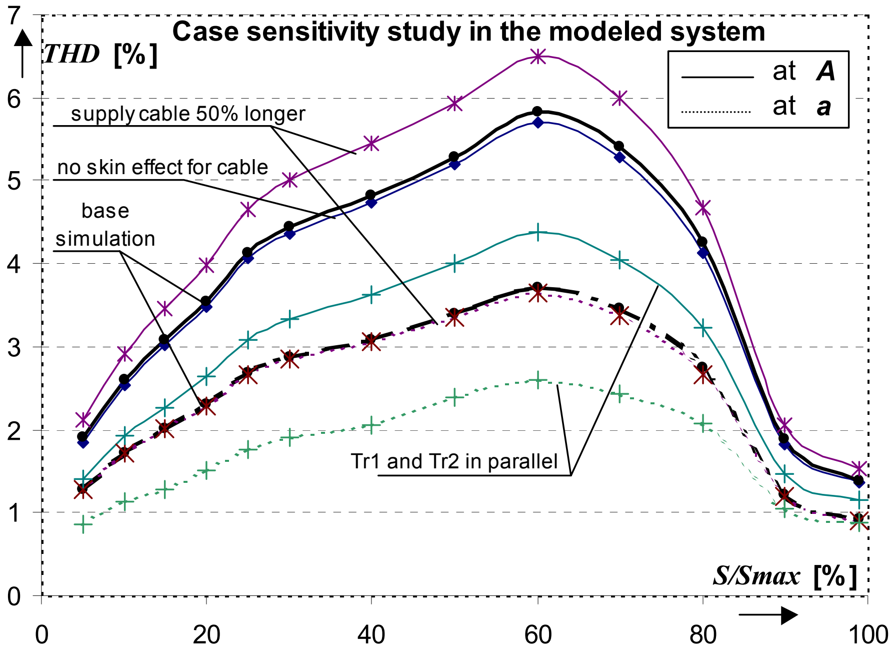

Fig. 4.9 Influence of the model parameter on the harmonic distortion at the clamps (a) and at the bus (A)

The problem with the upstream propagation can arise when the short-circuit power to load ratio decreases. This happens when the short-circuit power at substation decreases (smaller transformer) or the number of the load increases (many welders). The increase of the short circuit power (Tr1 and Tr2 in parallel) causes a reduction in the distortion over the system (Fig. 4.9). The variation of the supply cable length has considerable influence only on the *THD* at the clamps (Fig. 4.9). The inclusion of the skin effect in the low voltage cable model only minimally changes the results compared to the cases of length variation and short-circuit power modification.

The influence of the background harmonic content was reduced to the 5th harmonic, because in the studied system this one has the highest values, standing alone for the *THD* over the substations. The distortion emanated from the welder device comes mainly from the triple harmonics. Therefore, its propagation is blocked by the delta-star-ground step-down transformers. However, careful attention should be paid to the ground (neutral) cable which can be easily overheated in the case of multiple devices. In any case its diameter should be reduced (compared to the phase cable diameter).

4.3 DISTRIBUTION NETWORK - NON-LINEAR LOAD INTERACTION MODELING USING CROSSED FREQUENCY ADMITTANCE MATRIX

The improvement of the harmonic effect calculations can be achieved by including an interaction effect in the model that takes place, especially in weak networks between the non-linear, harmonic producing load, and the network through its impedance. In this work construction of a crossed frequency admittance matrix (CFA-Matrix) is presented for the non-linear load – a resistive welder. The basic algorithm for computation of a CFA-Matrix for non-linear loads representation was proposed in [91]. The method presented in [91] involves physically-based load modeling using direct measurement by a network simulation amplifier and is therefore limited to small consumer loads, like electronic ballasts, small induction motors or fluorescent lamps. The following applications of the method have been developed to describe electronically controlled loads [92], to decompose the load structure at the distribution level [93]. But all the presented approaches are limited to components with a small power ratio, and therefore only applicable to a limited set of distribution loads [94]. In this work an extension of this approach has been developed for non-linear load modeling with higher power ratio. This method utilizes a combined measurement-simulation approach to construct the CFA-Matrix for the source-sink representation of a resistive welding machine (source) with a maximal power of about 350 kVA that is connected directly to a distribution feeder (sink) (Fig. 4.10).

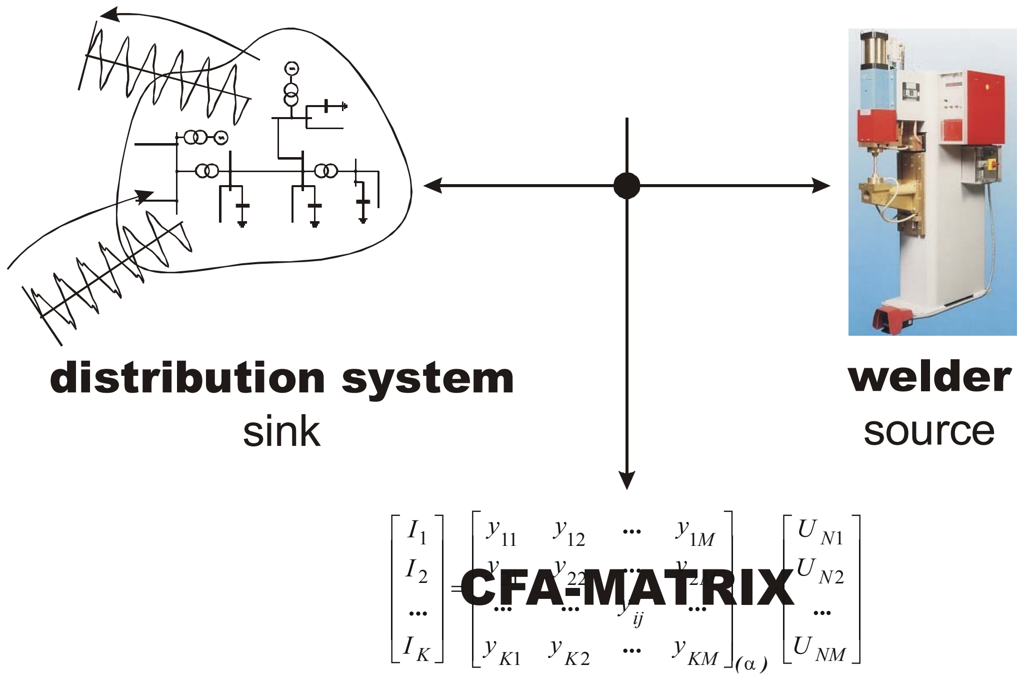

Fig. 4.10 Coupling representation for distribution network (sink for disturbance) – load (source of disturbance)

4.3.1 Algorithm of the method

In general, the distribution network voltage possesses a certain portion of waveform distortion in the form of harmonics, and, additionally, the network impedance varies in accordance to the load changes present both down and upstream of the distribution feeder. On the other hand, non-linear, electronically controlled loads that are connected to the network inject harmonic currents that are dependent on the supply voltage harmonic contents and magnitude. The inclusion of this effect can not be achieved using load models as in classical harmonic studies in frequency domain. The solution in harmonic domain is in such cases indispensable because this type of harmonic model takes into account the harmonic influence between harmonic currents and harmonic voltages of different orders. The harmonic domain solution with the help of the CFA-description is proposed in this work to acquire detailed information of the harmonic or inter-harmonic distortion at the points of special interest. The proposed method can be seen as a complementary one to the method of the whole system sensitivity study that is described in Chapter 5.

The algorithm of the proposed CFA-based approach covers measurements on the physical object, mathematical procedure for parameter identification of a non-linear load, modeling process of the load to acquire its characteristic at different network parameters and finally, the basic procedure for CFA-Matrix computation. The structure of the algorithm is presented in Fig. 4.11.

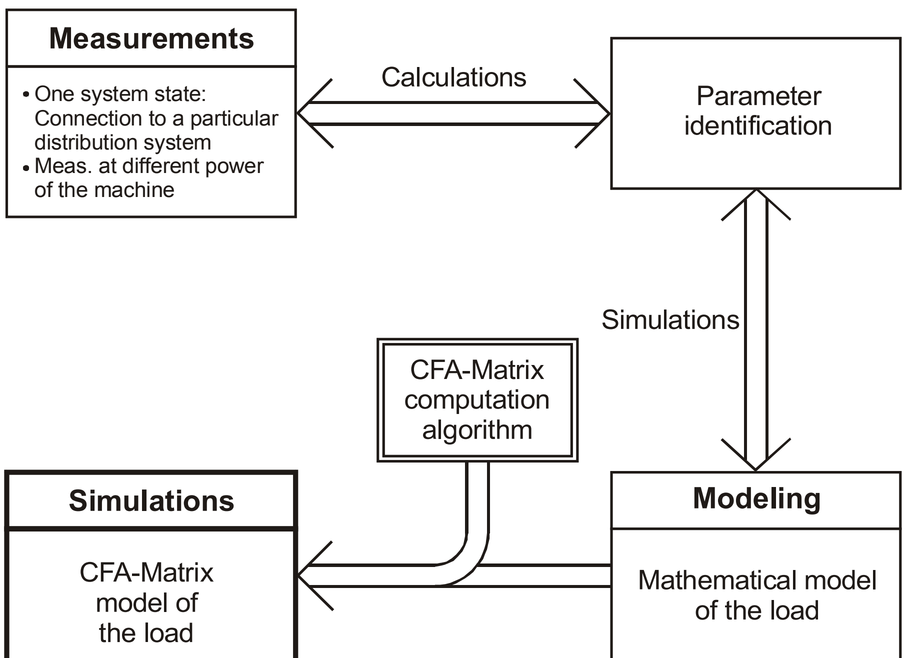

Fig. 4.11 The algorithm of the CFA- Matrix constructing process used for high power non-linear load representation

The parameter identification procedure is carried out in the first stage. This is essential for reflecting the influence of the machine's working-point, i.e. its actual welding power and material being welded, on the clamp-behavior of the welder. The goal here is to develop the welding machine model as non-linear impedance, seen from the clamps of the machine. A transmittance based procedure is used to model the clamp-behavior of the welder. In the next step the Matlab-Simulink® model of the welder is used to construct the CFA-Matrix during the simulation stage. Consecutively, the CFA-Matrix is extended by the network impedances.

4.3.2 Parameter identification procedure and the transmittance model of the resistance welding machine

In order to develop the device model that acquires different secondary load configurations of the machine, clamps currents and voltages of the welding machine were measured and evaluated for the chosen load configurations. As an example, the short-circuit - no metal being welded - configuration was used in the following considerations. Other welding configurations, for different metal sheets and plates, have been measured as well. The corresponding differences in the model structure are then indicated at the respective positions in the text.

The measuring arrangement is presented in Fig. 4.12. The welder is connected between phases L1 and L2 to reach greater welding currents. This is a standard connection as it is in an industrial system. The electrical quantities that were measured are represented in Fig. 4.12 by dotted circles.

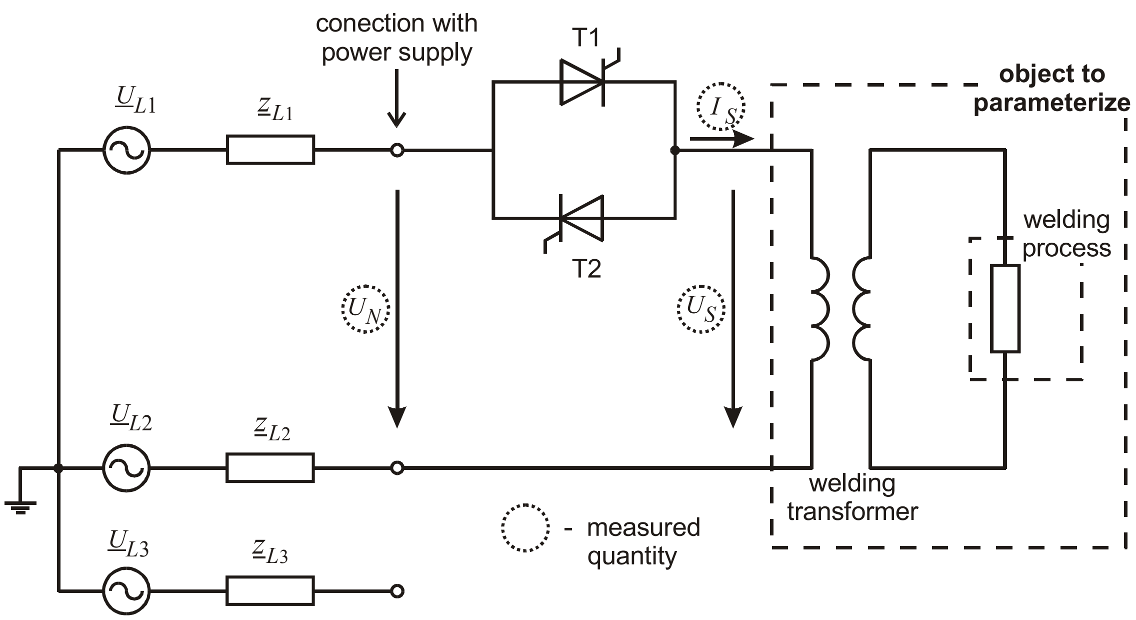

Fig. 4.12 Measuring arrangement for the identification of the welding process' parameters

The single-phase device draws currents from the network with a pulse rise of 0.5 A/µs (Fig. 4.3). The maximal apparent power of S_{max} = 350 kVA classifies it to the significant loads among loads at the distribution level.

The goal in the first stage of the method is to represent the welding machine as variable, non-linear impedance, as seen from the connection terminals. Since the exact data of the welding transformer (Fig. 4.12) is unknown and the welding process cannot be easily reproduced due to its stochastic behavior the transmittance-based approach was chosen to parameterize the welding process (Fig. 4.13). Moreover, the usage of the transmittance-based procedure in the modeling process allows for simulating the behavior of the load as a function of supply voltage parameters (magnitude and harmonic contents). It was assumed that the welding process can be characterized by the transmittance that is determined by the current $\underline{I}_S$ and the voltage $\underline{U}_S$. A schematic transformation of the structure is presented in the following figure.

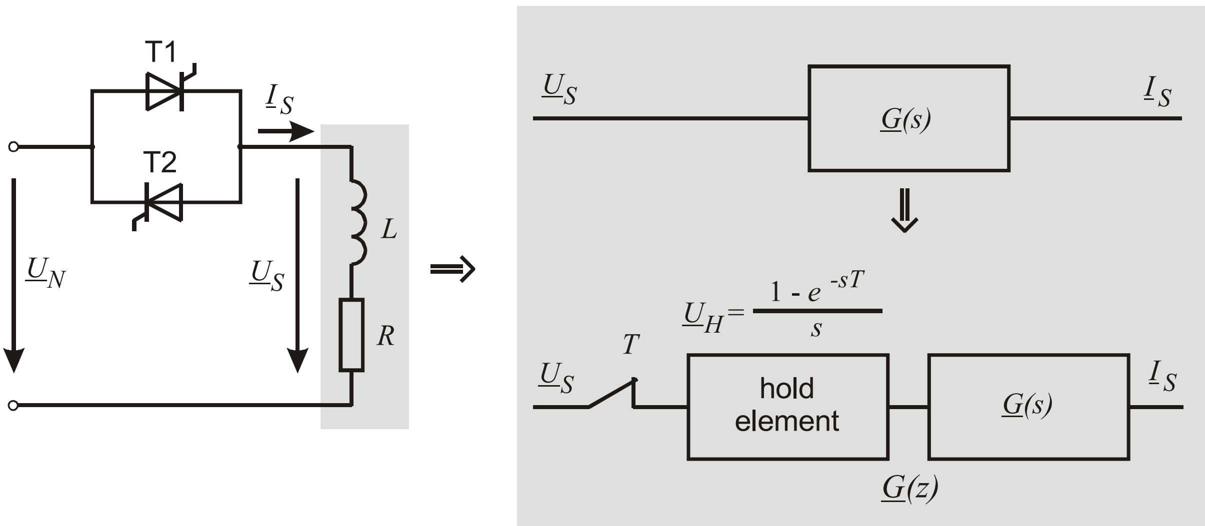

Fig. 4.13 Parameterization of the welding machine and transmittance based procedure for the measurement-based parameter identification

The welding process is characterized by an electrical load with quantities L and R (Fig. 4.13). Equation (4-5) describes the simple circuit:

$$u_S(t) = Ri_S(t) + L\frac{di_S(t)}{dt}. \tag{4-5}$$

The Laplace transformation of (4-5) leads to the expression (4-6):

$$\underline{U}_S(s) = R\underline{I}_S(s) + sL\underline{I}_S(s). \tag{4-6}$$

The transmittance that arises from (4-6) can be described in (4-7):

$$\underline{G}(s) = \frac{\underline{I}_S(s)}{\underline{U}_S(s)} = \frac{1}{R}\frac{\frac{R}{L}}{s+\frac{R}{L}} = \frac{1}{R}\frac{a}{s+a}, \tag{4-7}$$

where $a = R/L$. As a consequence of the measuring system used only digital signals are available for the identification process. Therefore, the continuous s-transmittance is transferred into the discrete domain (Fig. 4.13) by $\mathcal{Z}$-transformation as in (4-8):

$$\underline{G}(z) = \mathcal{Z}\left\{(1-e^{-sT})\frac{\underline{G}(s)}{s}\right\}, \tag{4-8}$$

where T is the sampling period.

From (4-8) follows the discrete transmittance (4-9):

$$\underline{G}(z) = \frac{\underline{I}_S(z)}{\underline{U}_S(z)} = \frac{1}{R}\frac{z-1}{z}\frac{z(1-e^{-aT})}{(z-1)(z-e^{-aT})} \Rightarrow \underline{G}(z) = \frac{1}{R}\frac{1-e^{-aT}}{z-e^{-aT}}. \tag{4-9}$$

The counter and the denominator of (4-9) are multiplied by z^{-1} in (4-10) to account for the hold element in Fig. 4.13:

$$\underline{G}(z) = \frac{\underline{I}_S(z)}{\underline{U}_S(z)} = \frac{\frac{1}{R}(1-e^{-aT})z^{-1}}{1-e^{-aT}z^{-1}}. \tag{4-10}$$

The equation (4-10) serves as the basis for the parameter identification of the welding process. In shorter form (4-10) can be written, as in (4-11):

$$\underline{I}_S(z) = e^{-aT}z^{-1}\underline{I}_S(z) + \underline{U}_S(z)\frac{1}{R}(1-e^{-aT})z^{-1}, \tag{4-11}$$

where $a_1 = e^{-aT}$ and $b_1 = \frac{1}{R}(1-e^{-aT})$. Representing (4-11) in time domain as in (4-12):

$$\underline{I}_S(kT) = a_1\underline{I}_S((k-1)T) + b_1\underline{U}_S((k-1)T), \tag{4-12}$$

with crms voltages and currents, the vector form (4-13) of the digital measured signal can be written:

$$\begin{bmatrix} \underline{I}_s(2T) \\ \underline{I}_s(3T) \\ \underline{I}_s(4T) \\ \underline{I}_s(5T) \\ .. \end{bmatrix} = \begin{bmatrix} \underline{I}_s(T) & \underline{U}_s(T) \\ \underline{I}_s(2T) & \underline{U}_s(2T) \\ \underline{I}_s(3T) & \underline{U}_s(3T) \\ \underline{I}_s(4T) & \underline{U}_s(4T) \\ .. & .. \end{bmatrix} \cdot \begin{bmatrix} a_1 \\ b_1 \end{bmatrix}. \tag{4-13}$$

For the identification of the process parameters an algorithm was applied that is based on the least-squares method. The identified parameters are presented in Fig. 4.14 as a function of the welding power of the machine. It can be seen that the parameters have different values at different power levels of the machine and this dependency changes non-linearly. This makes the acquisition of the CFA-Matrix cumbersome, because for each working point of the machine (i.e. each output power) new R and L have to be considered and that results in a different CFA-Matrix for each working point of the process.

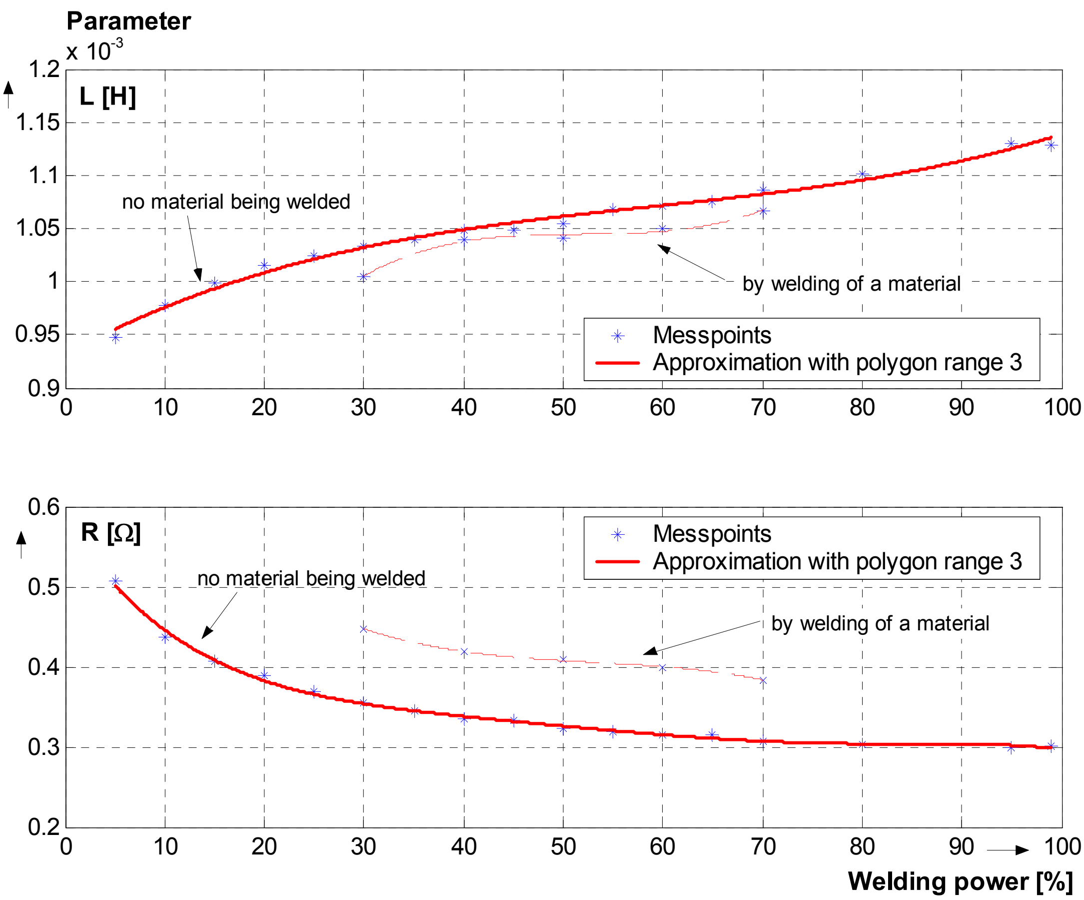

Fig. 4.14 Parameter L and R identified as a function of the welding power, for the short circuit welding condition and during the welding process of a metal plate

The influence of the material used can be seen clearly for the resistance, which finds its explanation in the conductivity of the material. The influence of the material used on the estimated inductance is small.

4.3.3 Derivation of a CFA matrix for the resistance welding machine

The next stage includes simulations within the Matlab-Simulink model in order to compute the CFA-Matrix. Since the network simulation amplifiers do not have enough output power to supply such a big device and there was no possibility to change the parameters of the supply voltage in the distribution network, the simulations have been carried out in a Matlab-Simulink environment. The computation algorithm is based on the assumption that the output current of the welder is a non-linear function of the supply voltage and the load behavior can be simulated around its working point by the CFA-Matrix $\underline{\boldsymbol{Y}}_{CFA}$, that will reflect the cross-frequency influence of the supply voltage on the current that is injected by the machine. This can be shortly noted as in (4-14):

$$\underline{\boldsymbol{i}}_S = F(\underline{\boldsymbol{u}}_N, \alpha) \Rightarrow \underline{\boldsymbol{i}}_S = \underline{\boldsymbol{Y}}_{CFA(\alpha)} \underline{\boldsymbol{u}}_N , \tag{4-14}$$

where α is a firing angle of the thyristors in the welder, $\underline{\boldsymbol{i}}_S$ and $\underline{\boldsymbol{u}}_N$ being the column vector of rms currents and voltages, respectively (Fig. 4.12). This can be interpreted as a transformation of the non-linear function F into the linear dependence of current and voltage in the form of the matrix $\underline{\boldsymbol{Y}}_{CFA}$ around each operation point of the machine. Writing again the right side of (4-14) $\underline{\boldsymbol{Y}}_{CFA(\alpha)}$ can be represented by (4-15):

$$\begin{bmatrix} \underline{I}_1 \\ \underline{I}_2 \\ \cdots \\ \underline{I}_K \end{bmatrix} = \begin{bmatrix} \underline{y}_{11} & \underline{y}_{12} & \cdots & \underline{y}_{1M} \\ \underline{y}_{21} & \underline{y}_{22} & \cdots & \underline{y}_{2M} \\ \cdots & \cdots & \underline{y}_{ij} & \cdots \\ \underline{y}_{K1} & \underline{y}_{K2} & \cdots & \underline{y}_{KM} \end{bmatrix}_{(\alpha)} \cdot \begin{bmatrix} \underline{U}_{N1} \\ \underline{U}_{N2} \\ \cdots \\ \underline{U}_{NM} \end{bmatrix}, \tag{4-15}$$

where K and M denote the maximal order of the analyzed current and voltage harmonic order, respectively. The element $\underline{y}_{ij}$, on the diagonal being $i = j$, describes in general the connection between the i^{th} ($i \in <1,K>$) current harmonic and the j^{th} ($j \in <1,M>$) voltage harmonic.

The following example can be used to describe the meaning of the elements of the CFA-Matrix. Assuming that the matrix is set up for only two harmonic orders, i.e. $K = M = 2$, (4-15) will be then reduced to (4-16):

$$\begin{bmatrix} \underline{I}_1 \\ \underline{I}_2 \end{bmatrix} = \begin{bmatrix} \underline{y}_{11} & \underline{y}_{12} \\ \underline{y}_{21} & \underline{y}_{22} \end{bmatrix}_{(\alpha)} \cdot \begin{bmatrix} \underline{U}_{N1} \\ \underline{U}_{N2} \end{bmatrix}, \tag{4-16}$$

or in open form as in (4-17):

$$\begin{aligned} \underline{I}_1 &= \underline{y}_{11} \cdot \underline{U}_{N1} + \underline{y}_{12} \cdot \underline{U}_{N2} \\ \underline{I}_2 &= \underline{y}_{21} \cdot \underline{U}_{N1} + \underline{y}_{22} \cdot \underline{U}_{N2} \end{aligned}, \tag{4-17}$$

the following conclusions can be made: The element $\underline{y}_{11}$ describes the effect of changes of the first harmonic of the voltage on the first harmonic of the current. The element $\underline{y}_{12}$ describes the effect of changes of the second harmonic of the voltage on the first harmonic of the current. The element $\underline{y}_{21}$ describes the effect of changes of the first harmonic of the voltage on the second harmonic of the current and, finally, the element $\underline{y}_{22}$ describes the effect of changes of the second harmonic of the voltage on the second harmonic of the current. These connections can be formed for arbitrary dimensions of the CFA-Matrix.

The computation algorithm for the derivation of the CFA-Matrix from the developed model is realized in the following steps:

a) At first the simulation with a purely sinusoidal input voltage is carried out to compute the column admittance vector $\underline{\mathbf{y}}_{K1}$ for the fundamental mode, where its element $\underline{y}_{i1}$ ($i \in \langle 1,K \rangle$) can be expressed like in (4-18):

$$\underline{y}_{i1} = \frac{\underline{I}_i}{\underline{U}_{N1}}, \tag{4-18}$$

where $\underline{I}_i$ is the rms current value of the i^{th} current harmonic, $\underline{U}_{N1}$ is the rms fundamental component of the voltage. Therefore, the vector $\underline{\mathbf{y}}_{K1}$ is the fundamental mode component that connects the i^{th} harmonic of the current with the first harmonic of the supply voltage, i.e. it is the first column of the CFA-Matrix computed, like in (4-19):

$$\begin{bmatrix} \underline{I}_1 \\ \underline{I}_2 \\ \cdots \\ \underline{I}_K \end{bmatrix} = \begin{bmatrix} \underline{y}_{11} \\ \underline{y}_{21} \\ \cdots \\ \underline{y}_{K1} \end{bmatrix} \cdot \underline{U}_{N1}. \tag{4-19}$$

b) The second step includes the simulations with a supply voltage that has harmonic contents. The simulations are carried out in series, each one at the different current harmonic orders, i.e. according to the pattern: {(3,1), (5,1), (7,1), ...}, so that the non-diagonal components $\underline{y}_{ij}$ ($i \neq j$) of the CFA-Matrix are computed, in accordance to (4-20):

$$\underline{y}_{ij} = \frac{\underline{I}_i - \underline{y}_{i1}\underline{U}_{N1}}{\underline{U}_{Nj}}, \tag{4-20}$$

where $\underline{U}_{Nj}$ is the rms voltage of the j^{th} harmonic, $\underline{y}_{ij}$ is the elements that connects i^{th} harmonic of the current, which is caused by j^{th} voltage harmonic. The supply voltage in the model is represented as a complex value since a change of phase leads to the change of CFA-Matrix computed currents.

In order to include network impedance into the calculations (Fig. 4.15), the following extension to the algorithm was applied.

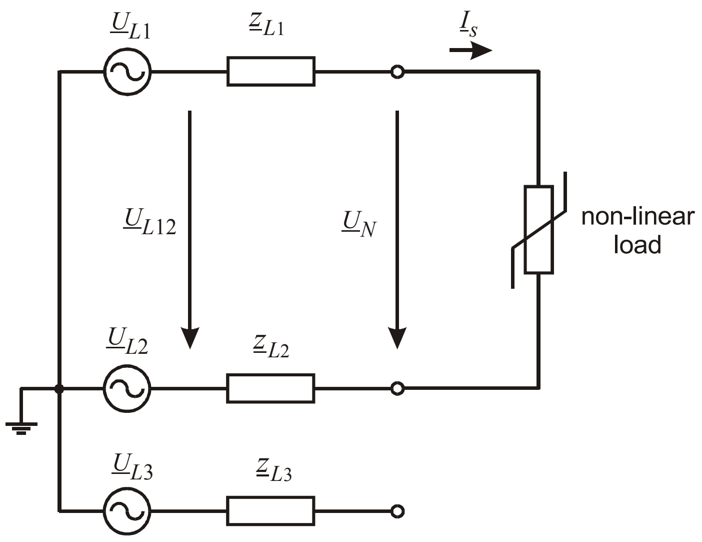

Fig. 4.15 The nonlinear load modeled with the impedance of a distribution network

The rms quantities shown in Fig. 4.15 can be described by the expression (4-21):

$$\underline{U}_{L12} = (\underline{z}_{L1} + \underline{z}_{L2}) \cdot \underline{I}_S + \underline{U}_N \,, \tag{4-21}$$

where $\underline{z}_{L1}$ and $\underline{z}_{L2}$ are the phase-to-ground impedance of the network for the fundamental frequency. Inserting expression (4-15) to (4-21) and building the phase-to-ground diagonal impedance matrices $\underline{\boldsymbol{Z}}_{L1}$ and $\underline{\boldsymbol{Z}}_{L2}$ for each considered harmonic orders leads to (4-22):

$$\underline{\boldsymbol{u}}_{L12} = (\underline{\boldsymbol{Z}}_{L1} + \underline{\boldsymbol{Z}}_{L2}) \cdot \underline{\boldsymbol{Y}}_{CFA(\alpha)} \cdot \underline{\boldsymbol{u}}_N + \underline{\boldsymbol{u}}_N \,, \tag{4-22}$$

where $\underline{\boldsymbol{u}}_{L12}$ and $\underline{\boldsymbol{u}}_N$ are column vectors of voltages containing rms voltage values for corresponding harmonic orders. After a manipulation of (4-22) expression (4-23) can be obtained:

$$\underline{\boldsymbol{u}}_N = (\underline{\boldsymbol{Z}}_{L12} \cdot \underline{\boldsymbol{Y}}_{CFA(\alpha)} + \boldsymbol{1})^{-1} \cdot \underline{\boldsymbol{u}}_{L12} \,, \tag{4-23}$$

where $\underline{\boldsymbol{Z}}_{L1} + \underline{\boldsymbol{Z}}_{L2} = \underline{\boldsymbol{Z}}_{L12}$. From this follows expression (4-24) for the current vector:

$$\underline{\boldsymbol{i}}_S = \underline{\boldsymbol{Y}}_{CFA(\alpha)} \cdot (\underline{\boldsymbol{Z}}_{L12} \cdot \underline{\boldsymbol{Y}}_{CFA(\alpha)} + \boldsymbol{1})^{-1} \cdot \underline{\boldsymbol{u}}_{L12} \,. \tag{4-24}$$

The network impedance matrix, $\underline{\boldsymbol{Z}}_{L12}$, in (4-24) is a diagonal matrix, since within the network the harmonic orders do not influence each other. The values for the network impedance result from the calculations that have been described in section 4.2 of this chapter. The values must be determined separately for each node of the distribution network [91].

Fig. 4.16 shows a complete Matlab-Simulink model with network impedance.

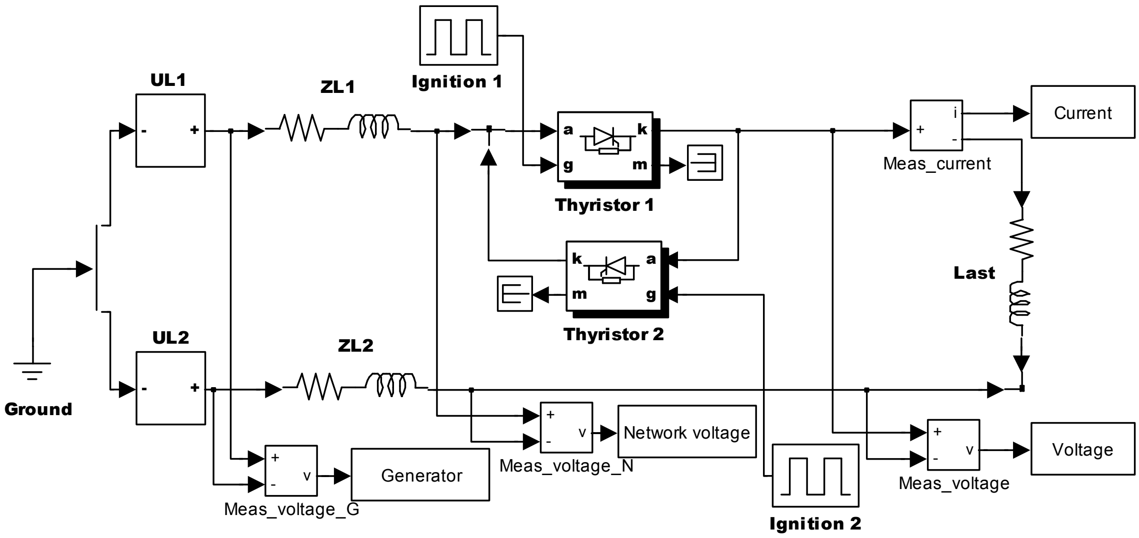

Fig. 4.16 Model of the welding machine with the identified parameters and network impedance

As an example, expression (4-25) shows the CFA-Matrix calculated for 60 % of the welding power:

$$\underline{Y}_{CFA\_60\%} = \begin{bmatrix} 0.6363 - 1.1582i & 0.3192 - 0.3293i & -0.2013 + 0.2227i & 0.0538 - 0.0777i \\ 0.1828 - 0.2564i & 0.3077 - 0.5697i & -0.0149 - 0.2022i & -0.0057 + 0.1030i \\ -0.0405 + 0.1155i & -0.0423 - 0.2037i & 0.1422 - 0.4036i & 0.0045 - 0.1102i \\ -0.0013 - 0.0327i & 0.0083 + 0.1209i & -0.0152 - 0.1120i & 0.0494 - 0.3019i \end{bmatrix} \quad (4\text{-}25)$$

Based on the calculations that have to be performed at each working point the influence of the supply voltage parameters changes on the behavior of the current that the welder injects into the network can be studied. Figures Fig. 4.17, Fig. 4.18, Fig. 4.19 and Fig. 4.20 show the changes of the disturbance emission by the change of the most important supply voltage parameters for practical situations. The calculations have been made assuming that the machine works with 60 % of the welding power.

The influence of the 5th harmonic supply voltage changes on the $THDi$ of the machine current (Fig. 4.17) show that a considerable dependency of the disturbance that are emitted by the machine exists. In a real situation the level of the 5th harmonics in the supply voltage reach 3 .. 6 % with varying phases. The closest look at current emission injection in this range enables one to estimate this emission properly within a range of the phase and amplitude variation of the 5th voltage harmonic.

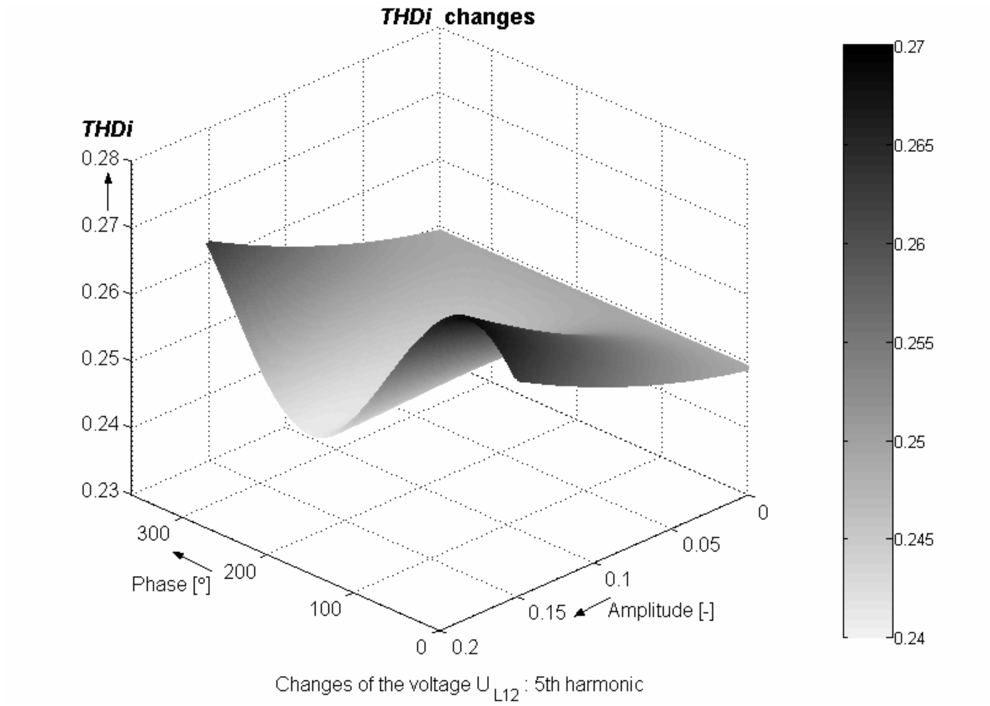

Fig. 4.17 Influence of the 5th harmonic voltage $\underline{U}_{L12}$ changes on the *THDi* of the current drawn by the machine

A sample result describing the influence of the 5th harmonic voltage changes on the first harmonic current drawn by the machine is presented in Fig. 4.18.

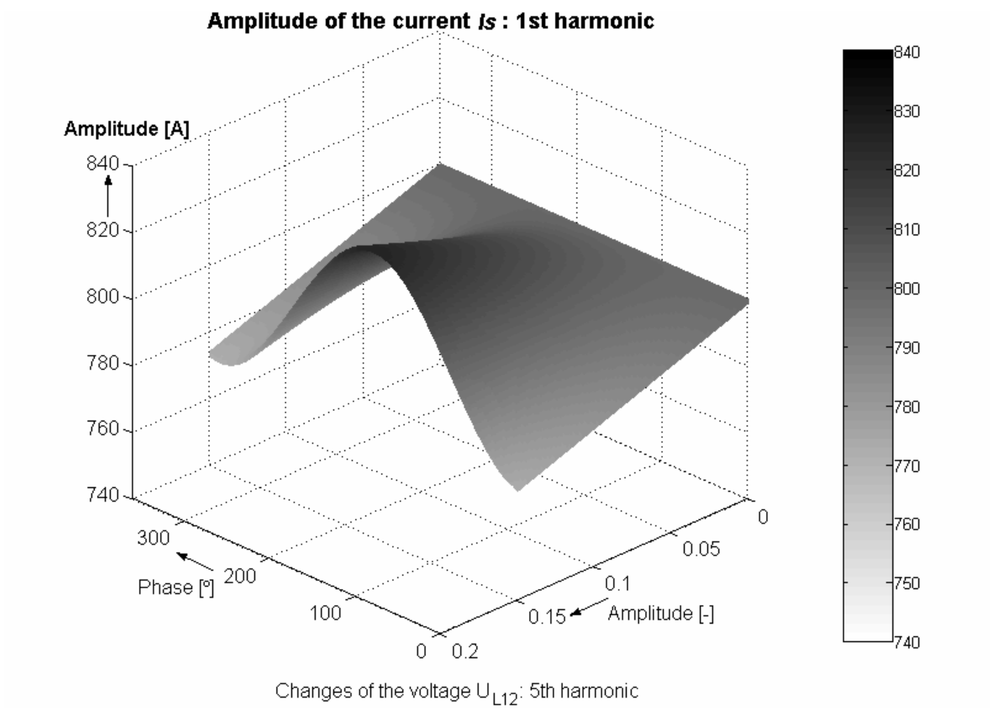

Fig. 4.18 Influence of the 5th harmonic voltage $\underline{U}_{L12}$ changes on the first harmonic current drawn by the machine

Again, the influence of the 5th voltage harmonic on the fundamental current can be clearly seen in Fig. 4.18. The current that is drawn by the welder at fundamental frequency is strongly dependent on the phase of the 5th supply voltage harmonic. This dependency is stronger for higher levels of this harmonic. The differences can be observed by comparing this effect with the influence that is induced by other harmonic orders, like the 3rd (Fig. 4.19) or 7th (Fig. 4.20).

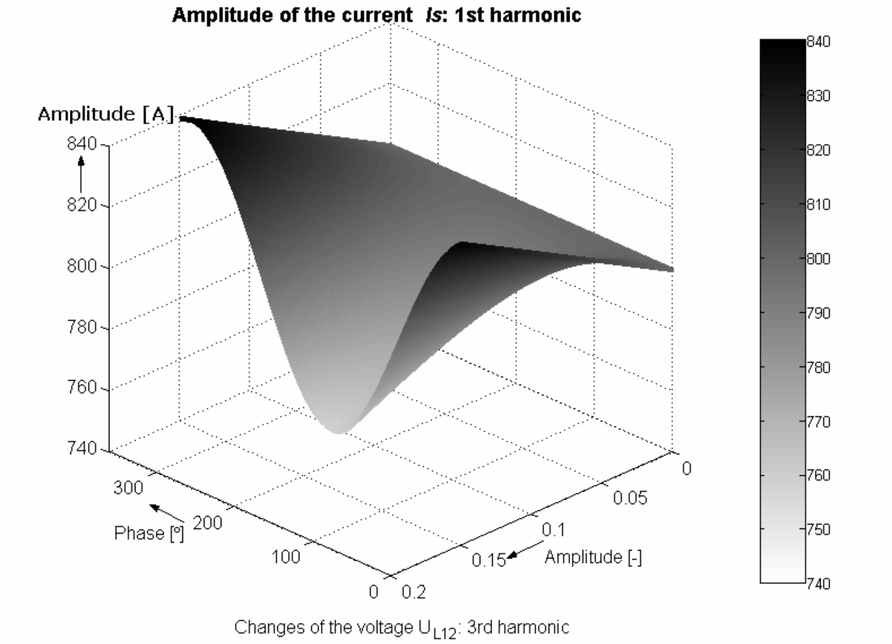

Fig. 4.19 Influence of the 3rd harmonic voltage $\underline{U}_{L12}$ changes on the first harmonic current drawn by the machine

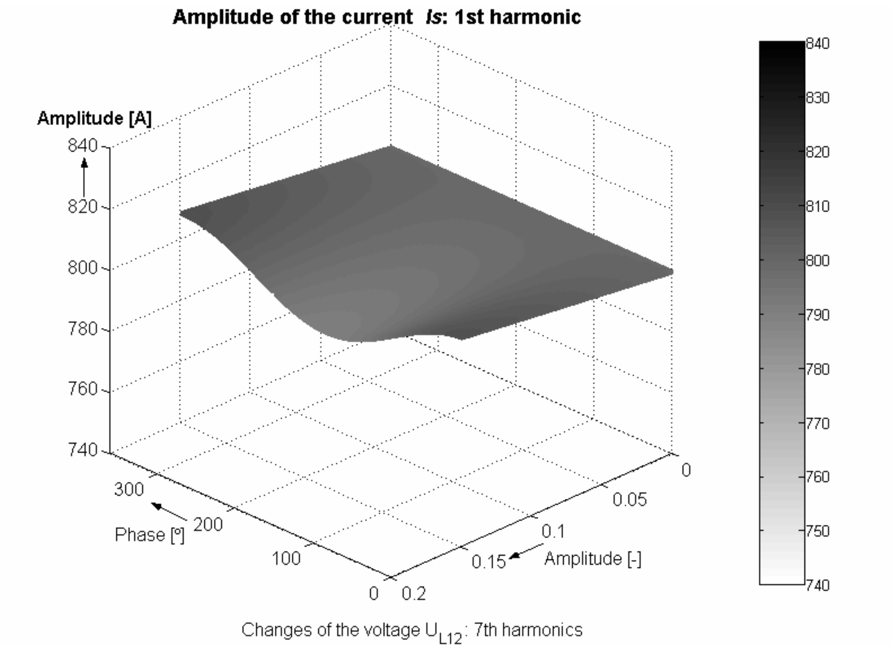

Fig. 4.20 Influence of the 7th harmonic voltage $\underline{U}_{L12}$ changes on the first harmonic current drawn by the machine

The 3rd harmonic of the supply voltage has a stronger effect on the fundamental current demanded by the welder, than the 5th, the changes of the 7th supply voltage harmonics influence the current only in a small amount. However, the phase dependency is maintained (Fig. 4.20). The impact of the higher harmonic orders of the voltage supply, not shown here, is correspondingly smaller.

In this way, the complete analysis can be carried out to quantitatively study the effects of the supply voltage harmonic contents on the harmonic emission of the non-linear load.

This type of modeling can be difficult for distribution system analysis in which many types of non-linear loads have a big influence on the voltage quality. Therefore, another method should first be applied to determine the most important places in the system to which much attention should be paid and which can then be analyzed with the help of CFA-Matrix method which was proposed in this chapter. The analysis method to make an entire overview of the potential problems that can arise is the topic of the next chapter.

5 SUSCEPTIBILITY ANALYSIS OF POWER NETWORKS TO CONDUCTED DISTURBANCES USING EIGENVALUES AND EIGENVECTORS

During operation, an electric power system is exposed to large and small external disturbances and responds to them by variation in state variables [95], [96]. Disturbances can occur at different places of the power system, and as a rule, produce a reaction of voltage magnitudes and phases at the same nodes, and, very often, due to the resonance phenomena a reasonable reaction at other, even remote, nodes. The response depends on the set of disturbances, their magnitude and such state-invariant factors as topology and parameters of the network elements, i.e. its inherent structure.

The analysis method proposed in this work is an active one that forecasts potentially susceptible nodes, which can be affected by harmonics or interharmonics, treated in this context as disturbances. The information included in the network structure, properly modeled and subjected to the eigenvalue analysis is, in the author's opinion, sufficient to claim a right to be a profitable analysis tool in the power quality area. One of the biggest advantages of the proposed analysis comparing it with statistical trials including separate simulations of every case is, above the significant time-reduction, the extraction property of the method. The method picks out only those nodes in the analyzed system at which the biggest variation to disturbances are supposed, enabling one to look at the whole system in a very selective and precise way. The deepest, precise analysis at only these nodes can then be performed using the improved supply-load modeling method, as proposed in the previous chapter.

Moreover, the usage of the method increases understanding of the system structure influence on the system behavior when there is the presence of external disturbances and shows which parts of the network can be affected due to the disturbance changes. This can then be used to find the system-structure-connected factors that cause sensors and to affect them purposefully both when operating and expanding a power system.

In this chapter a detailed description of the proposed method is given. Starting from the theoretical background, the basic properties of the method are shown in simple examples. Then, a real distribution system in which measurements surveys were done is subjected to the detailed analysis, which shows the advantages and difficulties of the method. The calculating results are compared with measurements, and discussed from different aspects of power quality area.

5.1 EIGENVALUE ANALYSIS USED FOR POWER SYSTEM STUDY

The initial stage of studying the power system sensitivity in steady states was associated with the sensitivity of the system performances to the changes that inevitably occur to the specified system [97] and with the analysis of the impact of input information errors on the results of state calculation [98]. At the same time, the spectral analysis was employed in some works to study dynamic system properties, in particular the modal analysis [99]. The latter allows for the estimation of the character of transients and the derivatives of the eigenvalues with respect to elements of the coefficient matrix and presents information for changing both the dynamic system properties as desired and the parameters of network elements. For this purpose a study is performed on the derivative of the minimum singular value with respect to the parameter of interest for the researcher [99].

Tiranuchit and Thomas illustrate the significance of determining the minimum singular value of the Jacobi matrix for evaluation of the system proximity to voltage instability [100]. In parallel, the possibility to increase the minimum singular value by installing capacitors at nodes corresponding to the maximum values of the right singular vector is shown. The interrelation between the minimum singular value of the Jacobi matrix and the nodal voltage is shown by Gao *et al* and is also devoted to voltage stability evaluation [101]. The idea of using the maximum components of the singular vector that correspond to the minimum singular value to choose the most informative set of measurements was applied by Gamm and Golub for detection of sensor nodes in an electric network by means of the spectral analysis [102]. The voltage in these nodes is most sensitive to external disturbances. Such an approach is applied in the works of Löf *et al* to solve the voltage collapse problem based on the singular analysis of the Jacobi matrix [103], [104]. The maximum component of the right singular vector is also used by Osowski, but for calculation of the coefficients of the Fourier-series expansion [105]. These approaches were applied to solve such energy problems as the analysis of operating reliability, reduction of voltage and power losses in distribution [106] and railway [107] power networks.

Taking the information which is present in the nodal admittance matrix, by means of the theory of norms, the inherent structures of power system networks were related to eigensystems reference frames [108]. The variety of power system problems, like voltage sensitivity, voltage control, fault levels and plan outage or reinforcement, was successfully related to such an analysis [109]. In the late 1990's and at the beginning of this century first approaches have appeared starting to use the inherent structure theory of networks to power system harmonics problems [110], [111].

In this work a novel, measurement-based consideration of problems that can be solved based on spectral analysis of the nodal admittance matrix of the analyzed system at other than fundamental frequencies is presented. The problem of singular value analysis of the Jacobi Matrix will not be treated in this context, however some remarks regarding this subject are given in Appendix 8.2. In the next section the theoretical background of the eigenvalue method will be described, starting from the basic frequency case and then extending the analysis to studies of quasi-stationary disturbances at harmonic and interharmonic frequencies by means of nodal admittance matrices constructed at the corresponding frequencies.

5.1.1 Theoretical background of the inherent network structure

Inherent structure theory of networks [108] draws attention to the role played by the eigensystem of the network matrix in relating currents and voltages. In power system analysis a very important position[1] takes the equation involving nodal admittance matrix $\underline{\boldsymbol{Y}}$ of power system with n nodes:

$$\underline{\boldsymbol{Y}}\,\underline{\boldsymbol{u}} = \underline{\boldsymbol{i}}, \tag{5-1}$$

where $\underline{\boldsymbol{u}}$ is a column vector of nodal voltages and $\underline{\boldsymbol{i}}$ is a column vector of nodal currents. The corresponding relationship between perturbations to voltages and currents can be written in (5-2):

$$\underline{\boldsymbol{Y}}\,\Delta\underline{\boldsymbol{u}} = \Delta\underline{\boldsymbol{i}}, \tag{5-2}$$

when the nodal admittance matrix remains unchanged. Equation (5-2) enables one to study, among others[2], voltage sensitivity to current perturbations, i.e the dependence between the nodal currents changes at each of n nodes in the studied power system and the resulting nodal voltage changes.

Considering that the complex nodal admittance matrix $\underline{\boldsymbol{Y}}$ can be reformulated in terms of its eigenvalues and eigenvectors (for a detailed explanation please see Appendix 8.2), the spectral theorem [113] allows one to write the matrix $\underline{\boldsymbol{Y}}$ in the form (5-3):

$$\underline{\boldsymbol{Y}} = \underline{\boldsymbol{V}}\,\underline{\boldsymbol{\Lambda}}\,\underline{\boldsymbol{V}}^T, \tag{5-3}$$

where $\underline{\boldsymbol{\Lambda}}$ is the diagonal matrix containing eigenvalues of the matrix $\underline{\boldsymbol{Y}}$. The matrix $\underline{\boldsymbol{V}}$ is a unitary matrix consisting of corresponding eigenvectors $\underline{\boldsymbol{v}}_1$, ..., $\underline{\boldsymbol{v}}_n$.

[1] A particularity of nodal admittance matrix in power system calculations lies in the possibility to build it directly from the branch list of a power network, without using other topological help matrices [112].
[2] There exists also possibility to regard current sensitivity to voltage perturbations or analogously voltage sensitivity to power perturbations or power sensitivity to voltage perturbations [108]. These cases will not be a subject to this work (more relevant to power flow than to harmonics and interharmonics).

Equation (5-3) describes the spectral decomposition[3] of the nodal admittance matrix $\underline{\boldsymbol{Y}}$ and represents the basis of the inherent structure theory of networks. The projection form of (5-3) has the form (5-4):

$$\underline{\boldsymbol{Y}} = \underline{\boldsymbol{v}}_1 \underline{\boldsymbol{v}}_1^T \underline{\lambda}_1 + \underline{\boldsymbol{v}}_2 \underline{\boldsymbol{v}}_2^T \underline{\lambda}_2 + \cdots + \underline{\boldsymbol{v}}_n \underline{\boldsymbol{v}}_n^T \underline{\lambda}_n \tag{5-4}$$

and can be also written compactly (5-5):

$$\underline{\boldsymbol{Y}} = \sum_{i=1}^{n} \underline{\boldsymbol{v}}_i \underline{\boldsymbol{v}}_i^T \underline{\lambda}_i \ , \tag{5-5}$$

where $\underline{\boldsymbol{v}}_i$ is the i-th eigenvector corresponding to the i-th eigenvalue $\underline{\lambda}_i$.

Taking into consideration equations (5-2) and (5-5) and keeping in mind the reversal rule for inverse product, the variations of the nodal voltages can be described as in (5-6):

$$\Delta \underline{\boldsymbol{u}} = \underline{\boldsymbol{Y}}^{-1} \Delta \underline{\boldsymbol{i}} = \sum_{i=1}^{n} \frac{\underline{\boldsymbol{v}}_i \underline{\boldsymbol{v}}_i^T}{\underline{\lambda}_i} \Delta \underline{\boldsymbol{i}} \ . \tag{5-6}$$

Analyzing power systems using vector space equations and matrix algebra the natural basis of comparison is matrix and vector norms[4]. Assuming that a constant current perturbation vector $\Delta\underline{\boldsymbol{i}}$ from (5-6) is rotated so as to coincide in turn with each of the eigenvectors $\underline{\boldsymbol{v}}_i$ then the l_2 norm (i.e. Euclidean norm) of the nodal voltage perturbations vector $\Delta\underline{\boldsymbol{u}}$, shown in (5-7)

$$\left\| \Delta \underline{\boldsymbol{u}} \right\| = \left\| \sum_{i=1}^{n} \frac{\underline{\boldsymbol{v}}_i \underline{\boldsymbol{v}}_i^T}{\underline{\lambda}_i} \Delta \underline{\boldsymbol{i}} \right\| \tag{5-7}$$

will be the maximum when the current perturbations vector is aligned with the eigenvector corresponding to the eigenvalue of smallest modulus [108].

In other words, assuming that the eigenvalues in the matrix $\underline{\Lambda}$ are ordered as their module increases and supposing an essential distinction between the smallest eigenvalue modulus and the other ones, the quotient ($\underline{\boldsymbol{v}}_i \cdot \underline{\boldsymbol{v}}_i^T$ / $\underline{\lambda}_i$) in (5-6) for the first element, i.e. for i = 1, appears to be the main contributor to the voltage changes at a particular node, determining alone sensitivity of the nodes to the current perturbation.

[3] Spectrum is a Latin word meaning “image”: When the light emitted by atoms passes through a prism it spreads out into a spectrum – a band of rainbow colors. Vibration frequencies correspond to the eigenvalues of a certain operator and are visible as bright lines in the spectrum of light that is emitted from the prism. Therefore the word spectrum has come to be applied to the complete set of eigenvalues of a matrix.

[4] For more detailed explanations please see Appendix 8.1.

Hence, (5-6) can be rewritten as in (5-8):

$$\Delta\underline{\boldsymbol{u}} \approx \frac{\underline{\boldsymbol{v}}_1 \underline{\boldsymbol{v}}_1^T}{\underline{\lambda}_1} \Delta\underline{\boldsymbol{i}} \ . \tag{5-8}$$

It follows from (5-8) that the elements connected with the minimum eigenvalue $\underline{\lambda}_1$ modulus make the greatest contribution to the voltage variations at a particular node. The sensitivity level is proportional to the corresponding components of the eigenvector $\underline{\boldsymbol{v}}_1$. The maximum module of the component $\underline{\boldsymbol{v}}_1$ determines the sensor node.

The l_2 norm of the nodal voltage perturbations vector from (5-8) can be written (5-9):

$$\left\|\Delta\underline{\boldsymbol{u}}\right\| \approx \left\|\Delta\underline{\boldsymbol{u}}_1\right\| = \frac{1}{\left|\underline{\lambda}_1\right|}\left|\sum_{i=1}^{n} \underline{\boldsymbol{v}}_{i1}^T \Delta\underline{\boldsymbol{i}}_i\right|, \tag{5-9}$$

where $\underline{\boldsymbol{v}}_{i1}^T$ is the i-th element of the first transposed eigenvector (connected with the first - the smallest - eigenvalue). The larger the difference between the smallest eigenvalue modulus and the other eigenvalues, the smaller the error ε (5-10) which results from the rejection of n–1 terms in transformation from (5-6) to (5-8), and it can be written:

$$\varepsilon = \left|1 - \frac{\left\|\Delta\underline{\boldsymbol{u}}_1\right\|}{\left\|\Delta\underline{\boldsymbol{u}}\right\|}\right| \cdot 100\% \, . \tag{5-10}$$

This error depends strongly on the difference between the smallest eigenvalue and the other eigenvalues, which in turn is connected with the structure and parameter of the studied network. Therefore, a detailed analysis of the system’s structure influence on the results of eigenvalue analysis is presented in the next section of this chapter.

5.1.2 Inherent network structure applied to power quality study

Since the inherent structure theory of networks involving eigenvalue analysis was successfully applied to voltage sensitivity investigations in power systems at the fundamental frequency, it can be extended to the study of the influence of quasi-stationary disturbances on the system operation [110], [111]. This means that a harmonic distortion prediction can be made utilizing the method shown in the previous section of this chapter, describing the most sensitive places in a power system from the harmonic or interharmonic distortion point of view. This needs to build a nodal admittance matrix $\underline{\boldsymbol{Y}}_f$ at each frequency f that can be of interest or in a general case to build a row of matrices from frequency f_1 to f_2 -with a defined frequency step- to study the system sensitivity in a specified frequency range.

Such process requires that the parameters of transformers, lines or cables, loads and power factor correction capacitors should be represented at the appropriate frequency f. The modeling basis for this was given in Chapter 4. In the case of general study on harmonic propagation in a distribution power system, the sensitivity of each node of the network to some harmonic frequency or frequencies is of great importance [114]. Therefore, it makes sense to construct the nodal admittance matrix for every frequency of interest for the power system being studied. The dependency between the disturbances present in the power system in the form of the nodal currents changes for each of the f-th considered frequencies, and the network response in term of its nodal voltages involves the nodal admittance matrix, with an analogous relationship to (5-2) given by (5-11):

$$\underline{\boldsymbol{Y}}_f \, \Delta\underline{\boldsymbol{u}}_f = \Delta\underline{\boldsymbol{i}}_f. \tag{5-11}$$

Then, the spectral decomposition of the nodal admittance matrix can be achieved for each frequency of interest:

$$\underline{\boldsymbol{Y}}_f = \underline{\boldsymbol{V}}_f \, \underline{\boldsymbol{\Lambda}}_f \, \underline{\boldsymbol{V}}_f^T, \tag{5-12}$$

where $\underline{\boldsymbol{\Lambda}}_f$ is the diagonal matrix with the eigenvalues of matrix $\underline{\boldsymbol{Y}}_f$ ordered as their value of modules increases. Equation (5-12) describes the spectral decomposition of the nodal admittance matrix $\underline{\boldsymbol{Y}}_f$ and represents the basis of the inherent structure theory of networks applied to the power quality study.

Analyzing the properties of this transformation in a similar way to the considerations presented in the first part of this chapter, it can be concluded that the term connected with the minimum eigenvalue $\underline{\lambda}_{1,f}$ makes the greatest contribution to the voltage variations at a particular node calculated for any frequency of interest. The sensitivity level of the system node to the disturbances taking place at a specific frequency is proportional to the corresponding components of the eigenvector $\underline{\boldsymbol{v}}_{1,f}$, making:

$$\Delta\underline{\boldsymbol{u}}_f \approx \frac{\underline{\boldsymbol{v}}_{1,f} \, \underline{\boldsymbol{v}}_{1,f}^T}{\underline{\lambda}_{1,f}} \cdot \Delta\underline{\boldsymbol{i}}_f \ . \tag{5-13}$$

Therefore, the anticipated voltage harmonic level at that node for corresponding harmonic frequency will be high.

If there is more than one eigenvalue significantly lower than the others, the analysis should be performed considering all of them and their corresponding eigenvectors. The quotient in (5-13) will be then extended from one component (i=1) to k components, where k is the number of considerably smaller eigenvalues and, correspondingly, eigenvectors and the analysis of the estimation error can be made analogously to that described for the case of fundamental frequency study.

This approach can be a valuable tool for analyzing a variety of power quality optimization problems, such as optimal placement of passive filters or nonlinear loads [115] and the proper selection of nodes that enable optimal set for power quality measurements [111].

5.2 SYSTEM STRUCTURE AND THE PROPERTIES OF THE METHOD

The problem of the influence of the system structure on the results of eigenvalue analysis will be studied in this section. As previous said one of the biggest advantages of the method is to take into account only several of the smallest eigenvalues and their corresponding eigenvectors. Therefore, it is necessary to study the influence of the change of the system structure parameters, like the change of admittance of one branch or at one node, on the results that are obtained using eigenvalue analysis.

5.2.1 General remarks

Equation (5-2) connects the nodal admittance matrix $\underline{\boldsymbol{Y}}$ with nodal voltage sensitivity $\Delta\underline{\boldsymbol{u}}$ to external disturbances as changes of nodal currents $\Delta\underline{\boldsymbol{i}}$. For simplicity of the considerations presented in this section the complexity of the elements will be omitted, keeping in mind that the method described in [116] and presented in the Appendix 8.2, allow for the simplification for nodal admittance matrices of real power systems.

The spectral decomposition enables the nodal admittance matrix $\boldsymbol{Y}$ to be written in terms of its diagonal eigenvalue matrix $\boldsymbol{\Lambda}$ and their corresponding eigenvectors, as in (5-3). From (5-3) the description of the diagonal eigenvalue matrix in terms of eigenvector matrices and nodal admittance matrix can be written as in (5-14):

$$\boldsymbol{\Lambda} = \boldsymbol{V}^T\boldsymbol{Y}\boldsymbol{V} = \begin{bmatrix} v_{11} & \cdots & v_{n1} \\ v_{12} & \cdots & v_{n2} \\ \cdots & \cdots & \cdots \\ v_{1n} & \cdots & v_{nn} \end{bmatrix} \begin{bmatrix} y_{11} & \cdots & y_{1n} \\ y_{21} & \cdots & y_{2n} \\ \cdots & \cdots & \cdots \\ y_{n1} & \cdots & y_{nn} \end{bmatrix} \begin{bmatrix} v_{11} & \cdots & v_{1n} \\ v_{21} & \cdots & v_{2n} \\ \cdots & \cdots & \cdots \\ v_{n1} & \cdots & v_{nn} \end{bmatrix}, \tag{5-14}$$

where for the smallest eigenvalue element (λ_1):

$$\lambda_1 = (v_{11}, \ldots, v_{n1}) \begin{bmatrix} y_{11} & \cdots & y_{1n} \\ y_{21} & \cdots & y_{2n} \\ \cdots & \cdots & \cdots \\ y_{n1} & \cdots & y_{nn} \end{bmatrix} \begin{pmatrix} v_{11} \\ \cdots \\ v_{n1} \end{pmatrix}. \tag{5-15}$$

Assuming that the branch l connects nodes p and q, the elements y_{pp}, y_{pq}, y_{qp}, y_{qq} of the nodal admittance matrix depend on admittance y_l of a branch l, and the derivative in (5-16) is true:

$$\frac{\partial y_{pp}}{\partial y_l} = \frac{\partial y_{qq}}{\partial y_l} = -\frac{\partial y_{pq}}{\partial y_l} = -\frac{\partial y_{qp}}{\partial y_l} = 1 . \tag{5-16}$$

For the smallest eigenvalue λ_1 the partial derivative on the admittance branch l can be written as in (5-17):

$$\frac{\partial \lambda_1}{\partial y_l} = \left(v_{11}, ..., v_{n1}\right) \begin{bmatrix} 0, & ..., & 0, & ..., & 0, & ..., & 0 \\ 0, & ..., & 1 & ..., & -1 & ..., & 0 \\ ... & ... & ... & ... & ... & ... & ... \\ 0, & ..., & -1 & ..., & 1 & ..., & 0 \\ 0, & ..., & 0, & ..., & 0, & ..., & 0 \end{bmatrix} \begin{pmatrix} v_{11} \\ ... \\ v_{n1} \end{pmatrix} = \left(v_{p1} - v_{q1}\right)^2 . \tag{5-17}$$

The derivative (5-17) describes the sensitivity of the minimum eigenvalue on the changes of the admittance branch. From (5-17) it can be stated that any change of branch admittance, for which square differences of the corresponding components of eigenvector connected with the smallest eigenvalue λ_1, has the biggest influence on the smallest eigenvalue of a nodal admittance matrix. Such branches are called *weak branches*. Analogously, regarding the influence of a change of the admittance, e.g. at node i, the derivative (5-18), which describes the influence of the shunt admittance parameter y_{shi} on the changes of the smallest eigenvalue, can be written:

$$\frac{\partial \lambda}{\partial y_{shi}} = \pm {v_{k1}}^2 . \tag{5-18}$$

In this way it is possible to obtain the node at which the changes of the admittance have the biggest influence on the smallest eigenvalue of a nodal admittance matrix. Such nodes are called *weak nodes*.

Now, the ways in which to decrease the difference between the smallest and the biggest eigenvalue, which leads to the improvement of the system sensitivity will be analyzed. At first, one can consider the impact of an additional branch (or any change in an admittance of existing branches) on the value of the smallest eigenvalue. According to the Weyl theorem[5] [113] the inequality (5-19) can be carried out:

$$\lambda_i(\boldsymbol{Y}) \le \lambda_i\left(\boldsymbol{Y} + \boldsymbol{b}\boldsymbol{b}^T\right), \tag{5-19}$$

[5] Weyl theorem shows that for the sum of the Hermitian matrices: $\boldsymbol{Y} + \boldsymbol{b}\boldsymbol{b}^T$ ($\boldsymbol{b}\boldsymbol{b}^T \neq \boldsymbol{0}$) is a positive semi-definite matrix of the rank 1.

where $i = 1, 2, ..., n - k$, n stands for the number of the nodes in the system, k is the number of nodes at which voltage is fixed (reference node). For the study of the power quality phenomena - at frequencies different to the basic one - mainly the earth node is quantified as a reference node. Keeping in mind that a nodal admittance matrix $\boldsymbol{Y}$ is defined as in (5-20):

$$\boldsymbol{Y} = \boldsymbol{K}\boldsymbol{Y_z}\boldsymbol{K}^T, \tag{5-20}$$

which can be written also as (5-21) for defining the elements as in the Weyl theorem:

$$\boldsymbol{Y} = \boldsymbol{K}\boldsymbol{Y_z}^{0.5}\,\boldsymbol{Y_z}^{0.5}\,\boldsymbol{K}^T. \tag{5-21}$$

Considering $\boldsymbol{K}$ as a node-branch-incidence matrix and $\boldsymbol{Y_z}$ as an admittance matrix of the system, vector $\boldsymbol{b}$ can be represented as in (5-22):

$$\boldsymbol{b} = \boldsymbol{k}_{il}\,\boldsymbol{y}_{il}^{1/2}\,, \tag{5-22}$$

where $\boldsymbol{k}_{il}$ is the column of the node-branch-incidence matrix, which corresponds to an added branch, or a branch, which admittance changes, and $\boldsymbol{y}_{il}$ represents the admittance of an added branch, or quantity of which the admittance of an existing branch changes.

The inequality (5-19) shows that the addition of a branch or an admittance increase of an existing branch leads to the fact, that the smallest eigenvalue λ_{min} of a such “improved” nodal admittance matrix will not be less than that of the nodal admittance matrix before the improvement. Conversely, a subtraction of a branch or admittance reduction of an existing branch, in inequality (5-19) denoted by a minus sign before matrix $\boldsymbol{bb}^T$, leads to the fact that the smallest eigenvalue λ_{min} of a such “worsened” nodal admittance matrix will not be bigger than of that from the nodal admittance matrix before this “worsening”.

Concluding, the usage of a Weyl theorem allows one to state than additional admittance or increase of admittance of any branch in the system does not decrease the value of the smallest eigenvalue of the nodal admittance matrix of the system. However, from (5-19) it does not follow that this action aides in the improvement of the conditionality of the nodal admittance matrix ($cond\,(\boldsymbol{Y})$), which is defined as a relation between the maximal eigenvalue λ_{max} and the minimal eigenvalue λ_{min}, as in (5-23):

$$cond\;(\boldsymbol{Y}) = \frac{\lambda_{max}}{\lambda_{min}}\,. \tag{5-23}$$

The conditionality number of a nodal admittance matrix can be interpreted as a degree of network heterogeneity. The bigger the conditionality number is, the more inhomogeneous the network is, i.e. the weak places can be found in the system.

Summarizing, changes of the system structure need a complete study considering both the smallest eigenvalue behavior and the conditionality number behavior in order to obtain a whole influence of any change in the system structure to the behavior of all eigenvalues of the corresponding nodal admittance matrix and its repercussions to the weak places in the system. A simple illustration of the problem can be made using the example presented in following section.

5.2.2 Illustration example

A chosen set of simple four-node-network configurations (Fig. 5.1) are considered. All branch admittances are assumed to be equal to 1, node 4 will be treated as a reference node, i.e. node at which the voltage can be fixed.

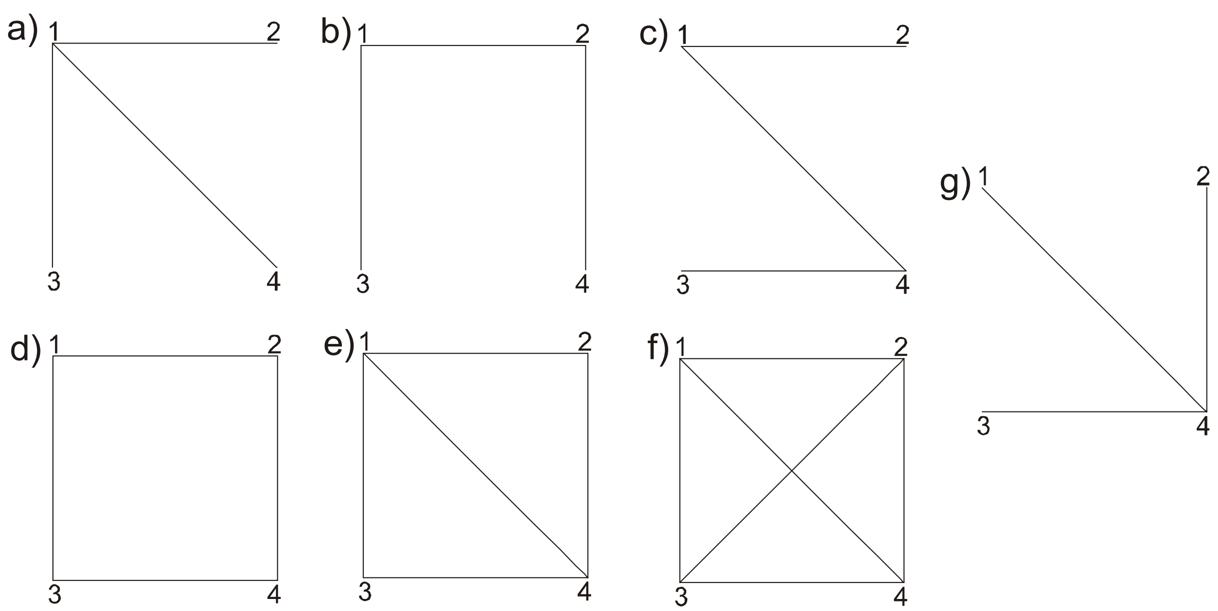

Fig. 5.1 Examples of four-nodes-networks

To begin with a nodal admittance was built for each of the cases and the eigenvalues were calculated together with the conditionality number, according to (5-23). The resulted matrix has three eigenvalues, which are shown in Tab. 5.1 from the smallest (λ_1) to the biggest (λ_3) together with the corresponding conditionality numbers. The results are also presented graphically in Fig. 5.2.

Table 5.1 The results for the different network configurations from Fig. 5.1

Circuit	λ1	λ2	λ3	*cond (Y)*
a	0.268	1	3.732	13.931
b	0.198	1.555	3.247	16.391
c	0.382	1	2.618	6.853
d	0.586	2	3.414	5.820
e	0.586	3.414	6	6.828
f	1	4	4	4
g	1	1	1	1

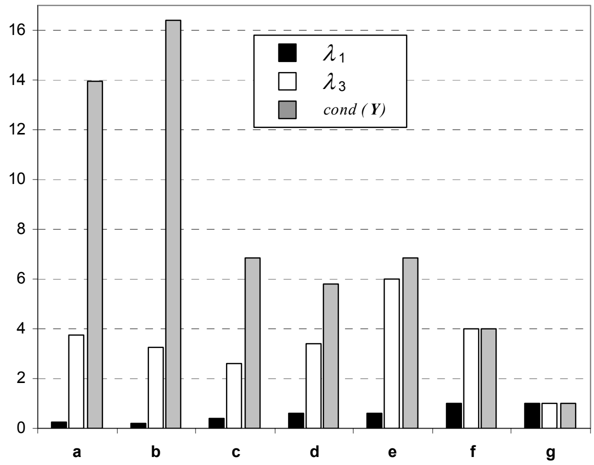

Fig. 5.2 Minimal (λ_1) and maximal (λ_3) eigenvalues and the conditionality number ($cond(Y)$) calculated for the network configurations from Fig. 5.1

Secondly, in circuit f (Fig. 5.1) the admittance of the branch connecting node 1 to slack node 4 was increased from 2 to 5-times (Tab. 5.2). For each admittance change the previously mentioned quantities were calculated and the results are presented in Tab. 5.2 and graphically in Fig. 5.3.

Table 5.2 The results for the different admittances of the branch 1-4 for the circuit from Fig. 5.1 f

Admittance of Branch 1-4	Circuit f			
	λ1	λ2	λ3	*cond (Y)*
1	1	4	4	4
2	1.268	4	4.732	3.732
3	1.438	4	5.562	3.867
4	1.551	4	6.450	4.160
5	1.628	4	7.372	4.529

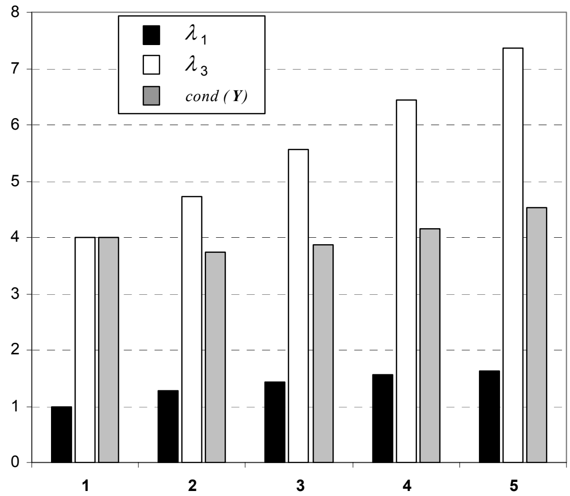

Fig. 5.3 Minimal (λ_1) and maximal (λ_3) eigenvalues and the conditionality number ($cond(Y)$) calculated for the different admittances of the branch 1-4 for the circuit from Fig. 5.1 f

The conclusions from the analysis of the results presented in Tab. 5.1 and Tab. 5.2 can be summarized as follows: The best conditionality of a nodal admittance matrix was obtained in case g (direct connection of nodes 1-3 with slack node 4 - Fig. 5.1). Such a network is equally strong, i.e. homogeneous, there are neither weak nodes nor weak branches in the network.

No other connection is distinguished by such good characteristic. For other connections the values both of smallest eigenvalue and of the conditionality number vary (Tab. 5.2). Interesting is that the closed-loop networks (Fig. 5.1 d, e, f) have a greater smallest eigenvalue than the opened-ones (Fig. 5.1 a, b, c), their conditionality number is generally not greater than for the opened-loop networks (Fig. 5.2). This proves the hypothesis that the connection to the reference node plays an important role in the network sensitivity.

Moreover, results obtained from the calculations of the eigenvalues by the gradual increase of the number of branches in one network scheme (Fig. 5.1 f) confirm the Weyl theorem (see the increasing values of the smallest eigenvalue in Tab. 5.2). However, a simultaneous increase of the biggest eigenvalue was also observed (Tab. 5.2). Looking closely at Fig. 5.3 it can be stated that the biggest eigenvalue increases quicker than the smallest one, which leads to the conclusion that the conditionality number will be worsened, having a minimum at 2-fold increase of the branch admittance. Concluding, thoughtlessly increasing the number of branches or even increasing the admittance of existing branches will not reduce the conditionality number of the nodal admittance matrix in every case. Therefore, no general conclusions can be done regarding the influence of admittance increase or decrease of a branch / branches on the behavior of the sensitivity of the analyzed network - a separate study for each case is in such situations indispensable.

As far as the influence of the shunts admittances are concerned the following consideration can be made. Analyzing results from Tab. 5.2 (Fig. 5.1 f) it can be assumed that the 2 - 5 fold increase of the admittance branch is equivalent to the introduction of an inductive shunt to the node 1 with the admittance that changes from 1 to 4. So that all conclusions made previously to that changes also apply to this case.

Concluding, the effective way to improve conditionality of a nodal admittance matrix is to fix a voltage at the nodes, especially at the sensor nodes. However, for the analysis of the nodal admittance matrices that are constructed for frequencies other than fundamental one, this is not the case because the only reference node is the earth and no other ‘fixation’ can be made. To repeat, a separate study for every case is in these situations indispensable.

Analogously, the error of the estimation of the system sensitive places using only the smallest eigenvalues and their corresponding eigenvectors can be assessed only through the whole analysis of the eigenvalues and the conditionality number: The smaller the difference between the smallest (first) eigenvalue and the next ones, the bigger the error of the estimation of the weak places. When the homogeneous system is considered, the biggest error occurs because of the fact that no weak places exist in such a system. However, such a case is not possible in real systems. Nevertheless, especially for small power systems, the inclusion of some of the smallest eigenvalues to the analysis is necessary to obtain reliable results in the estimation of the sensor places.

5.3 PRACTICAL APPLICATIONS OF THE METHOD FOR DISTRIBUTION SYSTEM SENSITIVITY EVALUATION

This section of the work includes several case studies showing the features of the spectral decomposition approach and its practical relevance on a real distribution system example. In the first part of this section the results of a measurement survey made in a real distribution network are described and commented on from the power quality indices point of view. Subsequent sections are devoted to the chosen sensitivity case studies, starting from the general case of eigenvalues of the system, then analyzing the influence of important modeling parameters such as load models on the results of the proposed method.

5.3.1 Long- term power quality measurements: a survey in a distribution network

In the distribution system (Fig. 5.4) some circuit breakers trips and a higher unbalance were signalized by the network operator. Therefore, a set of on-site measurements were made to follow up on the above mentioned problems. This distribution system is characterized by a single middle voltage grid connection (10 kV), at the station *west*. In this system a closed, middle-voltage (10 kV) loop-network (cables C2 .. C5) is used to supply the loads with the electrical energy through the step-down transformers at the nominal voltage 400 V (low side of the transformer) at a frequency of 50 Hz.

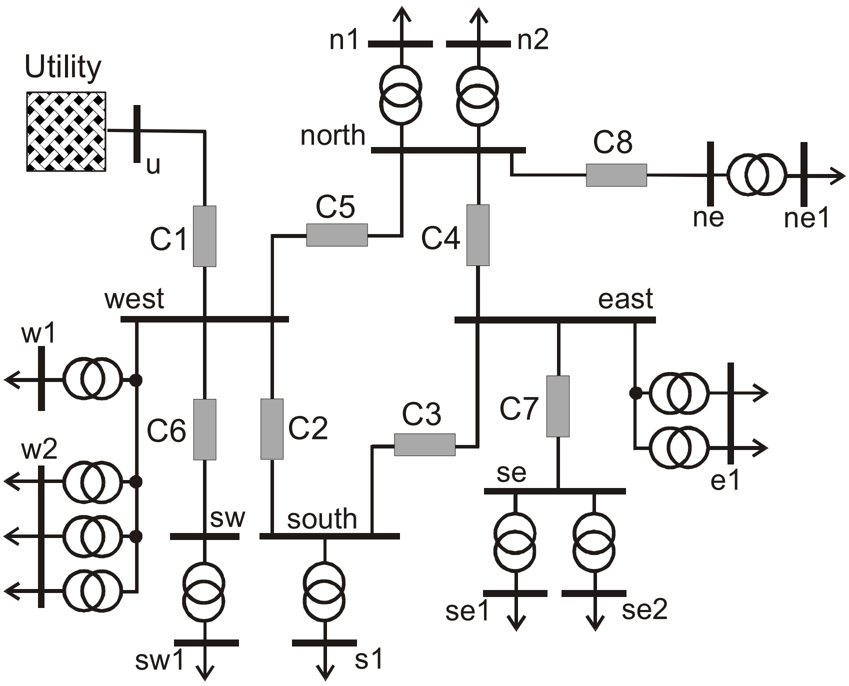

Fig. 5.4 Simplified test network scheme

The measurements were accomplished using the power quality measurement system described in Chapter 3 at several places of the distribution network from Fig. 5.4 within several months. In each case the measurements were recorded several times over a 24 hour period at the bus-bars of the transformers or at the individual outlets of the low-voltage side of the transformers. At each of these measuring points the quality of supply voltage was assessed concerning harmonics, in accordance with the standard [27], and the product standard [31]. This power quality survey was made in the system in order establish the actual level of the power quality factors as harmonics in quasi-stationary state. THD and HD for the harmonic frequencies up to 2.5 kHz were measured at the low-voltage buses of the substations according to prescriptions described in Chapter 2 and Chapter 3.

The power quality assessment system equipped with necessary plug-in units and special current and voltage probes making the measurement of the three-phase quantities possible was used to establish 24-hour and 7-days measurements at every measuring location. The measurements of the power drawn by loads and information about harmonic distortion present both in voltages and in currents was obtained concurrently, and for each data point a binary file was created. This binary file was configured in such a way that the analysis of the disturbances was possible in terms of short-interval (10-minutes) analysis of the quasi-stationary harmonics. The transfer of the measured data to the computer was performed automatically, so that each of the data points was saved on the workstation or notebook, establishing a data set, i.e., according to [45], in 10 minutes, 100 measurements. Hence, 144 data sets were created within each of the 24 hour measuring periods. In order to condense the large amount of data a statistical smoothing procedure was applied according to conditions specified in [45]. Namely, for each quantity X, e.g. THD, TDD, HD, in each data set (100 measurements in 10 minutes) a statistical position factor – a quantile χ_p of the rank $p = 0.95$ was built according to (5-24):

$$P\{X \leq \chi_p\} \geq p \,, \tag{5-24}$$

where P is a probability function of the quantity X. Such physical values, like currents, voltages and other direct measured values were calculated as their mean value over the 10 minute period. To increase understandability of the text in this work in future considerations the statistical description of the indices will be omitted. One should note that speaking about THD, TDD and HD is in terms of their 0.95 quantiles, and speaking about measured power, voltage and current is in terms of their above mentioned mean values.

The results of the survey are summarized in Fig. 5.5 The measurement points are presented as dots and the corresponding THD factors are shown as bars, indicating respective level utilizing a fulfillment of the bar. At places where measured values of individual harmonic have exceeded their compatibility levels an arrow together with the information of the corresponding harmonic order is placed.

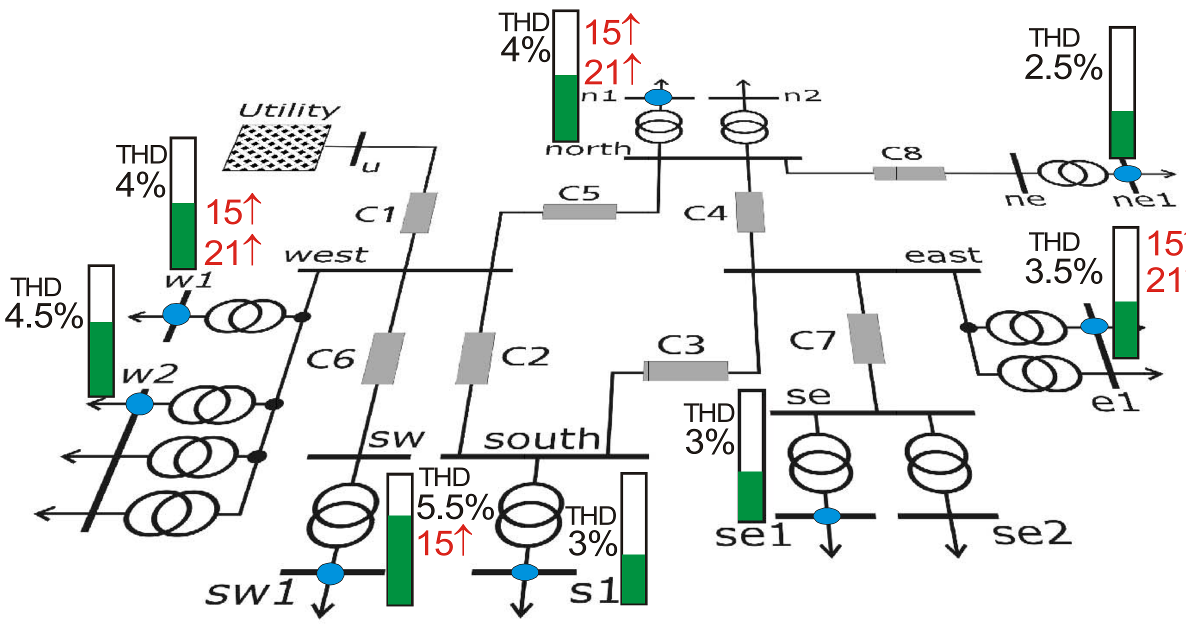

Fig. 5.5 *THD* level within the distribution network

The measurements recorded a relatively stable level of the *THD* factor at each substation, Fig. 5.5. Its value never exceeded 6 %, which is below the allowable 8 % limit for long-term harmonic distortion. The lower value of the *THD* was registered at node *ne1*, and was slightly above 2.5 %. The most problematic harmonics were the 15th and 21st, which at most of the substations reached or exceeded their compatibility levels provided in [27] – in this case 0.4 % and 0.3 %, respectively or the voltage characteristic provided in [31] – in this case 0.5 % both for 15th and 21st harmonic order. The biggest violations were recorded at node *w1*, *n1* and at node *sw1* [114], where the individual harmonic level of the 15th harmonic was nearly 0.7 % in the middle of the day (Fig. 5.11) The measurements performed at several nodes, e.g. *w1*, *w2* and *sw1*, will be described in detail regarding the interesting load types present at these nodes and the measurement results. The loads connected to node *w1* mainly consisted of lighting and office profile. The profile at node *w2* was mixed, with an air conditioning system being one of the bigger loads. At node *sw1* there were mainly offices with a lot of personal computers and computer laboratories.

Fig. 5.6 presents an overview of the distortion in the voltage of phase L1 at node *w1*. Beside the *THD*, the variations of individual *HD* factors for 3rd, 5th, 15th and 21st harmonics are also shown. It can be seen that there is no violation of the *THD*, 3rd and 5th *HD* limits, which in this case are 8 %, 5 % and 6 %, respectively according to standards [27] and [31]. However, between 7 and 15 o'clock some violations of the 15th and 21st harmonic level limits were observed, in this case 0.3 % and 0.2 %, respectively [25]. To see this clearly, the *HD* for 15th and 21st harmonic are presented in Fig. 5.7.

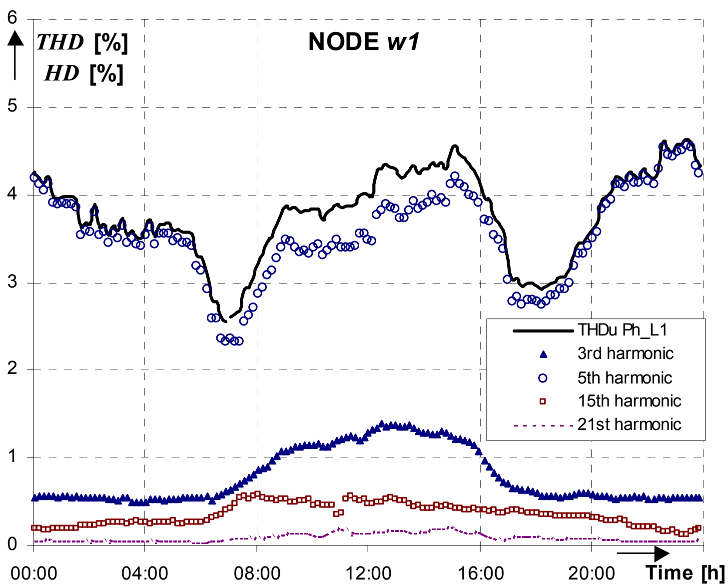

Fig. 5.6 *THD* and *HD* factors at node *w1* for phase L1

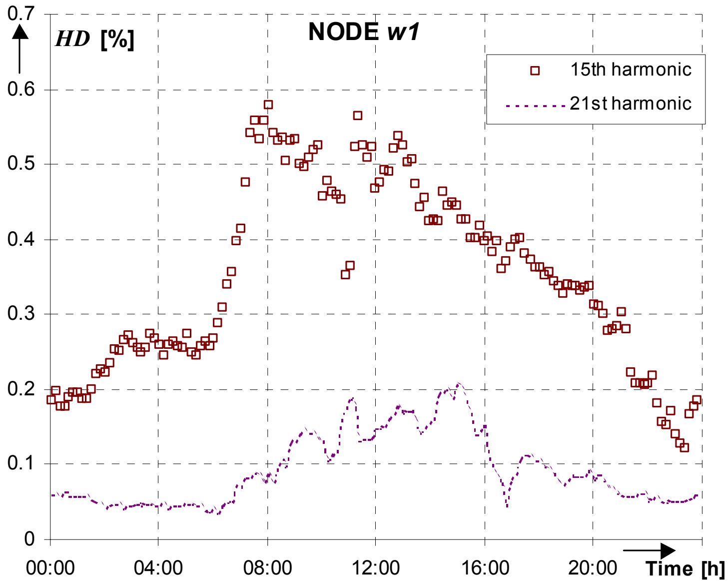

Fig. 5.7 *HD* factors for 15th and 21st harmonic orders at node *w1*

It can be seen that the 21st harmonic level lies close to the limit value of 0.2 % during that time. It can be also stated, that the *HD* values for both harmonics at night are essentially lower than those which were measured during the day. At this point it must be stated that the level of the 21st harmonic that was observed during that survey lies near to the measuring system error of about 1 % (see Table 3.1). It does not allow for unequivocal interpretation of these results as a limit violation. The 15th harmonic levels can be, however, interpreted as a clear compatibility level violation. In the newly issued standard [27], the compatibility levels are set for 15th and 21st harmonic at 0.4 % and 0.3 %, respectively. The evaluation of the measurement results in accordance with this standard brings a slight violation of the 15th harmonic compatibility level, as well. In the product norm [31], the limit values for each of the two mentioned harmonic orders are at 0.5 %. Evaluating according to this norm, a violation of the 15th harmonic limit can be stated, too.

The *TDD* was calculated based on the information gathered about the maximum demand load current (at the considered nodes *w1*, *w2* and *sw1* equal to about 400 A) and about the short-circuit power at every node. The variations of the *TDD* at the three nodes measured for phase L1 are shown in Fig. 5.8. It can be seen that the *TDD* at node *w2* lies below the other *TDDs*. It can be simply explained looking at Fig. 5.4, where at the low-voltage bus three transformers connected in parallel are working. The *TDD* at node *sw1* is above the 12 % limit proposed in [29].

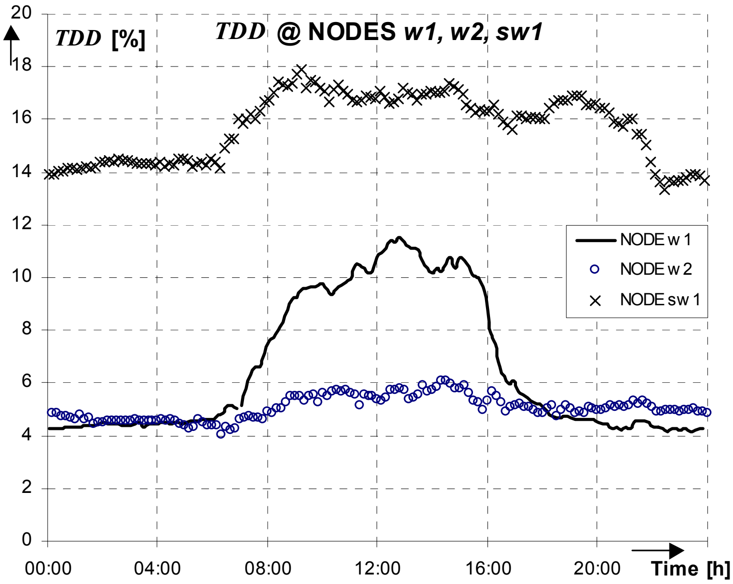

Fig. 5.8 ***TDD*** **of the currents measured at node *w1*, *w2* and *sw1***

The measurements of the voltage distortion at node *w2* (Fig. 5.9) has not confirmed its low distortion, as it can be presumed by looking at *TDD*. The reason is, that the current was measured at the bus of one of the three transformers, because there was no technical possibility to measure the whole current flowing out from the bus-bar *w2* to the loads. The voltage *THD* factor at node *w2* is about 5 % and this is comparable to the values at the other two nodes. However, during the measurements at node *w2* there was no violation of the voltage distortion limits (Fig. 5.9). The level of 5^{th} harmonic was only close to its limit value of 6 % during the night. It can be clearly seen that the 5^{th} harmonic is the main component in *THD* at node *w2*.

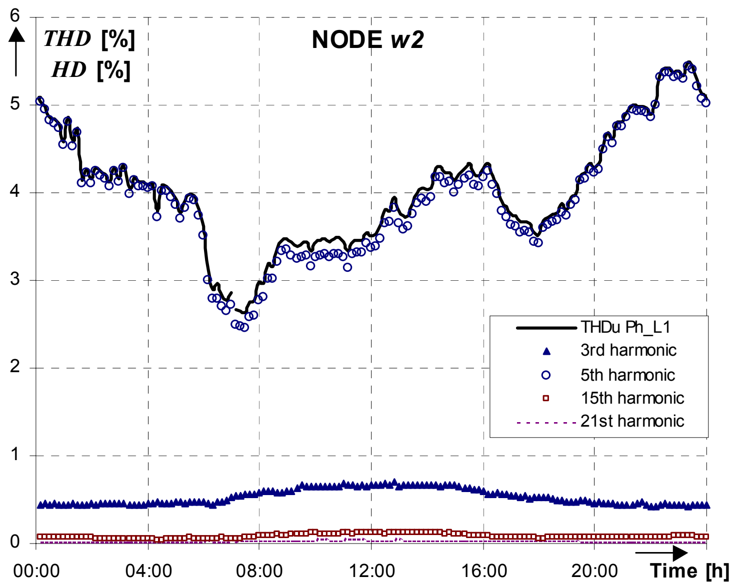

Fig. 5.9 ***THD*** **and** ***HD*** **factors at node *w2***

As far as the measurement place at node *sw1* is concerned a relatively stable level of the *THD* was observed (Fig. 5.10). Looking closely at the *HD* of 15^{th} and 21^{st} harmonics at this node (Fig. 5.11) a violation of their limits, especially for 15^{th} harmonic can be observed. This violation takes place mainly at night and among air conditioning devices the high unbalance present in the network is supposed to be the main source of disturbances at this and other nodes, where the distortion values for those triple harmonics (in balanced network being only zero sequence) have reached their limits.

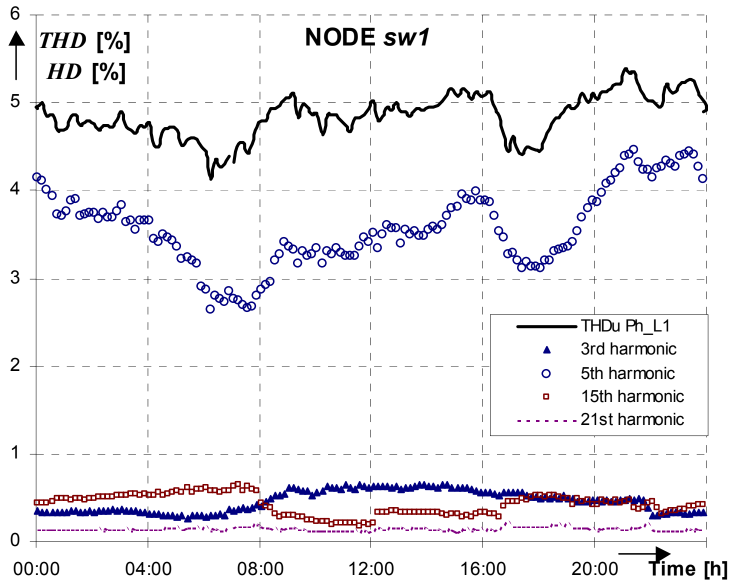

Fig. 5.10 ***THD*** **and** ***HD*** **factors at node *sw1***

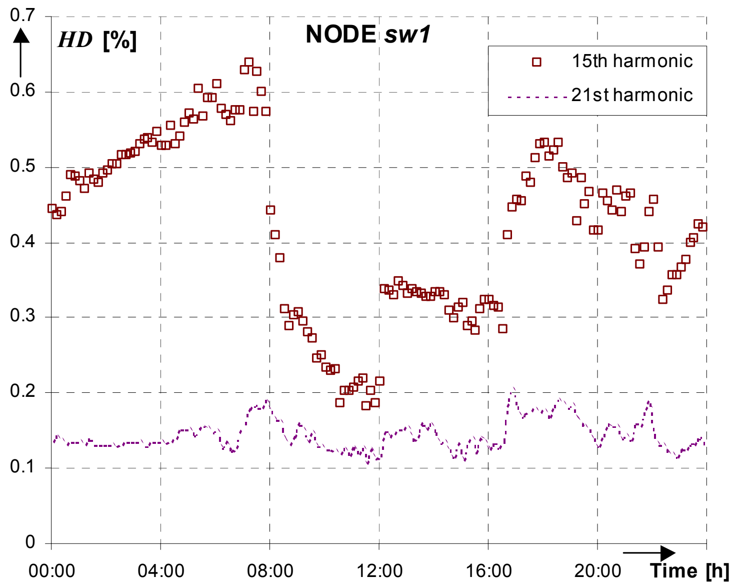

Fig. 5.11 ***HD*** **factors for 15^{th} and 21^{st} harmonics at node *sw1***

As a result of this, at several stations within this system relatively big amplitudes of current flowing through the neutral conductor have been measured. This can turn out to be a serious problem because of the standard practice in this network to reduce the diameter of the neutral wire. As an example, the measurement of the currents at the low voltage side of the transformer at bus *ne1* is presented in Fig. 5.12. The neutral conductor loading in Fig. 5.12 is comparable to the phase conductors. The spectrum of the current flowing in the neutral conductor is presented in Fig. 5.13.

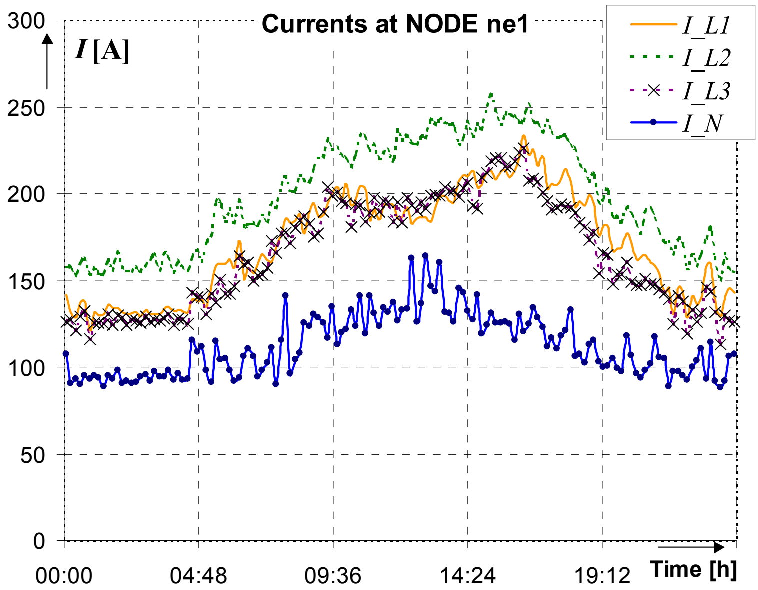

Fig. 5.12 Amplitude changes of the currents measured at bus *ne1* over 24 hours

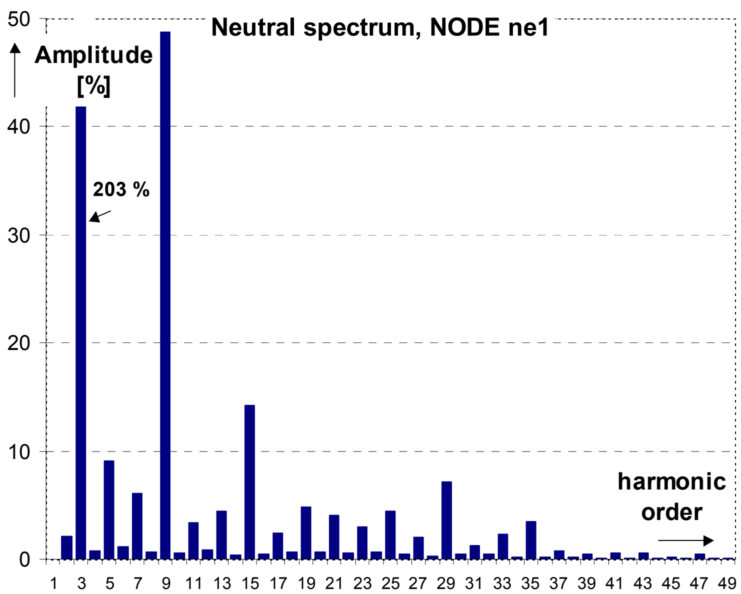

Fig. 5.13 Spectrum of the current flowing in neutral conductor at node *ne1*

A high presence of both the characteristic zero-sequence harmonics, like the 3rd, 9th and 15th and the non-characteristic [33] like the 5th and 7th can be observed. This is another example of the unbalance present in the network, mostly as a rule as an exception. Here, it is caused mainly by the primarily single-phase and non-linear loads present at this substation. Offices with PCs and PC laboratories with server pools, air conditioning devices and ventilation systems driven by electronic converters can be stated here as the main sources of the neutral overload. However, the long-term thermal current in this case was not reached, the situation can worsen in the case of increasing load, because of the common practice to use the under dimensioned neutral wire (normally realized as a half diameter or half number of wires for neutral as compared to the phase conductors). The second problem can arise in the case of a TN-C network, where a neutral conductor is used additionally as protective earth. This situation can be more critical and quite dangerous. In the described installation it was actually the case, and after first measurements the installation was upgraded to TN-S (from the low-voltage side). There is also another interesting fact, which can be obtained comparing all measurements of the 5th harmonic (Fig. 5.15) at every site, Fig. 5.14.

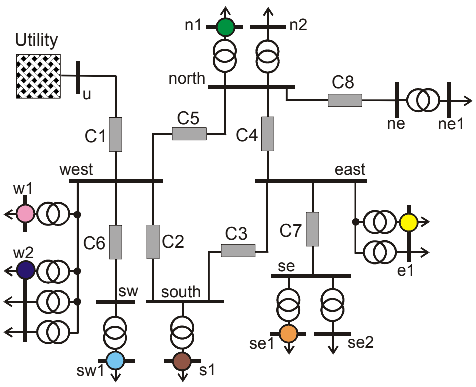

Fig. 5.14 Measurement sites

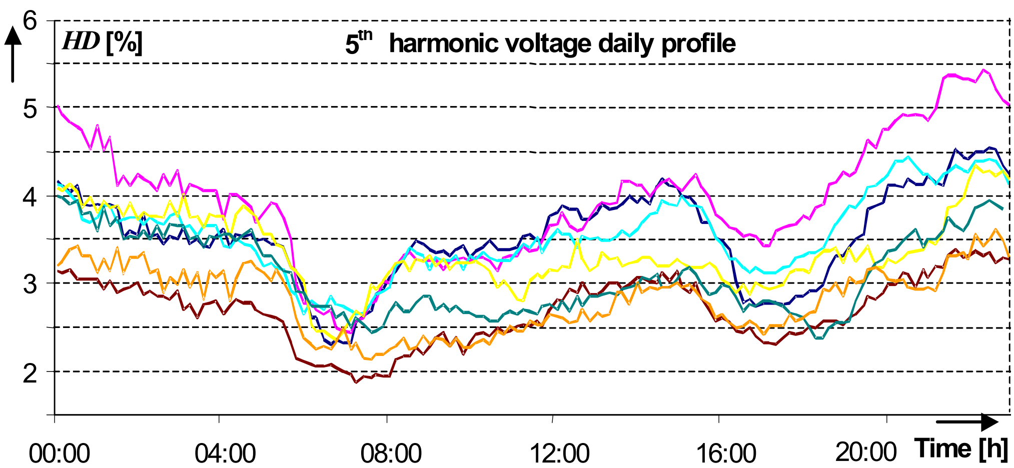

Fig. 5.15 Level of the 5th harmonic at every site

It is to be underlined that at every measurement site the 5th harmonic, and simultaneously the *THD* factor, have highest values during the night and early morning hours (Fig. 5.15) At these times the consumed power is small. Moreover, in Fig. 5.15 the daily curves of the level of the 5th harmonic have a clearly analogous shape, independent of time and place of measuring. Possible reasons for this could lie in the distortions, which reached the distribution network from the superordinated network or are continuously fed into the network by a local large consumer. Therefore, further measurements are necessary, in order to locate the exact sources of those disturbances. The method of the localization of sources of disturbances utilizes presented in the previous section inherent structure of network and first localization algorithm was published in the author's work [117].

Summarizing, the measurements give detailed but time-dependent information about harmonic distortion in the distribution system. This detailed information permits the synthesis of a statistical model (in its simplest form - average value) of the loads among the measurement time. Time, limiting measurement duration, can be a barrier which does not allow for a generalized analysis including all points of the system. Therefore, a combination of measurements with an analytical method which will give a general overview of the studied system and will help to identify the weak places is necessary. Therefore the eigenvalue analysis was carried out using this distribution system data and the results are described in the next section of this chapter.

5.3.2 The sensitivity analysis of the distribution system, linear load model

Building the nodal admittance matrix for the studied system requires a distribution system modeling routine. As already mentioned in Chapter 4, from the network structure point of view this procedure includes three important parts: modeling of the subsequent network connection point; modeling of the network elements and modeling of the load structure with harmonic sources. For the system in Fig. 5.4 the nodal admittance matrix was built for each harmonic order from the fundamental one to the 49th. In this section single-phase, positive sequence models according to those described in the previous chapter were used for the sake of their sufficient exactness for the, presented here, qualitative analysis. Summarizing, the supply system equivalent admittance was determined by equation (4-1) based on the short-circuit power S_k'' and the nominal voltage U_n. The middle voltage cables were represented by their pi-circuit, with both longitudinal and transversal elements expressed as frequency functions. The step-down transformers were modeled as a series resistance with the leakage inductance calculated from available rated impedance voltage u_{kr} and rated ohmic voltage drop u_{Rr}. The capacitance of the transformer and phase shifting components were not considered.

The power factor correction capacitors were precisely placed and modeled as susceptances with linear frequency dependence. Those equipped with chokes were represented respectively.

At first, loads were assumed to be linear, and their admittances were calculated directly from their power consumption. These values were taken both from measurements and from the grid carrier's data.

Eigenvalue analysis was executed for the 18 x 18 nodal admittance matrix according to the terms presented in previous sections of this chapter. The modules of eigenvector values corresponding to the smallest eigenvalue modulus for chosen low-voltage nodes are presented in Fig. 5.16. The biggest values for the eigenvectors in Fig. 5.16 indicate the nodes most sensitive to the analyzed harmonic orders. One can observe that the nodes *n1*, *e1*, *s1*, *sw1* and *w2* are the most sensitive to some of those harmonics. Therefore, this analysis makes the selection of the more important nodes possible. A special attention then has to be paid to the power quality at these nodes, especially by considerable presence of unbalanced loads. The nodes are indicated by arrows in Fig. 5.17. The nodes can be then selected for the on-site long-term power quality measurements (i.e. voltage and current inclusive neutral wire current), or in the case of considerable non-linear load presence, a detailed analysis that includes interaction modeling between the network and the load, as proposed in Chapter 4, should be carried out to obtain quantitative results about harmonic distortion at those nodes.

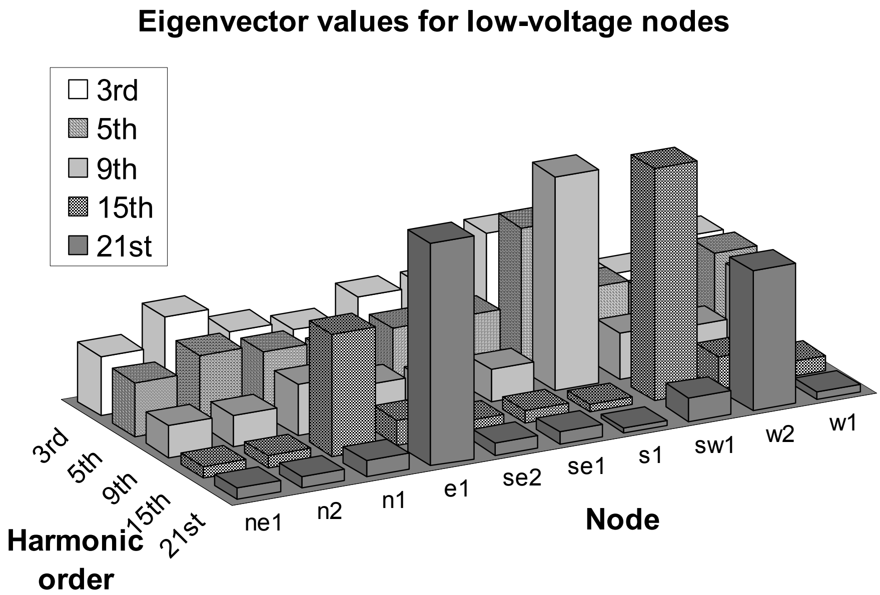

Fig. 5.16 Eigenvector values for the minimum eigenvalue calculated for low-voltage nodes in the studied system at chosen harmonic orders

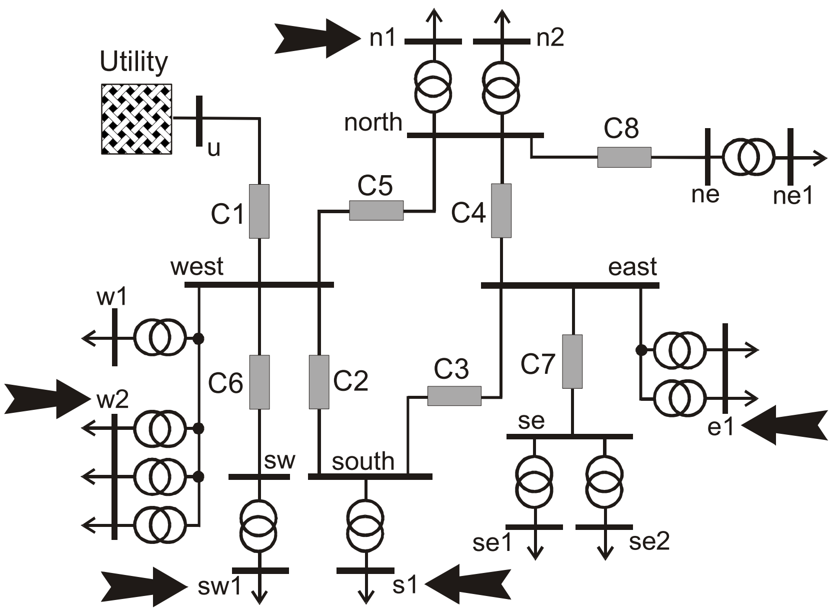

Fig. 5.17 Distribution system with the most considerable nodes to which attention should be paid in cases of unbalance for characteristic and non-characteristic harmonics

One should note that the method presented in this chapter only predicts the potentially most important and dangerous nodes in the distribution system. Problems arise with the installation of such loads that inject this kind of harmonic spectrum, to which the node is sensitive. The effect of load unbalance can therefore be considered knowing that the considerable neutral load was registered at node *ne1* (Fig. 5.12) that is non-sensitive to triplens (Fig. 5.16). If an analogous load configuration is installed at other nodes, e.g. *n1* or *sw1* – that are sensitive to triplens, this could cause many more problems because under unbalanced conditions not only characteristic harmonics will flow in the neutral conductor (triplens) or in line conductors (positive or negative sequence harmonics), but the non-characteristic orders will also appear. Detailed analysis including three-phase modeling and on-site considerations are needed, for such reference [33] seems to be of importance.

From Fig. 5.16 it can also be seen that node *sw1* is the most sensitive to the 15th harmonic (the biggest eigenvector value), therefore if a harmonic current of the 15th order would be injected in this node, the resulting voltage distortion would be big. The same can be said for the node *n1*. The results of the measurement survey have shown that the 15th harmonic seems to be the most problematic. The detected node sensitivity (i.e nodes *sw1* and *n1* being sensitive) shows good consistency with the measurement results. The comparison between measurement results for the 15th harmonic orders and the sensitivity analysis is shown in Fig. 5.18. Considering the 21st harmonics, the nodes *e1* and *w2* appear to be most sensitive. This situation was observed during measurements, as well, where some problems with 21st harmonic were registered at node *e1* (Fig. 5.5).

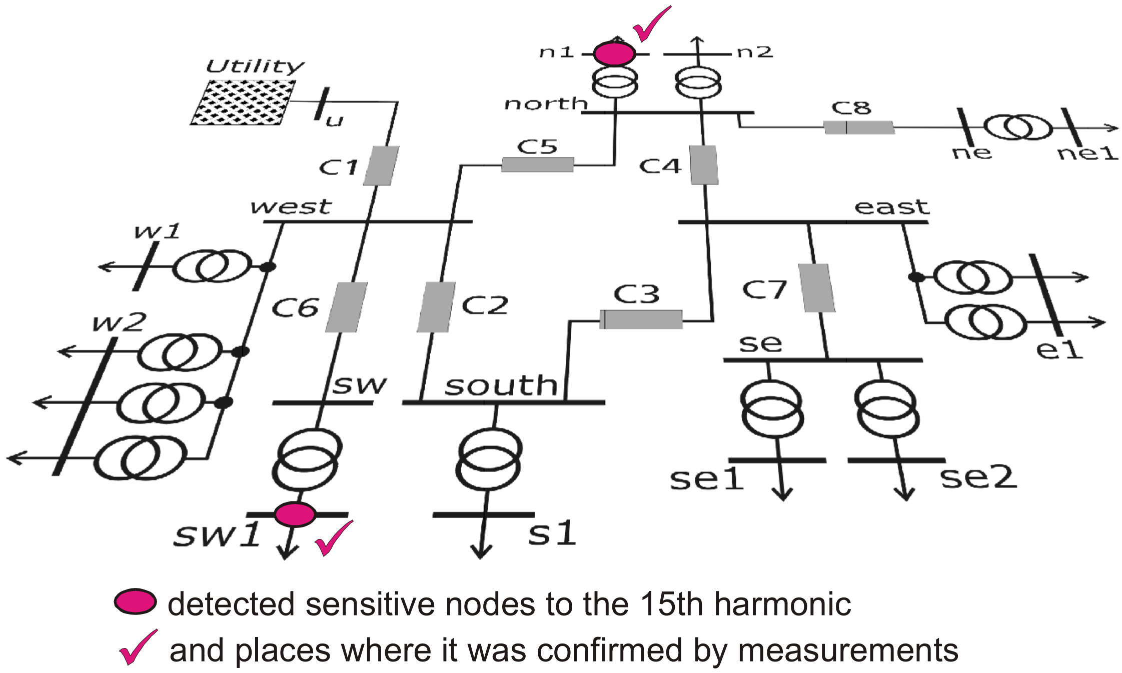

Fig. 5.18 Comparison measurements – sensitivity analysis, 15th harmonic case

Moreover, from Fig. 5.16 it can be stated that node *ne1* rises as an adverse node, being non-sensitive to the calculated harmonic orders. It can be generally observed that node *ne1*, having smaller a eigenvector value that corresponds to the respective four smallest eigenvalues, is more resistant to harmonic distortion than the other nodes considered above. The direction of harmonic propagation can be estimated in this way. The majority of distortion penetrates the generation node (e.g. flows to the power factor correction capacitor at that node), while a small amount of distortion 'flows' through the transformer to the grid which from the harmonic generation point is seen, in this case, as a considerably lesser impedance. The influence on the other nodes exists, but is relatively small.

As far as the error of the analysis is concerned, it must be stated that, as previously mentioned in section 5.1 of this chapter, the quantitative conclusions made analyzing only the eigenvector components that correspond to the smallest eigenvalue can be burdened with a considerable estimation error, especially when analyzing systems with closed loops, few generators and a small amount of lines/cables. This is in the case with the system analyzed in this section. In Fig. 5.19 the estimation error for the quantitative estimation of the voltage changes according to equation (5-10) is presented.

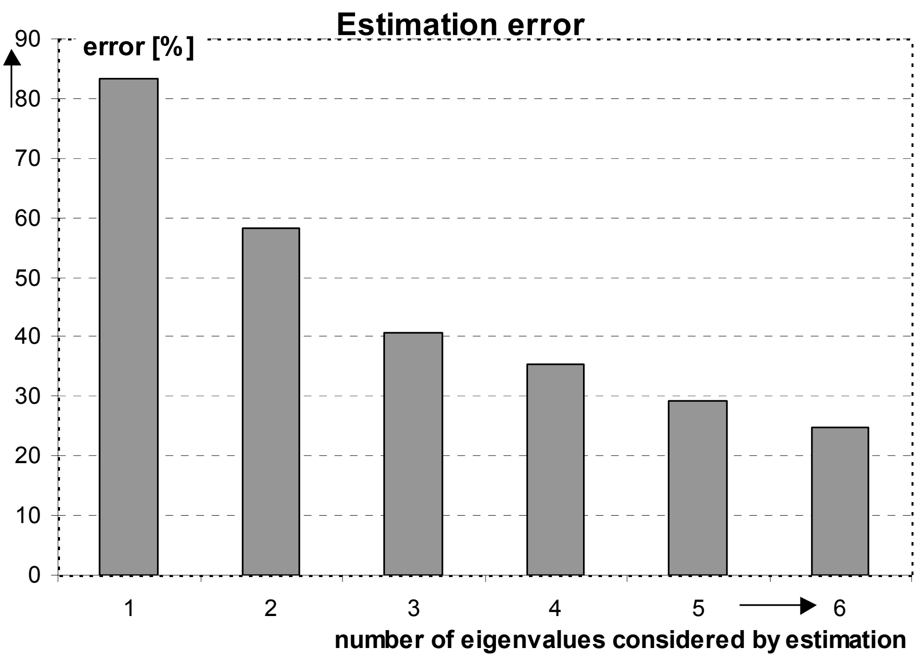

Fig. 5.19 Estimation error for the quantitative analysis, 15^{th} harmonic case

It can be seen that no serious quantitative conclusions can be made for the analyzed distribution system regarding only the components of the eigenvector connected with the smallest eigenvalue. The error in this case would be about 80 %, making the quantitative analysis unacceptable. In such cases, as previously mentioned, not only the smallest eigenvalue and its corresponding eigenvector values should be taken into consideration. However, for qualitative analysis proposed in this thesis, the conclusions about nodes sensitivity can be made satisfactorily when regarding only the smallest eigenvalue and its corresponding eigenvector components, as can be seen from Fig. 5.20. This graphic shows the components of the eigenvectors that correspond to the four smallest eigenvalues that have been obtained analyzing the nodal admittance matrix for the above mentioned 15^{th} harmonic case.

It can be observed that the nodes detected as sensitive when regarding only the components of the eigenvector that correspond to the smallest eigenvalue (dark rectangle in Fig. 5.20) remain sensitive by the analysis of components of eigenvectors that correspond to the second- and third smallest eigenvalues. For clearness in Fig. 5.20 the elements of eigenvectors that correspond to those three smallest eigenvalues are placed within two ellipses. In this case the sensor node detection (qualitative analysis) is assumed as sufficient and unequivocal. Analysis at other frequencies brings comparable results, however every case should be studied separately.

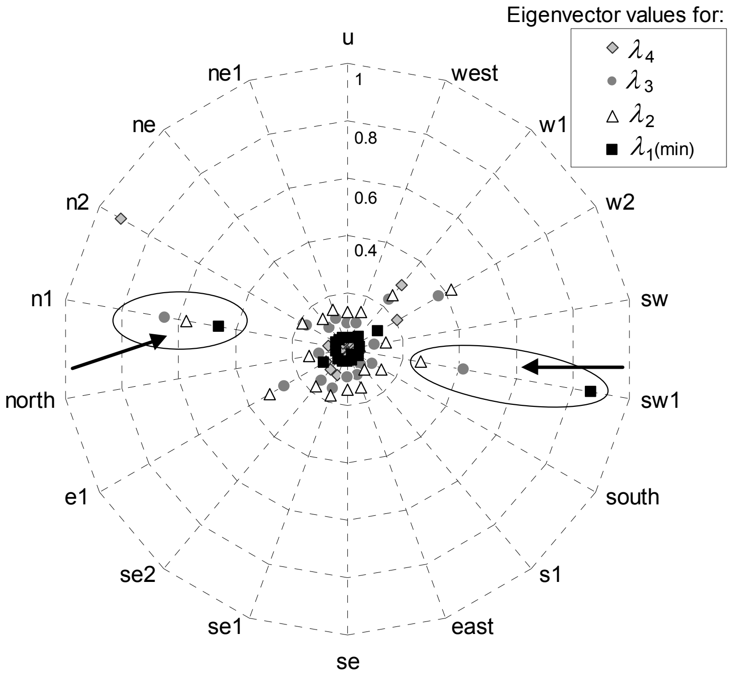

Fig. 5.20 Eigenvector values that correspond to the four smallest eigenvalues, analysis for 15th harmonics

Summarizing, the measurements, in general, are time consuming and cannot be done at every point of the distribution system to prove power quality. Therefore, computer simulation software is a convenient way to make an eigenvalue analysis of the nodal admittance matrix $\underline{Y}_h$ of the studied system and to find the critical points in the network considering their sensitivity to harmonics, as shown in this section. The evidence of the system elements plays an important role during the admittance matrix building process and influences the exactness of the method. In these investigations a good consistency has been shown allowing for the qualitative analysis of the distribution system. The method can be applied to collect information which gives an overview of the analyzed power system and shows the places that are, or can be, sensitive to harmonics. It can also be useful for finding the optimal harmonic filter location or in cases of finding of the most appropriate places to install new non-linear loads. The analysis of the nodal admittance matrix also answers the questions which of the nodal voltages are influenced and how sensitive are they to harmonic sources. The detailed, quantitative analysis can then be applied to the nodes of great influence, as proposed in Chapter 4, with the help of measurement-based CFA-Matrix simulations.

The analysis in frequency domain presented in this work can be built on the standard information including impedances of system elements and the characteristic or type of the non-linear loads. The influence of the load modeling on the behavior of the method will be described in the next section of this chapter.

5.3.3 Effect of the load modeling on the results of the analysis

To obtain the impact of the non-linear voltage-power characteristic of the loads on sensitivity analysis two modeling approaches were used in the calculations presented below. The problem of load modeling is more aggregate, because of the diversity of the load types and its different voltage-power characteristic. The first type of load model used – called *linear* stands for the loads with a linear voltage-power characteristic, like heating. The second type, with strong, non-linear characteristics (Fig. 5.21) is typical for the heavily-loaded induction machines [118] and was used to prove if the non-linear function, which combines the active and reactive power changes at the basic frequency with the nodal voltage changes, has an influence on the systems' nodes sensitivity variation to the conducted low-frequency disturbances in the form of harmonics [119].

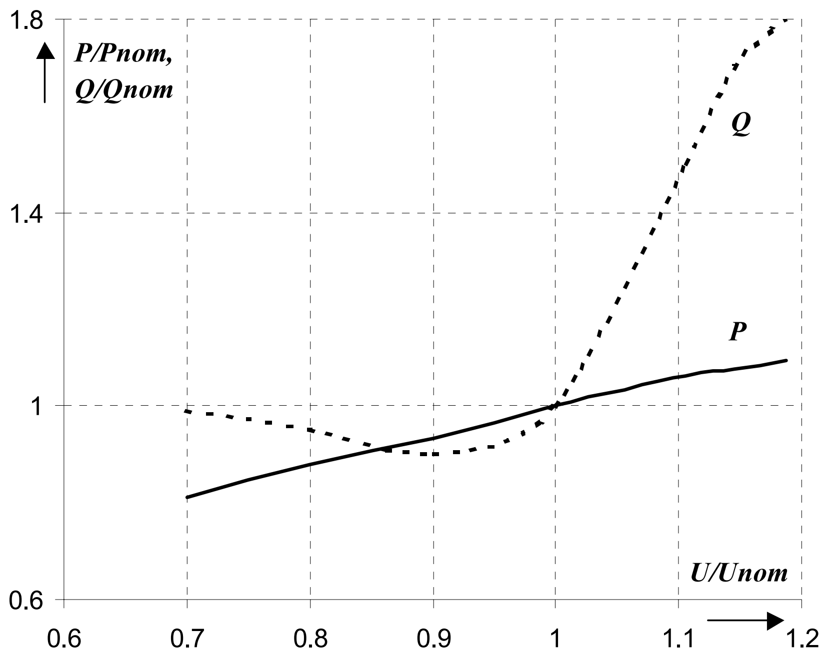

Fig. 5.21 Modeling of the load with non-linear P, Q = f(U) characteristic

This dependence between nodal voltage changes and the changes of the power of the load connected at this node can be written by using the so-called polynomial or ZIP load model [118], as in (5-25) and (5-26):

$$P = P_{nom} \cdot \left(a_0 + a_1 \frac{U}{U_{nom}} + a_2 \left(\frac{U}{U_{nom}} \right)^2 \right), \tag{5-25}$$

$$Q = Q_{nom} \cdot \left(b_0 + b_1 \frac{U}{U_{nom}} + b_2 \left(\frac{U}{U_{nom}} \right)^2 \right), \tag{5-26}$$

where P, Q are active and reactive power, respectively, obtained through the power flow calculation routine at the voltage U. The subscript nom stands for these values at nominal conditions. The a and b are polynomial coefficients. To better understand this phenomena and to estimate a potential risk connected to the harmonic pollution in the case of load variations in the system, a sensitivity analysis of the nodes in the studied system (Fig. 5.4) was carried out for the three cases:

- The sensitivity analysis of the system at minimum load;
- The sensitivity analysis of the system at maximum load;
- The load with non-linear voltage-power was connected at node *sw1* (detected sensor node) and the influence of its power on the sensitivity of the detected sensor nodes to harmonic distortion was studied.

Load flow was calculated for each case to obtain the voltages at the nodes and the load power. This was then used to include the loads admittances in the nodal admittance matrix of the system. Then, the nodal admittance matrix was built for the spectrum of frequencies which covers the measurement results, i.e. for the frequencies which correspond to the measured harmonics. After that the eigenvalue analysis was executed for the 18 x 18 nodal admittance matrix according to the terms presented in previous sections.

The results of the nodes sensitivity in the case of minimum load is shown in Fig. 5.22. It can be observed, that node *sw1* and node *n1* appear to be the most sensitive (the biggest values of the modules of the eigenvector components that correspond to the eigenvalue of minimum modulus – compare also with Fig. 5.16 gives analogous results) to those harmonic orders which were detected as problematic during the measurements (Fig. 5.5). Nodes *w1* and *w2* are more sensitive to the harmonic of order 5th, 7th and 9th, other nodes being ‘non-sensitive’ (e.g. node *se1*, also in Fig. 5.16). Comparing the results to those from Fig. 5.16 calculated for the average load conditions comparable conclusions can be drawn.

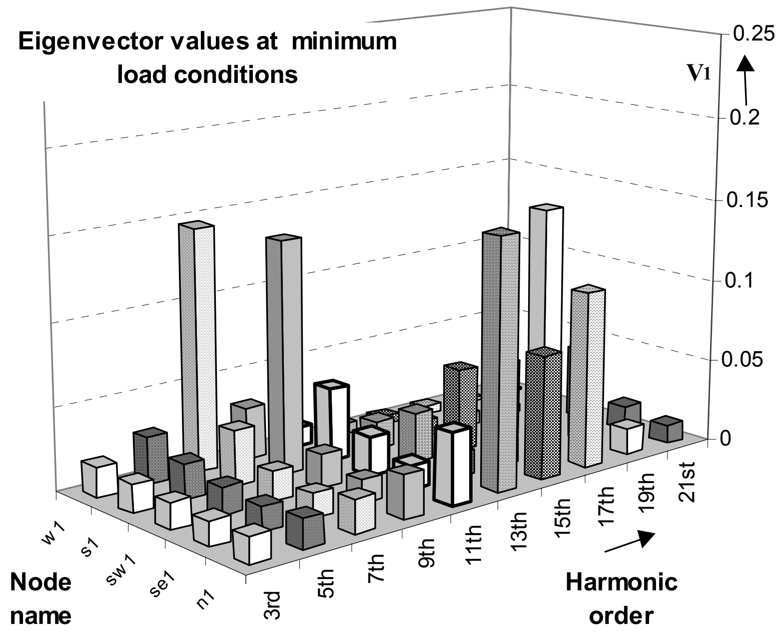

Fig. 5.22 Eigenvector values, which correspond to the minimum eigenvalue at minimum load conditions

In the second case, under maximum load conditions, the sensitivity of the nodes did not change considerably. Only the displacement of the frequencies (in the growing direction), to which the eigenvector values were maximal, was observed (Fig. 5.23).

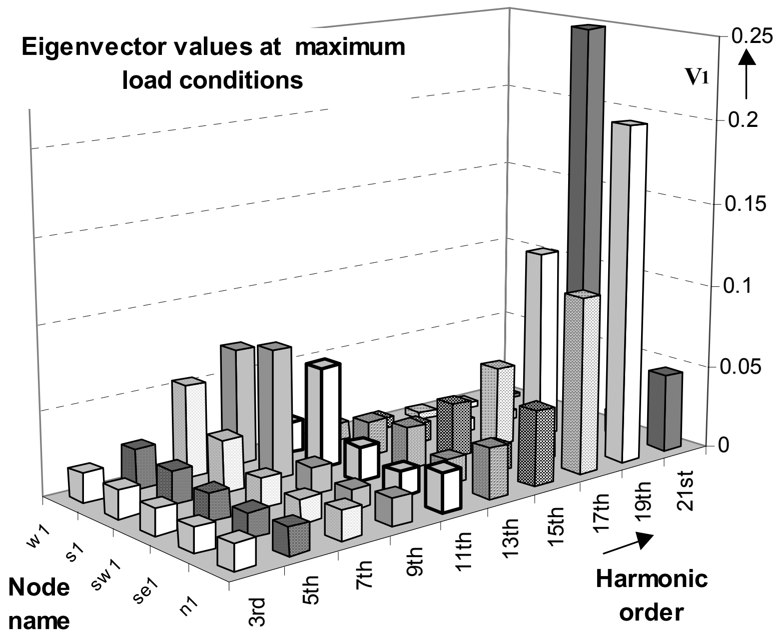

Fig. 5.23 Eigenvector values, which correspond to the minimum eigenvalue at maximum load conditions

In the third case, for the nodes, which were detected as the most sensitive a complementary analysis was executed including the non-linear load modeling (Fig. 5.21). The non-linear loads were connected to nodes *sw1* and *n1* and their power was changed from the minimum to the maximum value, both values have been taken from the measurements at those nodes. The results are shown in Fig. 5.24 and Fig. 5.25 for the 15th and 21st harmonic frequencies, respectively.

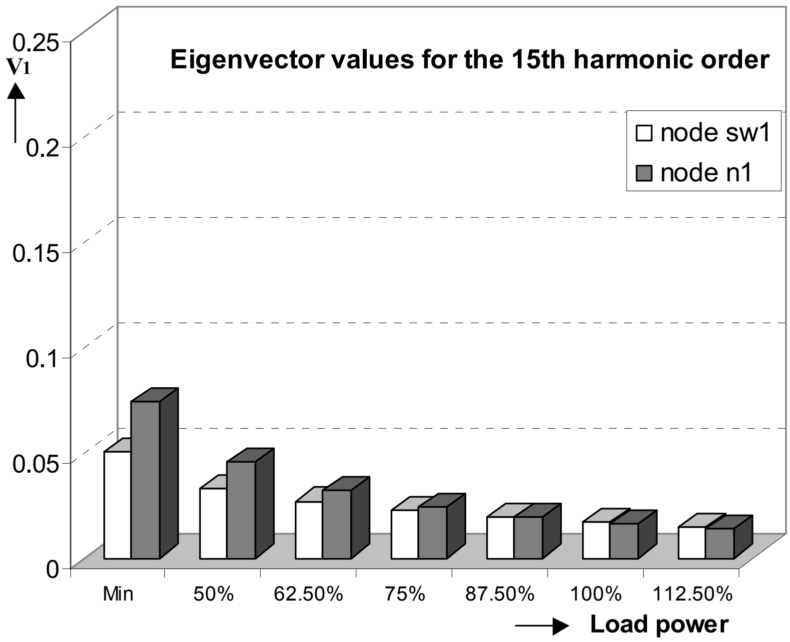

Fig. 5.24 Eigenvector values changes as a function of the non-linear load power calculated for 15th harmonic order

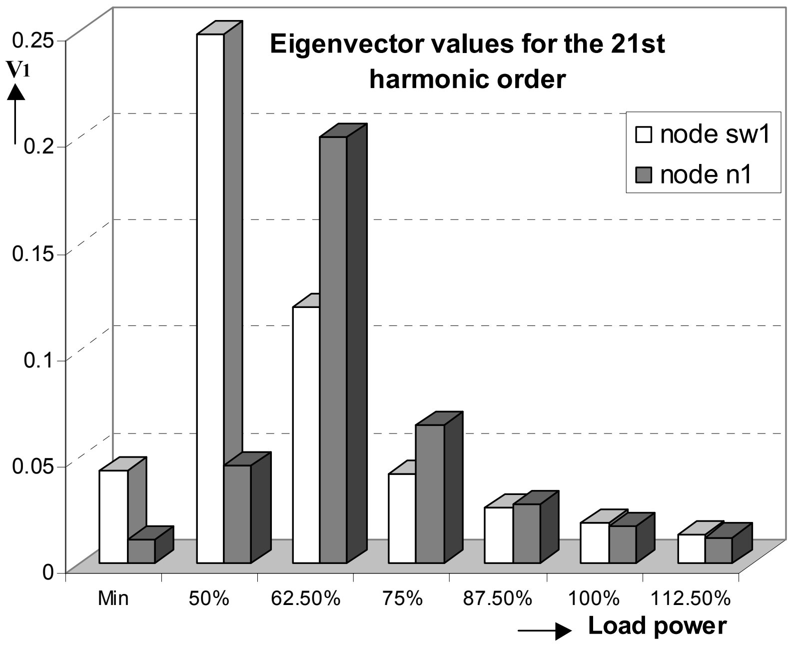

Fig. 5.25 Eigenvector values changes as a function of the non-linear load power calculated for 21st harmonic order

Again, the comparison of the measurement and spectral analysis results shows a good consistency. The biggest eigenvector component for the state of maximum and minimum loads corresponds in the nodes *sw1* and *n1* to the frequencies which lie near the 15th and 21st harmonic orders (Fig. 5.22, Fig. 5.23). This means that these are sensor nodes for the mentioned harmonics orders.

How already mentioned in section 5.3.2 one should note that the method predicts the potentially most important and dangerous nodes in the distribution system. This also explains why, if the source of disturbance is present at another node, the degradation of the electromagnetic environment (i.e. voltage characteristics) at this node also occurs, as with the 'non-sensitive' nodes *w1* and *e1* (Fig. 5.5).

The results of the case studies show clearly that the spectral analysis can be sensitive to the load changes and load type. By increasing the load the voltage sensitivity in nodes *sw1* and *n1* for 21st harmonic at the beginning increases and then decreases (Fig. 5.25), and for 15th harmonic the voltage sensitivity in nodes *sw1* and *n1* decreases (Fig. 5.24).

6 SUMMARY

In the scope of this work a novel, hybrid-method for power quality investigations was developed that is intended for the analysis of electric power distribution systems with respect to harmonics and interharmonics.

The increasing application of electronically controlled devices in recent years not only affects the secure and reliable operation of the power system, but it also makes the maintenance of the customers' supply parameters standards more complicated. As a result, the distribution power system is exposed to the new operational conditions and self-generates interferences, which not only decrease the efficiency of the energy transport within it, but also badly affect its immunity. Distortion propagation depends on the system configuration, its actual state in the sense of load variation, and on the non-linear load characteristics. Accurately recognizing the non-linear load placement and characteristics requires voluminous measurement data and depends on the load connection point conditions. This also creates problems for the power network operator: firstly, Where should the distortion sources be located? secondly, Which places in the distribution system are especially sensitive to the distortion? and finally, Which of the known mitigation methods will be recommended? It is, therefore, very important to know in advance how the power system will behave under new conditions; what susceptibility level at which point in the system can be expected. This information can help to identify threatening conditions in a power system before an interruption or disturbance occurs. In this work a novel method for the harmonic and interharmonic study in distribution systems was proposed for finding and analyzing the disturbances in the nodes of the system that are sensitive to harmonics or interharmonics.

In the initial part of the work, the subject of power quality and its interrelation to the field of electromagnetic compatibility was clarified with respect to the standards and regulations. Synthesizing this information a comprehensive classification of the power quality phenomena was presented and analyzed. It was stated that the quality of supply requires much stricter monitoring than what is currently in practice for two main reasons. On the one hand, there exists a tough resonance danger caused by the increasing share of non-linear loads by simultaneous decreasing number of resistive loads, and, on the other hand, the fact of increased cost pressure which arose due to the changes in the electricity market has made the evaluation of power quality at the PCC between the utility and the consumer more necessary than ever.

The concept of an appropriate measurement system for the evaluation of power quality in distribution systems was presented in the second part of the work. The application of the algorithms used was the central goal of the developed measurement system whose flexible construction enables one to study both the behavior of the system in a long-term perspective, i.e. observing and comparing trends of the PQ indices over a long period of time in a measurement survey, and to also measure and analyze power quality problems that arise at the cross-section of disturbing devices.

In the third part of this work the concepts for both the electrical system's equipment and for the non-linear and linear load modeling in frequency domain were presented and then discussed in a measurement-based example. It was discovered that the improvement of the harmonic simulations can be achieved by including in the model an interaction effect that takes place between the non-linear, harmonic producing load - disturbance source -, and the network via its impedance - disturbance sink. Synthesizing this, a measurement-based method was presented which includes this interaction effect in the constructed model with the help of a crossed frequency admittance matrix in the harmonic domain. For the reasonable employment of the routine, the nodes in the analyzed system that are most sensitive to disturbances have to be found at first. Therefore, the core of the hybrid-method developed in the work builds an approach which is based on information coming from the structure of the analyzed power system and utilizes eigenvalue analysis of the nodal admittance matrix of the system, i.e. the inherent structure theory of network. The inherent structure theory of networks involving eigenvalue analysis that was successfully applied to voltage sensitivity investigations in power networks was extended here to the harmonic distortion prediction, which in this case can help to describe the most sensitive places in a distribution system from the expected distortion point of view.

The work in this thesis focuses on the power system's sensitivity analysis to quasi-stationary disturbances, like harmonics or interharmonics. The investigations showed that this approach enables one to study the sensitivity of the power system taking into account only one (as in the case of most power systems) or a few components that come from the spectral decomposition of the nodal admittance matrix of the analyzed system. This improves the understandability of the final results and is advantageous especially in cases of systems with many nodes and adverse conditions with respect to the voltage and current distortion that result from a variety of disturbing loads present in a system with low short-circuit power.

As far as the modeling process is concerned, it was discovered that the proper system model development should concentrate on the precise short-circuit data assessment: starting from supply cable length, through middle voltage supply network parameters and ending with a correctly assumed short circuit power at the PCC. The source of error in the system model was the background noise which was difficult to include within the model. The derivation of a daily curve for the distortion present at a given place helped in understanding the phenomena in a real system. The modeling process of the non-linear load was assisted by synchronous measurements which helped to parameterize the model in a way which enabled reaching the interaction source-sink. However, the procedure can be difficult to apply when there are multiple harmonic current sources in the system.

The usage of this ‘pro-active’ method to estimate a potential risk connected to the harmonic pollution turned out to be important, especially with regard to standards and norms in the power quality area. Above all, in the scope of the mentioned circumstances the practice to use the under dimensioned neutral wires and TN-C type of network should be reconsidered, especially in cases with a high ratio of non-linear and single-phase load. The best method for power quality analysis, although clearly not possible in every case, is to make on-site measurements and on-site evaluation of the harmonic problems within the system. The enlargement of the allowable harmonic distortion limits can have an apparent effect on the equipment functionality and therefore, on-site monitoring is necessary. Clarification of the problems can then be made by detailed analysis. Therefore, the analytical method proposed in this contribution can indicate a set of most sensitive nodes to which special attention should be paid when considering the load structure currently present in a studied system, is able to analyze the potential harmonic problems and can then be used to choose the nodes for on-site monitoring.

A closer study of the case of multiple devices and the influence of unbalance on the distortion propagation can be the subject of future considerations, where a holistic approach combining statistical data of loads and network impedances with measurement-based analytical methods can improve the thoroughness of the analysis.

7 ZUSAMMENFASSUNG

Im Rahmen der Arbeit wurde eine Methode der Spannungsqualitätsanalyse vorgestellt, die zur Untersuchung von Oberschwingungen und Zwischenharmonischen in Verteilungsnetzen besonders geeignet ist.

Der zunehmende Einsatz von elektronisch gesteuerten Geräten führt zur Beeinträchtigung der Energiequalität in elektrischen Netzen. Die resultierende Spannungs- und Stromverzerrung kann für empfindliche Einrichtungen gefährlich sein, besonders dann, wenn der Oberschwingungspegel nahe an den Störfestigkeitspegeln der angeschlossenen Betriebsmittel liegt oder diese überschreitet. Die in der Arbeit vorgestellte Methode findet die bezüglich Oberschwingungen und Zwischenharmonischen gefährdetsten Stellen in einem Verteilungssystem heraus. Somit wird eine Vorab-Analyse zur Ergreifung der notwendigen Maßnahmen ermöglicht.

Zunächst wurde das Thema Spannungsqualität und ihr Zusammenhang mit der elektromagnetischen Verträglichkeit aus Sicht der Normen und Vorschriften erläutert. Darauf aufbauend wurde eine grundlegende Klassifikation der Spannungsqualitätsereignisse vorgestellt und analysiert. Es wurde festgestellt, dass die Spannungsqualität aus verschiedenen Gründen zunehmend überwacht werden muss - einerseits aufgrund verstärkter Resonanzgefahr durch wachsenden Anteil nichtlinearer Verbraucher bei gleichzeitig sinkenden Anteil ohmscher Lasten und andererseits, da der durch den veränderten Energiemarkt verstärkte Kostendruck die Evaluierung auch unter wirtschaftlichen Gesichtspunkten notwendig macht. Das Konzept eines entsprechend entwickelten Messsystems zur Beurteilung der Spannungsqualität in Verteilungsnetzen wurde vorgestellt. Der Einsatz der verwendeten Beurteilungsalgorithmen stand hierbei im Zentrum des Messsystems, deren flexibler Aufbau sowohl langzeitige Spannungsqualitätsmessungen aber auch Emissionsmessungen an einzelnen Geräten normgerecht ermöglicht.

Im Weiteren wurden Modellierungsansätze für elektrische Betriebsmittel sowie sowohl lineare- als auch nicht-lineare Lasten für die Modellierung im Frequenz-Bereich vorgestellt. Dabei wurde verdeutlicht, dass das Zusammenwirken zwischen der Störquelle - nichtlinearer Last - und der Störsenke - dem Versorgungsnetz - sehr wesentlich für die Genauigkeit der Simulationen ist. Darauf aufbauend wurde eine messungsbasierte Methode vorgeschlagen, um die zu berücksichtigenden Nichtlinearitäten mit Hilfe einer Crossed-Frequency-Admittance-Matrix im Harmonischen-Bereich zu modellieren. Ein Beispiel illustriert detailliert dieses Verfahren, so dass alle Abhängigkeiten und Wechselwirkungen deutlich werden.

Um die in der Arbeit entwickelte Methode sinnvoll durchführen zu können, müssen im Voraus die sensitivsten Knoten in einem Verteilungsnetz gefunden werden. Deshalb wurde als Kern der entwickelten Methode ein Verfahren vorgeschlagen, das auf der internen Struktur des zu analysierenden Netzes basiert. Nachdem die mathematischen Grundlagen dieses spektralen Ansatzes vorgestellt wurden, wurde eine Beispielanalyse am realen Netz durchgeführt um die Eigenschaften dieser qualitativen Methode zu veranschaulichen.

Die Untersuchungen zeigten, dass die Methode zur Beurteilung von Spannungsqualität in Verteilungsnetzen wirkungsvoll anwendbar ist und zu besserer Genauigkeit bei Simulationen führt. Durch die Filterungseigenschaft der Spektralanalyse wurde eine bessere Selektivität der Analyse erreicht als bei herkömmlichen Methoden der Spannungsqualitätsanalyse. Das ist besonders bei Verteilungsnetzen von Vorteil, bei denen ungünstige Verhältnisse bezüglich Spannungs– und Stromqualität, hervorgerufen durch niedrige Kurzschlussleistungen und eine Vielzahl von Störquellen in den Verteilungsnetzen, entstehen.

8 APPENDIX

8.1 INNER PRODUCT AND NORMS OF VECTORS

In this work an *Euclidean inner product* and *Euclidean vector norm* are used.

Let $\underline{\boldsymbol{W}}$ denote a square nonsingular[1] $n \times n$ matrix. The inner product of n-dimensional column vectors $\underline{\boldsymbol{x}}$ and $\underline{\boldsymbol{y}}$ with respect to $\underline{\boldsymbol{W}}$, denoted as $\langle \underline{\boldsymbol{x}}, \underline{\boldsymbol{y}} \rangle_{\underline{\boldsymbol{W}}}$, is the dot[2] product:

$$\langle \underline{\boldsymbol{x}}, \underline{\boldsymbol{y}} \rangle_{\underline{\boldsymbol{W}}} = (\underline{\boldsymbol{W}}\,\underline{\boldsymbol{x}}) \cdot (\underline{\boldsymbol{W}}\,\underline{\boldsymbol{y}})^* . \tag{7-1}$$

If $\underline{\boldsymbol{W}} = \boldsymbol{1}$, where $\boldsymbol{1}$ is the identity[3] matrix, then the subscript in (7-1) is dropped, and the inner product in (7-2):

$$\langle \underline{\boldsymbol{x}}, \underline{\boldsymbol{y}} \rangle = \underline{\boldsymbol{x}} \cdot \underline{\boldsymbol{y}}^* \tag{7-2}$$

is called *Euclidean inner product*. If $\underline{\boldsymbol{x}}$ and $\underline{\boldsymbol{y}}$ are also real, then the Euclidean inner product reduces to the dot product of the two vectors.

A *norm* for an arbitrary finite dimensional vector $\underline{\boldsymbol{x}}$ is a measure of the length or magnitude of the vector and is a real-valued function. There are many alternative definitions of norms for measuring the magnitude of a vector [113]. The most common inner-product generated vector norm is defined in (7-3):

$$\|\underline{\boldsymbol{x}}\|_{\underline{\boldsymbol{W}}} = \sqrt{\langle \underline{\boldsymbol{x}}, \underline{\boldsymbol{x}} \rangle_{\underline{\boldsymbol{W}}}} . \tag{7-3}$$

In this work the *Euclidean* (or l_2) *norm* (7-4) is used, which is a special case of the inner-product norm when $\underline{\boldsymbol{W}} = \boldsymbol{1}$:

$$\|\underline{\boldsymbol{x}}\|_2 = \sqrt{\langle \underline{\boldsymbol{x}}, \underline{\boldsymbol{x}} \rangle} . \tag{7-4}$$

The *Euclidean norm* can also be treated as a special case of the l_p norm:

$$\|\underline{\boldsymbol{x}}\|_p = \left(|\underline{x}_1|^p + |\underline{x}_2|^p + \cdots + |\underline{x}_n|^p \right)^{\frac{1}{p}} \tag{7-5}$$

for $p = 2$. In most cases in this work the subscript 2 in (7-4) is dropped.

[1] A square matrix is said to be *singular* if it does not have an inverse.
[2] The *dot product* $\boldsymbol{x} \cdot \boldsymbol{y}$ of two vectors of the same order is obtained by multiplying the corresponding elements of $\boldsymbol{x}$ and $\boldsymbol{y}$ and then summing the elements.
[3] An identity matrix is a diagonal matrix in which all of the diagonal elements are equal to unity.

8.2 CALCULATION OF EIGENVALUES AND EIGENVECTORS OF COMPLEX MATRICES

In this work a Matlab (which stands for Matrix Laboratory) eigenvalue routine was used to obtain the eigenvalues and eigenvectors of the nodal admittance matrix $\underline{\boldsymbol{Y}}$. Since only the modules of the eigenvalues and eigenvectors were subjected to the analysis, the problem of complexity of the eigenvalues and eigenvectors is not critical in the cases concerned in this work. However, for the proper placing of the cases studied in this work and for explanation of the complex eigenvalue calculation problem several comments are presented in this part of appendix.

Matrices that are real and symmetric are of special importance in praxis due to their special properties [113]. However, in the power engineering praxis the usual case are matrices with complex elements. The extension of the real and symmetrical class of matrices to all matrices which are symmetric and have complex elements is of less value since matrices of this extend class do not have many of the more important properties of real, symmetric matrices. The most useful extension is to the class of matrices of the form (7-6):

$$\underline{\boldsymbol{A}} = (\boldsymbol{D} + i\boldsymbol{F}), \tag{7-6}$$

where $\boldsymbol{D}$ is real and symmetric and $\boldsymbol{F}$ is real and skew-symmetric, i.e:

$$\boldsymbol{F}^T = -\boldsymbol{F}. \tag{7-7}$$

Matrices of this class are called *Hermitian matrices*. Therefore if $\underline{\boldsymbol{A}}$ is *Hermitian*, then from the definition:

$$\underline{\boldsymbol{A}} = (\underline{\boldsymbol{A}}^*)^T, \tag{7-8}$$

where $\underline{\boldsymbol{A}}^*$ denotes the matrix whose elements are the complex conjugates of those of $\underline{\boldsymbol{A}}$. The matrix $(\underline{\boldsymbol{A}}^*)^T$ is frequently denoted by $\underline{\boldsymbol{A}}^H$ and is referred to as the Hermitian transposed matrix. For vectors, similarly, $\underline{\boldsymbol{x}}^H$ is the row vector with components equal to the complex conjugates of those of the column vector $\underline{\boldsymbol{x}}$. The notation is convenient and has the advantage that results proved for Hermitian matrices may be converted to the corresponding results for real symmetric matrices by replacing $\underline{\boldsymbol{A}}^H$ with $\boldsymbol{A}^T$ and $\underline{\boldsymbol{x}}^H$ with $\boldsymbol{x}^T$ [116]. For real symmetric matrices, real eigenvalues imply real eigenvectors, but the eigenvectors of a complex Hermitian matrix are in general complex.

Since for all practical cases the nodal admittance matrix $\underline{\boldsymbol{Y}}$ is a complex symmetrical matrix, for which real and imaginary part properties (7-9) and (7-10) can be written:

$$\boldsymbol{G}^T = \boldsymbol{G} \text{ and} \tag{7-9}$$

$$\boldsymbol{B}^T = \boldsymbol{B}. \tag{7-10}$$

where $\boldsymbol{G}$ is the conductance matrix and $\boldsymbol{B}$ is the susceptance matrix (both having real elements), it therefore makes sense to extend the construction of (7-6) as described in [116], pp. 342, to the form (7-11). This is a useful representation of the nodal admittance matrix as a symmetrical[4] matrix with real elements:

$$\underline{\boldsymbol{Y}} = \begin{pmatrix} -\boldsymbol{B} & \boldsymbol{G} \\ \boldsymbol{G} & \boldsymbol{B} \end{pmatrix}. \tag{7-11}$$

Such construction can be advantageous, especially for large power system studies, enabling the complexity of $\underline{\boldsymbol{Y}}$ to be avoided. This allows for the sensitivity determination of the series $\Delta\boldsymbol{u}_a$ and the shunt $\Delta\boldsymbol{u}_r$ components of nodal voltages to changes of the real $\Delta\boldsymbol{i}_a$ and the imaginary $\Delta\boldsymbol{i}_r$ components of nodal currents:

$$\Delta\,\underline{\boldsymbol{u}} = \begin{pmatrix} \Delta\boldsymbol{u}_r \\ \Delta\boldsymbol{u}_a \end{pmatrix} = \begin{pmatrix} -\boldsymbol{B} & \boldsymbol{G} \\ \boldsymbol{G} & \boldsymbol{B} \end{pmatrix}^{-1} \begin{pmatrix} \Delta\boldsymbol{i}_a \\ \Delta\boldsymbol{i}_r \end{pmatrix}. \tag{7-12}$$

In other words, as a result of the eigenvalue calculations of such a matrix (7-11) the eigenvalues are real and are coincident. However, the presence of such coincident eigenvalues does not affect the accuracy with which they are determined, and only one vector is needed in the subspace of the eigenvectors corresponding to each double eigenvalue. All vectors in this subspace correspond to the same complex eigenvector and the obtained real eigenvalues are equal to the modules of the complex eigenvalues obtained from the Matlab eigenvalue routine.

As far as the non-symmetrical matrices are concerned the method described in this work can be used as well. However, a non-symmetrical matrix $\underline{\boldsymbol{Y}}$ will be then subjected to the singular value decomposition. The susceptibility analysis can be undertaken analogously considering the singular value of the smallest modulus and its corresponding singular vectors.

[4] Matrix $\underline{\boldsymbol{Y}}$ will be non-symmetrical when the transformer transformation factors are complex values (i.e. with phase-shifting), but this is not the case in this work.

9 LIST OF REFERENCES

[1] DUGAN, R. C.; MCGRANAGHAN, M. F.; BEATY, H. W.: Electrical Power Systems Quality. McGraw-Hill, New York , 1996, ISBN 0070180318.

[2] WAKILEH, G. J.: Power System Harmonics: Fundamentals, Analysis and Filter Design. Springer, Berlin Heidelberg New York, 2001, ISBN 3540422382.

[3] DUGAN, R. C.; MCGRANAGHAN, M. F.; SANTOSO, S.; BEATY, H. W.: Electrical Power Systems Quality (2nd edition). McGraw-Hill, New York, 2003, ISBN 007138622X.

[4] ACHA, E.; MADRIGAL, M.: Power System Harmonics, Computer Modelling and Analysis. John Wiley & Sons, Chichester, England, 2001, ISBN 047152175-2.

[5] BOLLEN, M.: Understanding Power Quality Problems, Voltage Sags and Interruptions. IEEE Press, New York, 2000, ISBN 0780347137.

[6] BERNARD, S.: Harmonic Pollution. Power Quality Online Assurance Magazine, ISSN 1068-4085, www.powerquality.com, call date: Nov. 2000.

[7] LONIE, B.: Proactive Power Quality Program. PQ Today Magazine, Vol. 1, No. 2, 1995.

[8] ARRILLAGA, J.; SMITH, B. C.; WATSON, N. R.; WOOD, A. R.: Power System Harmonic Analysis. John Wiley & Sons, Chichester, 1997, ISBN 0471975486.

[9] ARRILLAGA, J.; WATSON, N. R.; CHEN, S.: Power System Quality Assessment. John Wiley & Sons, Chichester, 2001, ISBN 0471988650.

[10] 89/336/EEC: European Council Directive on the approximation of the laws of the Member States relating to electromagnetic compatibility, amended by Directives 91/263/EEC, 92/31/EEC, 93/68/EEC, 93/97/EEC.

[11] IEC 61000-1-1, 1992: Electromagnetic compatibility: General - Application and interpretation of fundamental definitions and terms.

[12] BLUME, D.; SCHLABBACH, J.; STEPHANBLOME, T.: Spannungsqualität in elektrischen Netzen. VDE-Verlag, Berlin, 1999, ISBN 3800722658.

[13] UNION OF THE ELECTRICITY INDUSTRY EURELECTRIC (editor): Network of Experts for Standardization; Power Quality in European Electricity Supply Networks (1st edition). Ref: 2002-2700-0005, Brussels, Feb. 2002.

[14] SCC 22: Standards Coordinating Committee on Power Quality. Charter, http://www.standards.ieee.org.

[15] EN 61000-4-30, 2002 (draft): Electromagnetic compatibility: Testing and measuring techniques – Power quality measurements method.

[16] IEEE STANDARD 100-1996 (6th edition): IEEE Standard Dictionary of Electrical and Electronics Terms. IEEE, New York, 1997.

[17] IEEE STANDARD 1100-1992: IEEE Recommended Practices for Powering and Grounding Sensitive Electronic Equipment. IEEE, New York, 1992.

[18] ELECTRIC POWER RESEARCH INSTITUTE EPRI, Palo Alto, California, USA, http://www.epri.com.

[19] GONSCHOREK, K. H.; SINGER, H.: Elektromagnetische Verträglichkeit. Grundlagen, Analysen, Maßnahmen. Teubner, Stuttgart, 1992, ISBN 3519061449.

[20] GOEDBLOED, J.: Electromagnetic Compatibility. Prentice Hall, New York, 1992, ISBN 0132492938.

[21] HABIGER, E. ET AL.: Handbuch Elektromagnetische Verträglichkeit. Grundlagen, Maßnahmen, Systemgestaltung 2nd ed. Verlag Technik, Berlin, 1992, ISBN 3341009930.

[22] SCHWAB, A. J.: Elektromagnetische Verträglichkeit (3rd edition). Springer, Berlin, 1994, ISBN 3540576584.

[23] EN 61000-2-5, 1995: Electromagnetic compatibility: Environment - Classification of electromagnetic environments. Basic EMC publication.

[24] IEEE STANDARD 1159-1995: IEEE Recommended Practices on Monitoring Electric Power Quality. IEEE, New York, 1995.

[25] EN 61000-2-2, 1993: Electromagnetic compatibility: Environment - Compatibility levels for low frequency conducted disturbances and signaling in public low-voltage power supply systems.

[26] FORSCHUNGSGEMEINSCHAFT FÜR HOCHSPANNUNGS- UND HOCHSTROMTECHNIK E.V. (editor): FGH Technischer Bericht 284: Spannungsqualität. Mannheim, 1996.

[27] EN 61000-2-2, 2002: Electromagnetic compatibility: Environment - Compatibility levels for low frequency conducted disturbances and signaling in public low-voltage power supply systems.

[28] HERMANN, N.: Vergleich ziviler und militärischer EMV-Normen. Internationale Fachmesse und Kongress für Elektormagnetische Verträglichkeit, Düsseldorf, Germany, 2000, pp. 363-370.

[29] IEEE Standard 519-1992: IEEE Recommended Practices and Requirements for Harmonic Control in Electrical Power Systems. IEEE, New York, June 1992.

[30] HALPIN, S. M.: Overview of Revisions to IEEE Standard 519-1992. CIGRE and IEEE PES Symposium on Quality and Security of Electric Power Delivery Systems, Montreal, Canada, Oct. 2003, session IIIa, Paper 301.

[31] EN 50160, 1999: Voltage characteristics of electricity supplied by public distribution systems.

[32] KLOSS, A.: Netzrückwirkungen der Leistungselektronik (2. Auflage). VDE – Verlag, Berlin, 1996, ISBN 3800721570.

[33] KREBS, R.: Analysis der Anisotropien dreiphasiger Betriebsmittel. Ph.D. Dissertation, Technical Dept., Univ. Erlangen-Nuremberg, 1990.

[34] IEEE INTERHARMONIC TASK FORCE, CIGRÉ 36.05/CIRED 2 CC02 VOLTAGE QUALITY WORKING GROUP (editor): Interharmonics in Power Systems. Jointly prepared paper, 1999.

[35] BACHRY, A.; CZARNECKI, T. K.; DÖBBELIN, R.; MECKE, H.; STYCZYNSKI, Z.: Zwischenharmonische in elektrischen Energieversorgungsnetzen, hervorgerufen durch gepulste technologische Lasten. Internationale Fachmesse und Kongress für Elektromagnetische Verträglichkeit, Düsseldorf, Germany, Feb. 2004, pp. 767-774.

[36] 85/374/EEC: European Council Directive on the approximation of the laws, regulations and administrative provisions of the Member States concerning liability for defective products, amended by Directive 1999/34/EC.

[37] GUTIÉRREZ-IGLESIAS, J. L.: Power Quality Costs. EURELECTRIC Third Power Quality Workshop, Brussels, Belgium, Nov. 2003.

[38] GRETSCH, R.: Summary Session 1. EURELECTRIC Third Power Quality Workshop, Brussels, Belgium, Nov. 2003.

[39] BACHRY, A.; ORTHS, A.; STYCZYNSKI, Z.; RUHLE, O.; WINTER, W.: Standardized Models of Distributed Energy Sources for Power Network Planning Using NETOMAC. 14th International Power Systems Computation Conference PSCC'02, Sevilla, Spain, June 2002, session 11, Paper 4.

[40] BACHRY, A.; ORTHS, A.; BÖSE, C.; RUHLE, O.: Einfluss von verteilten Erzeugern und Speichern auf Netzplanung und Netzbetrieb. VDE-Kongress 2002, Dresden, VDE–Verlag GmbH Berlin Offenbach, Oct. 2002, Bd. 1, pp. 395-400, ISBN 3800727234.

[41] ORTHS, A.; BACHRY, A.; BÖSE, C.; RUHLE, O.; STYCZYNSKI, Z.: Dispersed Generation in Distribution Networks: Performance Simulation Based on New Planning Technique's Results - Case Study. 17th International Conference on Electricity Distribution CIRED, Barcelona, Spain, May 2003, session 4, Paper 83.

[42] BUCHHOLZ, B. M.; BÖSE, C.: The impact of dispersed power generation in distribution systems. CIGRE and IEEE PES Symposium on Quality and Security of Electric Power Delivery Systems, Montreal, Canada, Oct. 2003, session V, Paper 502.

[43] ORTHS, A.: Multikriterielle, optimale Planung von Verteilungsnetzen im liberalisierten Energiemarkt unter Verwendung von spieltheoretischen Verfahren. Ph.D. Dissertation, Faculty of Electrical Engineering and Information Technology, Otto-von-Guericke-Univ. Magdeburg, 2003.

[44] BIERWIRTH, M.: Softwareentwicklung zur erfassung und erkennung der leitungsgeführten Störungen in elektrischen Netzen. Student's Thesis, Faculty of Electrical Engineering and Information Technology, Otto-von-Guericke-Univ. Magdeburg, 2002 (unpublished).

[45] EN 61000-4-7, 1993 (Ed.1): Electromagnetic compatibility: Testing and measuring techniques – General guide on harmonics and interharmonics measurements and instrumentation, for power supply systems and equipment connected thereto.

[46] EN 61000-4-7, 2002 (Ed.2): Electromagnetic compatibility: Testing and measuring techniques – General guide on harmonics and interharmonics measurements and instrumentation, for power supply systems and equipment connected thereto.

[47] FOURIER, J. B. J.: Théorie Analytique de la Chaleur. (book), Paris, 1822.

[48] KREYSZIG, E.: Advanced Engineering Mathematics (8th edition). John Wiley and Sons, Chichester, 1999, ISBN 047133328X.

[49] KUO, F. F.: Network Analysis and Synthesis (2nd edition). John Wiley and Sons, Chichester, 1996, ASIN 0471511188.

[50] BRIGHAM, E. O.: The Fast Fourier Transform, An Introduction to Its Theory and Application. Prentice-Hall, New York, 1973, ISBN 013307496X.

[51] SHANG, L.: Wavelet Transform Applications in Power Systems. Ph.D. Dissertation, Faculty of Engineering Sciences, Univ. Erlangen-Nuremberg, 2002.

[52] CICHOCKI, A.; ŁOBOS, T.: Artificial Neural Networks for Real-Time Estimation of Basic Waveforms of Voltages and Currents. IEEE Transactions on Power Systems, May 1991, Vol. 9, No. 2, pp. 612-618.

[53] TANAKA, K.: An Introduction to Fuzzy Logic for Practical Applications. Springer, Berlin Heidelberg New York, 1996, ISBN 0387948074.

[54] ŁOBOS, T.; LEONOWICZ, Z.; REZEMER, J.; KOGLIN, H.-J.: Advanced signal processing methods of harmonics and interharmonics estimation. 7th International Conference on Developments in Power System Protection, April 2001, pp. 315-318.

[55] LEONOWICZ, Z.: Modern Methods Of Spectral Analysis In Power Systems (in Polish). Ph.D. Dissertation, Faculty of Electrical Engineering, Wroclaw Univ. of Technology, Wroclaw, 2000.

[56] LEM NORMA D 6000 SERIES: Wide Band Power Analyzer, User's Guide and Technical Specifications. LEM NORMA GmbH, Neudorf, Austria, 1998, www.lem.com.

[57] NATIONAL INSTRUMENTS PCI-6120 SERIES: Data Acquisition Card, User's Guide and Technical Specifications. National Instruments Germany GmbH, Munich, 2003, www.ni.com.

[58] Directives concerning the Protection of Telecommunication Lines against Harmful Effects from Electricity Lines, CCIT, Geneva, Switzerland, 1963.

[59] ETXEBERRIA-OTADUI, I.; BACHA, S.; BACHRY, A.; STYCZYNSKI, Z.; FRACCHIA, M.; STUART, M.: Power Electronic Converters for Railway Infrastructure Upgrading: Advantages and Potential Risks. Proc. Conference on Power Systems and Communication Systems for the Future, Beijing, China, Sept. 2002, session VII, Paper 4.

[60] STYCZYNSKI, Z.; BACHA, S.; BACHRY, A.; ETXEBERRIA- OTADUI, I.: Improvement of EMC in Railway Power Networks. 10th IEEE International Conference on Harmonics and Quality of Power ICHQP, Rio de Janeiro, Brazil, Oct. 2002, Paper 26.

[61] ETXEBERRIA- OTADUI, I.; BACHA, S.; STYCZYNSKI, Z.; BACHRY, A.; COURTOIS, C.; TALIBART, A.; FRACCHIA, M.: SVC, A Real Alternative for Railway Infrastructure Upgrading – HVB2 European Project Test Results. 10th European Conference on Power Electronics and Applications EPE 2003, Toulouse, France, Sept. 2003, Paper 760.

[62] CZARNECKI, L. S.: Scattered and Reactive Current, Voltage, and Power in Circuits with Nonsinusoidal Waveforms and Their Compensation. IEEE Transactions on Instrumentation and Measurement, June 1991, Vol. 40, No. 3, pp. 563-567.

[63] FERRERO, A.; SUPERTI-FURGA, G.: A New Approach to the Definition of Power Components in Three-Phase Systems Under Nonsinusoidal Conditions. IEEE Transactions on Instrumentation and Measurement, June 1991, Vol. 40, No. 3, pp. 568-577.

[64] EMANUEL, A. E.: Apparent and reactive powers in three-phase systems, In search of a physical meaning and a better resolution. European Transactions on Electrical Power Engineering ETEP, 1993, Vol. 3, No. 1, pp. 7-14.

[65] AKAGI, H.; NABAE, A.: The p-q theory in three-phase systems under non-sinusoidal conditions. European Transactions on Electrical Power Engineering ETEP, 1993, Vol. 3, No. 1, pp. 27-31.

[66] DEPENBROCK, M.: The FBD-Method, A Generally Applicable Tool for Analyzing Power Relations. IEEE Transactions on Power Systems, May 1993, Vol. 8, No. 2, pp. 381-387.

[67] PRETORIUS, J. H. C.; VAN WYK, J. D.; SWART, P. H.: An Evaluation of Some Alternative Methods of Power Resolution in a Large Industrial Plant. IEEE Transactions on Power Delivery, July 2000, Vol. 15, No. 3, pp. 1052-1059.

[68] BUDEANU, C. I.: Puissances reactives et ficitves. Institute Romain de l'Energie, publication 27, Bucharest, Romania, 1927.

[69] CZARNECKI, L. S.: Power related phenomena in three-phase unbalanced systems. IEEE Transactions on Power Delivery, July 1995, Vol. 10, No. 3, pp. 1168-1176.

[70] FRYZE, S.: Active, reactive and apparent power in circuits with non-sinusoidal voltage and current (in Polish). Przegl. Elektrotech., 1931, No. 7, pp. 193-203; ibid. 1931, No. 8, pp. 225-234; ibid. 1932, No. 22, pp. 673-676; ETZ Elektrotech., 1932, Z. 53 (in German).

[71] IEEE WORKING GROUP ON NONSINUSOIDAL SITUATIONS: Practical Definitions for Powers in System with Nonsinusoidal Waveforms and Unbalanced Loads: A Discussion. IEEE Transactions on Power Delivery, Jan. 1996, Vol. 11, No. 1, pp. 79-101.

[72] FILIPSKI, P. S.: Apparent Power – A misleading Quantity in the Non-sinusoidal Power Theory: Are all Non-Sinusoidal Power Theories Doomed to Fail? European Transactions on Electrical Power Engineering ETEP, 1993, Vol. 3, No. 1, pp. 21-26.

[73] EMMANUEL, A. E.: The Buchholz-Goodhue Apparent Power Definition, The practical Approach for Nonsinusoidal And Unbalanced Systems. IEEE Transactions on Power Delivery, April 1998, Vol. 13, No. 2, pp. 344-350.

[74] CZARNECKI, L. S.: An orthogonal decomposition of the current of non-sinusoidal voltage sources applied to non-linear loads. International Journal on Circuit Theory and Applications, 1983, Vol. 11, pp. 235-239.

[75] BUCHHOLZ, F.: Die Drehstrom-Scheinleistung bei ungleichmäßiger Belastung drei Zweige. Licht und Kraft, Jan. 1922, No. 2, pp. 9-11.

[76] BACHRY, A.; STYCZYNSKI, Z.; ŁOBOS, T.: The Analysis of Low Voltage Distribution Power System Under Non-sinusoidal Conditions – Case Study. 4th International Conference on Power Networks PNET2000, Wroclaw, Poland, ISSN-0324-9778, July 2000, pp. 583-591.

[77] STYCZYNSKI, Z.; BACHRY, A.: The Influence of the High Power Ratio Non-linear Loads on the Low Voltage System Operation – Case studies. International Conference on Power System Transients IPST'2001, Rio de Janeiro, Brazil, June 2001, pp. 120-125.

[78] IEEE TASK FORCE ON HARMONICS MODELING AND SIMULATION: Modeling and Simulation of the Propagation of Harmonics in Electric Power Networks. IEEE Transactions on Power Delivery, Jan. 1996, Vol. 11, No. 1, pp. 452-474.

[79] CIGRE WORKING GROUP 36-05: Harmonics, characteristic parameters, methods of study, estimates of existing values in network. Electra, July 1981, No. 77, pp. 35-54.

[80] VEREINIGUNG DEUTSCHER ELEKTRIZITÄTSWERKE - VDEW-E.V. (editor): Grundsätze für die Beurteilung von Netzrückwirkungen. Verlags- und Wirtschaftsgesellschaft der Elektrizitätswerke m.b.H. - VWEW, Frankfurt am Main, 1992.

[81] HOFMANN, L.; OSWALD, B. R.: New transmission line model with frequency dependent parameters in the time domain. 13th International Power Systems Computation Conference PSCC'99, Trondheim, Norway, June 1999, pp. 1040-1046.

[82] REFORMAT, M.; WOODFORD, D.; WACHAL, R.; TARKO, N. J.: Non-linear load modeling for simulations in time domain. 8th IEEE International Conference on Harmonics and Quality of Power ICHQP 1998, Athens, Greece, Oct. 1998, pp. 506-510.

[83] IEEE PES (editor): Tutorial on Harmonics Modeling and Simulation. 98TP125-0, Piscataway, New Jork, 1998.

[84] SANKARAN, C.: Power Quality. CRC Press, Boca Raton London New York, 2002, ISBN 0849310407.

[85] MANJURE, D. P.; MAKRAM, E. B.: Impact of Unbalance on Power System Harmonics. 10th IEEE International Conference on Harmonics and Quality of Power ICHQP 2002, Rio de Janeiro, Brazil, Oct. 2002, Paper 01.

[86] IEEE TASK FORCE ON HARMONICS MODELING AND SIMULATION: Impact of aggregate linear load modeling on harmonic analysis: A comparison of common practice and analytical models. IEEE Transactions on Power Delivery, April 2003, Vol. 18 , No. 2, pp. 625-630.

[87] ELECTROTEK CONCEPTS (editor): SuperHarm® - an Electrotek Harmonic Simulation Program: User's Guide. Version 4.3, Knoxville, Tennessee, USA, Nov. 2002.

[88] ASEA BROWN BOVERI (editor): Switchgear Manual, a Pocket Book (9th edition). ABB Schaltanlagen GmbH, Mannheim, Germany, 1993.

[89] XU, W.; MARTI, J. R.; DOMMEL, H.: A multiphase harmonic load flow solution technique. IEEE Transactions on Power Systems, 1991, Vol. 6, No. 1, pp. 174-182.

[90] BACHRY, A.; STYCZYNSKI, Z.: An Investigation of Voltage Quality in Distribution Systems With Pulsed Power Loads - Modeling Method Verified by Synchronous Measurements. 17th International Conference on Electricity Distribution CIRED, Barcelona, Spain, May 2003, Session 2, Paper 41.

[91] FAURI, M.: Harmonic Modelling of Non-Linear Loads by means of Crossed Frequency Admittance Matrix. IEEE Transactions on Power Systems, 1997, Vol. 12, No. 4, pp. 1632-1638.

[92] FUENTES, J. A.; GABALDÓN, A.; MOLINA, A.; CÁNOVAS, F. J.: Harmonic Modelling of Electronically Controlled Loads. 2000 IEEE PES Summer Meeting, Washington, USA, Vol. 3, pp. 1805-1810.

[93] FUENTES, J. A.; GABALDÓN, A.; MOLINA, A.; GÓMEZ, E.: Development and Assessment of A Load Decomposition Method Applied at The Distribution Level. IEE Gener. Transm. Distrib., 2003, Vol. 150, No. 2, pp. 245-251.

[94] MOLINA, A.; GABALDÓN, A.; FUENTES, J. A.; ÁLVAREZ, C.: Implementation and Assessment of Physically Based Electical Load Models: Application to Direct Load Control Residential Programs. IEE Gener. Transm. Distrib., 2003, Vol. 150, No. 1, pp. 61-66.

[95] WEEDY, B. M.; CORY, B. J.: Electric Power Systems (4th edition). John Wiley & Sons, Chichester, 1998, ISBN 0471976776.

[96] VAN CUSTEM, T.; VOURNAS, C.: Voltage Stability of Electric Power Systems. Kluwer Academic Publishers, Boston, 1998, ISBN 0792381394.

[97] LAUGHTON, M. A.: Sensitivity in Dynamical System Analysis. Journal of Electronics and Control, 1964, 17, No.5, pp. 577-591.

[98] PECHON, J.; PIERCY D.; TINNEY, W. F.; TWELT, O. Y.: Sensitivity of power systems. IEEE Trans. on Power Apparatus and Systems, 1968, Vol. 89, No. 8, pp. 1381-1388.

[99] PORTER, B.; GROSSLEY, R.: Modal control, Theory and applications. Taylor and Francis, London, 1972, ASIN 0850660572.

[100] TIRANUCHIT, A.; THOMAS, R. J.: A Posturing Strategy Against Voltage Instabilities in Electric Power Systems. IEEE Transactions on Power Systems, 1988, Vol. 3, No. 1, pp. 87-93.

[101] GAO, B.; MORISON, G. K.; KUNDUR, P.: Voltage Stability Evaluation Using Modal Analysis. IEEE Transactions on Power Systems, 1992, Vol. 7, No. 4, pp. 1529-1542.

[102] GAMM, A. Z.; GOLUB, I. I.: Detection of weak places in a power system (in Russian). Izv. RAS, Energetika, No. 3, 1993, pp. 83-92.

[103] LÖF, P-A.; SMED, T.; ANDERSSON, G.; HILL, D. J.: Fast Calculation of A Voltage Stability Index. IEEE Transactions on Power Systems, 1992, Vol. 7, No. 1, pp. 54-64.

[104] LÖF, P-A.; ANDERSSON, G.; HILL, D. J.: Voltage Stability Indices For Stressed Power Systems. IEEE Transactions on Power Systems, 1993, Vol. 8, No. 1, pp. 326-335.

[105] OSOWSKI, S.: SVD Technique for Estimation of Harmonic Components in A Power System, A Statistical Approach. IEE Gener. Transm. Distrib., 2001, Vol. 141 No. 5, pp. 473-479.

[106] GAMM, A. Z.; GOLUB, I. I.; SCHNEIDER, P. W.; STYCZYNSKI, Z.: Power Network Operation Parameters in Distribution System with Energy Storages. Gdansk – Jurata, Poland, June 1999, Vol. 5, pp. 35-42.

[107] GOLUB, I. I.; STYCZYNSKI, Z.; BACHA, S.: Comparison of the Voltage Support Methods in the Railway Supply System Using Singular Value Methods. International Conference on Electrical Power Engineering PowerTech, Budapest, Hungary, Aug. 1999, Paper BPT99-137-24.

[108] LAUGHTON, M. A.; EL-ISKANDARANI M. A.: On The Inherent Network Structure. 6th Power Systems Computation Conference PSCC, Darmstadt, Germany, 1978, pp. 188-196.

[109] LAUGHTON, M. A.; EL-ISKANDARANI M. A.: The Structure of Power Network Voltage Profiles. 7th Power Systems Computation Conference PSCC, Lausanne, Switzerland, 1982, pp. 845-851.

[110] CARPINELLI, G.; RUSSO, A.; RUSSO, M.; VERDE P.: Inherent Structure Theory of Networks and Power System Harmonics. IEE Gener. Transm. Distrib., 1998, Vol. 145, No. 2, pp. 123-132.

[111] GAMM, A. Z.; GOLUB, I. I.; TKACHYEV, A. A.: Localization of Test Points for Measurement of Power Quality Indices. IEEE Power Tech Conference, Porto, Portugal, Sept. 2001, Paper QSR2-072.

[112] OSWALD, B.: Netzberechnung, Berechnung stationärer und quasistationärer Betriebszustände in Elektroenergieversorgungsnetzen. VDE Verlag, Berlin Offenbach, 1992, ISBN 3800717182.

[113] HORN, R. A.; JOHNSON, CH. R.: Matrix Analysis. Cambridge University Press, New York, 1990, ISBN 0521386322.

[114] BACHRY, A.; STYCZYNSKI, Z.: A Method For A Sensitivity Analysis of the Distribution System To Harmonic Distortion. 10th IEEE International Conference on Harmonics and Quality of Power ICHQP, Rio de Janeiro, Brazil, Oct. 2002, Paper 63.

[115] CARAMIA, P.; RUSSO, A.; VARILONE, P.: The Inherent Structure of Network for Power Quality Issues. 2001 IEEE PES Winter Meeting, Vol. 1, pp. 176-185.

[116] WILKINSON, J. H.: The Algebraic Eigenvalue Problem. Oxford University Press, New York, 1962, ISBN 0198534183.

[117] BACHRY, A.; KOROVKIN, N.; NITSCH, J.; STYCZYNSKI, Z.: Ein Ansatz zur Lokalisierung von Störungsquellen in elektrischen Energienetzen. Internationale Fachmesse und Kongress für Elektromagnetische Verträglichkeit, Düsseldorf, Germany, Feb. 2004, pp. 95-102.

[118] MACHOWSKI, J.; BIALEK, J. W.; BUMBY, J. R.: Power System Dynamics and Stability. John Wiley & Sons, Chichester, 1997, ISBN 047197174X.

[119] BACHRY, A.; GOLUB, I. I.; STYCZYNSKI, Z.: An Evaluation of Distribution Power System Susceptibility to Low Frequency Conducted Disturbances Under Different Load Conditions. 15th International Zurich Symposium & Technical Exhibition on Electromagnetic Compatibility EMC Zurich'03, Zurich, Switzerland, Feb. 2003, pp. 589-592.